Molecular and Mechanical Signatures in Epidermal Development and Differentiation

by

Alexandra Prado Mantilla

Department of Cell Biology
Duke University

Defense Date: November 13, 2024

Approved:

Terry Lechler, Advisor

Purushothama Rao Tata, Co-Chair

Debby Silver, Co-Chair

Stacy Horner

Dissertation submitted in partial fulfillment of the requirements for the degree of Doctor of Philosophy in the Department of Cell Biology in The Graduate School of Duke University
2024

ABSTRACT

Molecular and Mechanical Signatures Driving Epidermal Development and Differentiation

by

Alexandra Prado Mantilla

Department of Cell Biology
Duke University

Defense Date: November 13, 2024

Approved:

Terry Lechler, Advisor

Purushothama Rao Tata, Co-Chair

Debby Silver, Co-Chair

Stacy Horner

An abstract of a dissertation submitted in partial fulfillment of the requirements for the degree of Doctor of Philosophy in the Department of Cell Biology in The Graduate School of Duke University
2024

Abstract

Formation of the skin barrier requires rapid proliferation coupled with differentiation and stratification of the embryonic epidermis. Basal progenitors give rise to progeny throughout development – first to intermediate cells, a transient proliferative suprabasal cell population, and later to spinous cells. Neither the function nor the differentiation trajectory of intermediate cells has been documented. We generated transcriptomes of intermediate and spinous cells and identified specific markers that distinguish these two populations. Further, we found that intermediate cells express a subset of genes in common with granular cells of the epidermis – the terminal living cell type that helps establish the barrier. Lineage tracing revealed that most intermediate cells directly transition to granular cells without expressing markers specific to spinous cells, thus revealing a distinct lineage pathway leading to granular fate. In addition to their transcriptional similarities, intermediate and granular cells both had hallmarks of increased actomyosin contractility. We found that rather than simply lying downstream of cell fate pathways, contractility was sufficient to suppress spinous fate and promote granular gene expression. Together, these data establish the molecular and mechanical characteristics of the developing epidermis that allow this tissue to rapidly develop barrier activity. Additionally, I developed an inducible mouse model that enables the controlled knockdown of endogenous proteins in both a temporal and spatial manner using the Tet-ON system. This *in vivo* tool allows for the degradation of GFP-tagged proteins as early as 6 hours post-induction, providing a precise means to determine the specific timing and location of protein function within the organism.

Dedication

Para mi familia, que siempre, con su amor, apoyo y comprensión, me motiva a ser mi mejor versión. Sin ustedes, no habría llegado al final de este doctorado. Desde aquellos inicios, trepando las dunas de Huacachina, cuando los días eran soleados y felices, hasta ahora, que la vida es muy distinta y estamos lejos, siguen siendo mi apoyo incondicional frente a todas las adversidades de la vida. Los amo.

Contents

List of Figures

Acknowledgements

First, I would like to thank my PhD advisor, Terry Lechler, for his mentoring and guidance during this challenging process.

I thank the members of my thesis committee, Purushothama Rao Tata, Debby Silver and Stacy Horner, for their invaluable scientific insights throughout my work.

I am thankful to the past and current members of the Lechler lab for their feedback and support. Special thanks to Julie for assistance with the mouse colony.

I am grateful to the friends I met along this journey for their emotional and intellectual support. I will always cherish their friendship and continue to look up to them.

Most importantly, I am deeply grateful to my family, whose unconditional love and support have been my foundation throughout these years.

1 Introduction

1.1 Introduction to epidermal cell types and architecture

The entire epidermis is attached to an underlying basement membrane, which separates it from the dermis below. The cells directly in contact with the basement membrane are basal progenitor cells that express keratin 5 and 14 (K5/14) and are responsible for the rapid turnover of the tissue and for wound healing. Above these are differentiated cells, collectively referred to as "suprabasal" that express keratin 1 and 10 (K1/10). There are a number of distinct cell types that keratinocytes move through on their path through differentiation and eventual death. In the adult epidermis, spinous cells are the direct progeny of differentiating basal cells, which then progress through a granular cell fate before their eventual death and formation of the cornified layer, the outermost layer of the skin (Figure 1.1) (Prado-Mantilla & Lechler, 2023b).

1.1.1 Basal cells

Basal cells have a clear basal side defined by their attachment to the basement membrane. At this site, there is an enrichment for the hemidesmosomal α6/β4-integrin complex, which is likely stabilized at this site by interactions with the underlying extracellular matrix (ECM). In the absence of α6 or β4-integrin, the epidermal attachment to the underlying basement membrane is lost (van der Neut et al., 1996), resulting in blistering and conditions such as junctional epidermolysis bullosa (Niessen et al., 1996; Ruzzi et al., 1997). Common lateral markers of simple epithelia, like E-cadherin, are found at all cell-cell contact sites of these cells, including the "apical" region, which makes contact with overlying spinous cells. To our knowledge, there have been no reports showing specific apical enrichment of transmembrane proteins. These cells also lack tight junctions which normally demarcate the borders of apical and lateral membranes. While it is unclear whether the apical membrane is polarized, there is clear evidence that the apical region of the cell is specified and marked by core polarity machinery like Par3 and Gai3 (T. Lechler & E. Fuchs, 2005; Williams et al., 2014). This localization depends on both cell-cell

and cell-ECM adhesion as it requires both α-catenin and β1-integrin. Furthermore, the cytoplasm is clearly polarized as both the centrosome and the Golgi Apparatus are consistently apical to the nucleus (Lechler & Fuchs, 2007).

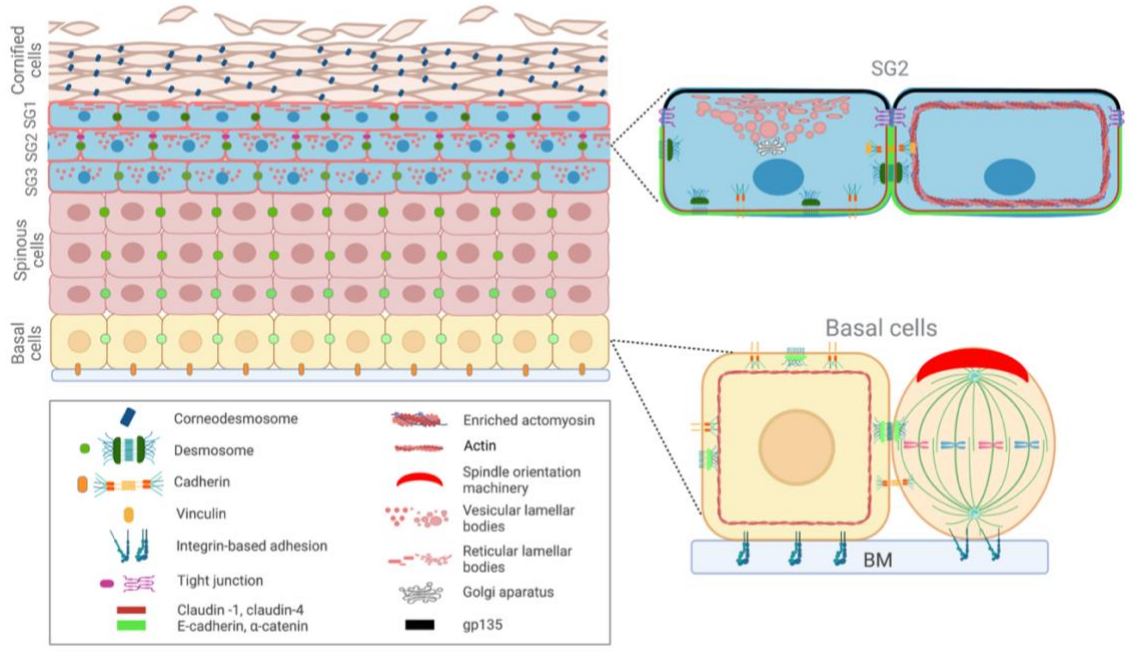

Figure 1.1: Diagram of epidermal architecture and cellular composition

Schematic of the architecture of the epidermis highlighting differences in cellular composition across different epidermal cell layers. Figure from (Prado-Mantilla & Lechler, 2023b)

During early development of the epidermis, basal progenitors divide planar to the underlying basement membrane (T. Lechler & E. Fuchs, 2005; Smart, 1970; Williams et al., 2011). These symmetric divisions give rise to two basal daughters. However, concomitant with the stratification of the epidermis, a substantial number of divisions become perpendicular and/or oblique to the underlying basement membrane. A number of lineage tracing and live imaging studies have demonstrated that these are functionally asymmetric – giving rise to one basal cell and one cell that is born into the suprabasal layer of the epidermis (Box et al., 2019; Poulson & Lechler, 2010). The ability to orient these spindles requires both cell-cell and cell-ECM adhesion

(T. Lechler & E. Fuchs, 2005). Perpendicular alignment of the spindle to produce asymmetric cell divisions is controlled by a core spindle orientation machinery that is polarized to the apical cortex of dividing cells. These divisions are essential for proper stratification and differentiation of the epidermis, as disruption of the core machinery results in randomized or symmetric cell divisions and profound defects in epidermal morphology (Moreci & Lechler, 2021; Seldin et al., 2016; Williams et al., 2011; Zhong et al., 2022).

While a role for spindle orientation in epidermal morphogenesis is evident, the connections to cell fate remain stubbornly murky. In the interfollicular epidermis, activation of Notch signaling is an essential driver of differentiation (Blanpain et al., 2006). Although the molecular connections between spindle orientation and Notch activation in the skin are unknown, it is clear that Notch signaling lies downstream of spindle orientation (Williams et al., 2011). There are likely both intrinsic and extrinsic cues that robustly guide cell fate, complicating this analysis. Notably, a specific population of basal progenitor cells fated to form hair follicles also divides asymmetrically (Ouspenskaia et al., 2016). The molecular machinery required for these asymmetric cell divisions has both overlapping and distinct components with surrounding basal progenitors (Byrd et al., 2016; Moreci & Lechler, 2021). Further, these divisions have an impact on Wnt signaling to control cell fate (Moreci & Lechler, 2021). Together, these findings show diversity in both the molecular machinery and the downstream signaling pathways of asymmetric cell divisions.

After embryonic stratification, maintenance of tissue architecture does not require precise control of spindle orientation. Rather, cell delamination from the basal layer supports homeostasis (Rompolas et al., 2016). There have been some reports of delamination occurring even in the embryonic epidermis, though neither the rate of this, nor its importance for stratification has been determined (Miroshnikova et al., 2018). Basal cells give rise to the first differentiated cell type, spinous cells.

1.1.2 Intermediate cells

Intermediate cells are a transient cell population that exists uniquely during development for only 1 to 2 days. These cells constitute the first layer of K1/10-expressing suprabasal cells and are formed at E14.5, when basal cells start dividing perpendicularly to the underlying basement membrane(T. Lechler & E. Fuchs, 2005; Smart, 1970). Then, they are located between the basal layer and the periderm. This cell population has unique characteristics like the fact that they are differentiated and yet are capable of proliferating. In addition, they are able to proliferate without attachment to the basement membrane, unlike basal cells that require dermal-epidermal junctions and their signaling cues to proliferate (Rousselle et al., 2022). The proliferation of differentiated epidermal cells in the epidermis does not occur later in development nor in adults unless in rare sporadic occasions (Cockburn et al., 2022) or in cutaneous diseases (Niehues et al., 2022). It is worthwhile to note that in the epidermis of adult humans during homeostasis conditions, there are cycling suprabasal cells (Pontiggia et al., 2022); however, this does not occur in mice.

It's currently broadly accepted in the literature that intermediate cells mature into spinous cells, given that suprabasal proliferation stops later in development and granular cells are formed. However, there is no direct evidence of the transition from intermediate cell to spinous cell fate occurring.

1.1.3 Spinous cells

Spinous cells are differentiated keratinocytes that express K1/10 and are postmitotic. They lie immediately above the basal layer, making them the first suprabasal cells in the mature epidermis. The onset of spinous cells starts after E15.5. At this point and later during epidermal development, basal cells give rise to spinous layers, also called stratum spinosum, by asymmetric cell divisions. However, in the adult epidermis, spinous cells originate directly from basal cells that commit to differentiation (Simpson et al., 2011). In this case, basal cells start expressing differentiation markers and stop expressing components that attach them to the basement

membrane, like hemidesmosomes and integrins (Cockburn et al., 2022; Haensel et al., 2020; Wang et al., 2020). As a result, these cells delaminate and move up to the suprabasal layer. Here, keratinocytes form stronger intercellular interactions by an increased number of desmosomes (Simpson et al., 2011). Desmosomes are intercellular junctions that mediate cell-cell adhesions and, by connecting with actin and keratin, help anchor this network of intermediate filaments to the plasma membrane. In this way, they help maintain tissue structures and provide cells with mechanical stability while also contributing to mechanosensing (Angulo-Urarte et al., 2020; Hatzfeld et al., 2017).

Desmosomes cover the entirety of spinous cells' surface. Although there are already desmosomes in the basal layers, their composition varies depending on their location throughout the epidermis. Overexpressing Dsg2, a desmosome component that is only present in basal cells, in suprabasal layers induced EGFR downstream signaling, which resulted in slightly impaired differentiation, hyperproliferation in basal and suprabasal layers, and pre-malignant papilloma (Brennan et al., 2007). On the other hand, Dsg1, which is increased in suprabasal layers, is necessary for repressing EGFR activity in an epidermal organotypic model, thus promoting differentiation (Getsios et al., 2009). Therefore, desmosomes seem to play a role in the switch from proliferation to differentiation in the epidermis (Johnson et al., 2014; Park, 2022).

Another event that occurs when keratinocytes pass from basal to spinous fate is that as they exit the cell cycle, their centrosomes become inactivated. In this way, centrosomes lose microtubule-organizing activity as they no longer co-localize with many microtubule anchoring proteins, and their microtubules undergo re-organization and localize cortically (Moreci & Lechler, 2020). *In vivo* experiments in the epidermis suggest that microtubules are important for maintaining cell shape and are implicated in junctional strength (Muroyama & Lechler, 2017; Ning et al., 2021). In addition, the higher layers of spinous cells that are further in the differentiation process start to become more flattened and start to produce Involucrin, an

important structural protein involved in the initial step of cornification, a process that occurs in terminal differentiation (Furue, 2020).

1.1.4 Granular cells

Two layers in the epidermis – the granular and cornified layers – compromise distinct aspects of the epidermal barrier. The outermost barrier is the stratum corneum, which is composed of enucleated cornified keratinocytes immersed in a complex lipid network that provides a watertight environment (Baroni et al., 2012; Blank, 1953; Brandner et al., 2015). The inner barrier is composed of tights junctions (TJs) in the stratum granulosum/granular layer (Furuse et al., 2002; Tellkamp et al., 2014; Tunggal et al., 2005), which seal neighboring cells and are especially important to prevent loss of water from within the body.

Cells in the granular layer, also called stratum granulosum, produce crucial components for the epidermal barrier formation. Some of the cornified envelop precursors that granular cells synthesize include structural proteins like loricrin, Involucrin and small proline-rich proteins (SPRRs). In addition, they produce keratin-associated proteins like profilaggrin, and trichohyalin, and numerous S100A Ca^{2+}-binding proteins. Curiously, all the genes encoding the previously mentioned proteins are located within 1.9Mbp of genomic DNA on human chromosome 1q21. This genomic region is called the epidermal differentiation complex (EDC), while in mice, they are located on chromosome 3 (Matsui, 2023; Mischke et al., 1996). Granular cells also start producing water-insoluble protein structures in their cytoplasm that are mainly composed of loricrin and profilaggrin, the precursor of filaggrin, which causes keratin bundling and condensation important for later cornification (Freeman & Sonthalia, 2024).

Granular cells also have the important function of synthesizing lipids and other components that are secreted to the extracellular space through membrane-bound organelles called lamellar bodies (LB) to form part of the stratum corneum (Mahanty & Setty, 2021). Cargo components of LB include precursor lipids, and enzymes necessary for processing them into their

final lipid products, as well as proteolytic enzymes important for desquamation, and other proteins like corneodesmosin (Ishida-Yamamoto et al., 2004). Therefore, LB formation is crucial for the establishment of the epidermal barrier, and their defective biogenesis or secretion is linked to diseases with defective barrier function like atopic dermatitis and severe ichthyosis syndromes (Elias & Wakefield, 2014; Feingold, 2012; Ishida-Yamamoto et al., 2018; Montpetit et al., 2008; Sakai et al., 2007).

The stratum granulosum is composed of three layers in the human skin: the granular layer closest to the spinous cells (SG3), the intermediate granular layer (SG2), and the outermost granular layer adjacent to the stratum corneum (SG1) (Furuse et al., 2002; Kubo et al., 2009; Yoshida et al., 2013). Granular cells change in protein content, structural conformation, and organelle reorganization while continuing to differentiate and move up through the different granular layers. Similarly, during this process, their LBs undergo changes in structure and location within the cell.

Several studies have proposed different models of LB's morphology and secretion of their cargo (den Hollander et al., 2016; Elias et al., 1998; Landmann, 1986; Norlen, 2001; Norlen et al., 2003). However, a recent study elucidated the highly detailed 3D structure of LB throughout the different layers of stratum granulosum in human skin (Yamanishi et al., 2019). In the SG3 layer, the LB are vesicular. When they transition to SG2, some LB fuse with the apical plasma membrane and show a reticular structure, while others remain as vesicles. Furthermore, in SG2, the tubular branches of TGN extend underneath the apical reticular network of lamellar bodies and connect to the apical vesicular lamellar bodies. Beneath the cornified layer, in SG1 cells, most LBs are fused to the plasma membrane and form a reticular network in the apical side of the outermost granular layer, in accordance with previous studies (Yamanishi et al., 2019). Thus, cells in the second granular layer direct their organelles and secrete important components for barrier formation to their apical membrane, but the mechanisms involved remain undefined.

In addition to SG2 cells being able to direct target apically, they are uniquely characterized by having tight junctions within the epidermis. TJ components, such as occludin and zonula occludens-1 (ZO1), are concentrated at TJ sites between SG2-SG2 junctions (Furuse et al., 2002; Kubo et al., 2009; Yoshida et al., 2013). Additionally, cells in this layer have enriched cortical organization of F-actin compared to spinous layers (Rubsam et al., 2017). While adherens junctions are present in cell-cell contacts throughout all epidermal layers, vinculin, a cytoskeletal protein that couples adherens junctions to the actomyosin complex (le Duc et al., 2010), is enriched in SG2 (Rubsam et al., 2017). SG2 segregate these cell adhesions such that TJs are found between their apical edges, while underneath there is a basolateral network of vinculin-rich adherens junctions (Rubsam et al., 2017) (Figure 1.1) (Prado-Mantilla & Lechler, 2023b).

1.1.5 Cornified layer

The stratum corneum is the final product of epidermal development and provides a physical permeability barrier against external pathogens, chemicals, or UV radiation. Cornification is the process where keratinocytes undergo programmed cell death and become corneocytes. During this process of terminal differentiation, the contents produced while they were granular cells, including structural components and lipids, become crosslinked at the cell periphery by transglutaminases 1 (Tgm1), 3, and 5, forming the cornified layer. Transglutaminases become activated with increased Ca2+ levels, potentially produced by organelle degradation, including the endoplasmic reticulum and mitochondria, which store Ca2+ (Eckhart et al., 2013; Haftek, 2014).

After organelle disintegration, keratin filaments form a dense network that occupies all the interior of the cell, providing them with mechanical strength. These flattened corneocytes are strongly tightened together by corneodesmosomes (Ishida-Yamamoto & Igawa, 2015). These junctions are modified desmosomes and are only present in between cornified keratinocytes. They play a role as adhesive structures in the cornified layer and in maintaining thickness of the

stratum corneum (Jonca et al., 2002). While they originate from desmosomes, their major structural difference is the presence of corneodesmosin (CDSN) in the extracellular region of corneodesmosomes. Desquamation, the process of shedding terminally differentiated keratinocytes from the cornified layer, occurs when degradation of their external structure is completed. CDSN is secreted by LBs, as well as proteases, including kallikrein-related proteases and their inhibitors, which control the desquamation process (Ishida-Yamamoto et al., 2005; Ishida-Yamamoto et al., 2004; Jonca et al., 2011; Raymond et al., 2008).

Granular cells synthesize precursor barrier lipids like ceramides, cholesterol, and free fatty acids, in the Golgi apparatus and endoplasmic reticulum and are then secreted to the extracellular space through LBs. These precursor lipids are processed by enzymes also secreted by LBs and, once in the intercellular space, are arranged into stacked sheets that are observed in the intercellular spaces throughout the cornified layers. This highly organized lipid matrix is called lipid lamellae and acts as a water-repellent that also cements corneocytes together in the stratum corneum (Bouwstra & Ponec, 2006; Feingold, 2012; Mahanty & Setty, 2021).

To form a functional epidermal barrier, lipids in the intercellular lipid matrix undergo progressive molecular arrangements that result in polarized organization of lipid structures along the stratum corneum. As observed by cryo-EM, the lipid lamellae undergo five different maturation stages in their progress through the cornified layers (Narangifard et al., 2018; Narangifard et al., 2021). In human skin, secreted lipids start as a highly folded, highly hydrated lipid bilayer present in LBs of granular cells. After several steps of reorganization, a mature skin barrier structure is formed at the third to fifth cornified layer, exhibiting stacked lipid bilayers of fully stretched ceramides, with cholesterol associated with ceramide's shorter sphingoid tail, while free fatty acids are associated with ceramides' longer fatty acid tail (Narangifard et al., 2021; Norlen et al., 2022) (Prado-Mantilla & Lechler, 2023b).

1.1.6 Mechanical differences across the epidermis

The varied tissues that comprise the main layers of the skin (epidermis, dermis, and hypodermis) have different mechanical characteristics. The epidermis is mainly composed of keratinocytes, though there are a number of additional resident cell types. The dermis consists of connective tissue, which contains fibrous proteins like collagen (18-30% of dermis volume), and lower amounts of elastin and other components. This is in addition to the cellular components including fibroblasts, vasculature, etc. Lastly, the innermost layer, or hypodermis, contains adipocytes that function as both a cushion and a regulator of other aspects of skin biology (Festa et al., 2011; Joodaki & Panzer, 2018). A recent study reported stiffness levels of the different layers of the human skin *in vivo*. They measured the Young's modulus of the forearm of healthy volunteers: epidermis (~4 MPa), dermis (40 kPa), and hypodermis (15 kPa) (Feng et al., 2022). This indicates that there are mechanical differences across the main layers of the skin.

During development, mechanical cues are not evenly distributed across the forming epidermis. Recent studies have shown that anisotropic tissue deformations, like growth rate and morphological changes, induce stretching and crowding in the basal cell layer. These events coordinate polarity alignment and produce different cell geometries and tension levels along the planar axis of the epidermis (Aw et al., 2016).

While adherens junctions are found throughout the epidermis, they are thought to be in a distinct, high-tension state in granular cells. Adherens junctions are mechanosensitive structures that couple intercellular junctions to the cytoskeleton (le Duc et al., 2010). They become engaged under tension, which is thought to involve conformation changes in the adaptor protein a-catenin, allowing increased association with vinculin and potentially other actin-binding proteins (Yonemura et al., 2010). In SG2 cells, there are increased levels of cortical F-actin, suggesting higher stiffness. Consistently, vinculin, a-18 (an antibody that recognizes a mechanosensitive conformation of a-catenin) (Yonemura et al., 2010), as well as phosphorylated myosin light chain

were high in granular cells, indicating increased actomyosin contractility in these layers (Rubsam et al., 2017). Engagement of these adherens junctions and generation of intercellular tension is mediated by E-cadherin and is required for proper barrier function (Tunggal et al., 2005). E-cadherin also plays a key role in regulating the polarized localization and activation of EGFR, which restricts TJ formation to the SG2 layer, thus allowing the assembly of a functional epidermal barrier (Rubsam et al., 2017).

Depletion of MyoIIA and B in mouse epidermis resulted in reduced tension and severe defects in TJ barrier function *in vivo* (Sumigray et al., 2011). Further, this work demonstrated that microtubules, which become strongly associated with the cell cortex in granular cells (Lechler & Fuchs, 2007), recruit myosin- II to the cell cortex resulting in adherens junction engagement, which promotes proper TJ function (Sumigray et al., 2011). Accordingly, loss of Lis1, which is required for microtubule reorganization to the cell cortex in differentiated keratinocytes, resulted in loss of both cortical microtubules and of tight junction barrier activity, leading to perinatal lethality in mice (Lechler & Fuchs, 2007; Sumigray et al., 2011). These studies suggest that high cytoskeletal tension within the granular layers is necessary for epidermal barrier formation.

A recent study explored the tension levels in stratified epithelia using atomic force microscopy in the mouse back skin epidermis of a wild-type E18.5 embryo. Interestingly, with the help of antibody staining to differentiate epidermal layers, they found that granular layers were four times stiffer than basal layers (Fiore et al., 2020), confirming that granular cells are physically under higher tension than layers underneath.

Overall, previously mentioned studies suggest that tight control of contractility may be important for many aspects of epidermal biology. Accordingly, when contractility was increased in differentiated cells of the epidermis (through genetic mechanisms), there were dramatic consequences. These included both cell-autonomous effects on adhesions as well as non-cell autonomous effects on the proliferation, motility, and cell fates of underlying progenitor cells

(Ning et al., 2021). These data highlight the importance of spatially controlled regulation of contractility within a tissue (Prado-Mantilla & Lechler, 2023b).

1.2 Overview of epidermal development

In mice, epidermal development starts at embryonic day (E) 8.5, when the K8/K18-expressing surface ectoderm starts expressing a transcription factor crucial for epidermal lineage specification, p63 (Mills et al., 1999; Yang et al., 1999). By E9.5, K8/18 is replaced by K5/K14, marking the event called epidermal commitment, and giving rise to the epidermal basal layer (Byrne et al., 1994; Jackson et al., 1981). At this point, epidermal cells are a simple polarized epithelium and have a free apical surface, a hallmark of simple epithelia. Then, the periderm, a specialized cell population composed of polarized cells with tight junctions, covers the surface of the epidermis, starting shortly after its commitment.

Epidermal stratification defines the process in which the epidermis transitions from a monolayer to a stratified multilayered epithelium that functions as a barrier. This process in mice begins at E14.5 when basal cells start dividing perpendicularly to the underlying basement membrane and give rise to the first layer of K10-expressing differentiated cells, nominated intermediate cells (Terry Lechler & Elaine Fuchs, 2005; Smart, 1970). Intermediate cells are located between the basal layer and the periderm and are a transient cell population that exists only for 1 to 2 days. These differentiated cells are still capable of proliferating without attachment to the basement membrane, unlike later differentiated epidermal cells. By E16.5, suprabasal layers are composed of spinous cells and granular cells. A day before birth, at E18.5, a cornified layer of terminally differentiated keratinocytes that functions as an epidermal barrier is already present (DuBrul, 1972) (Figure 1.2). The periderm, which provides an anti-adhesive coating for the developing epidermis, is replaced as the fully differentiated and dying squames of the cornified envelope are initially produced. Consistently, in the absence of periderm, there are fusions of digits and within the palate (Richardson et al., 2014).

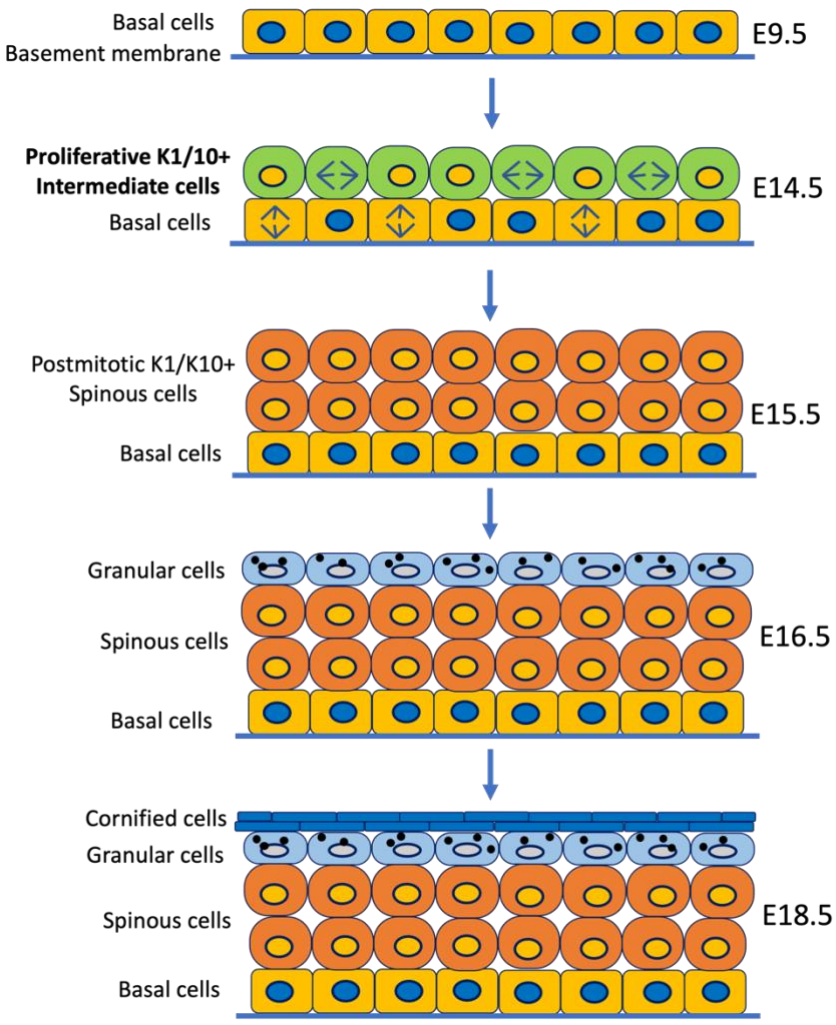

Figure 1.2: Diagram depicting the currently established model of epidermal stratification during development

The current model of epidermal development proposes that intermediate cells first differentiate into spinous cells, then into granular cells, and finally into terminally differentiated corneocyte cells.

1.3 Signaling pathways and transcription factors governing epidermal development

Multiple signaling pathways play significant roles in regulating epidermal development during epidermal fate commitment, inducing epidermal stratification and commitment to terminal differentiation. After gastrulation, the ectoderm can give rise to either the neuroectoderm, which gives rise to the nervous system, or the surface ectoderm, which gives rise to the epidermis and its

appendages. The decision between epidermal or neural commitment depends on a balance of different signaling pathways like Wnt, bone morphogenetic proteins (BMPs), and fibroblast growth factors (FGF). In the absence of Wnt signaling, the ectoderm responds to FGFs and inhibits BMP signaling, and the ectodermal cells acquire a neural fate. However, Wnt signaling blocks the ectoderm from responding to FGF, resulting in the expression of BMPs, and ectodermal progenitor cells adopt epidermal fate. The K8/18 expressing cells in the surface ectoderm will later become the epidermis (Fuchs, 2007). In the following sections, I will focus on the signaling pathways and important transcription factors involved in epidermal development.

1.3.1 Epidermal Fate Commitment

The hallmark of epidermal fate commitment is the replacement of K8/18 for K5/14 in the surface ectoderm, signaling that these cells are becoming basal keratinocytes. Involved in this process is the transcription factor p63, family of the tumor suppressor p53, a master regulator of proliferation and differentiation. p63 expression begins between E8.5 and E9.5, shortly before K5/14 appearance. p63 is critical for epidermal morphogenesis, as mice lacking p63 fail to develop epidermis and other epithelial tissues (Mills et al., 1999; Yang et al., 1999). Different p63 isoforms and their targets are implicated in initial epidermal fate commitment.

p63 can be expressed as multiple functional protein isoforms, including isoforms that contain the N-terminal transactivator domain (TAp63) or lack it (DNp63) (Yang et al., 1998). TAp63 is present during the early stages of epidermal development (Koster et al., 2006; Koster et al., 2004; Laurikkala et al., 2006) and is required for commitment to epidermal stratification by mediating K14 expression through AP-2γ (Koster et al., 2006). Even though DNp63 is mainly expressed in the later stages of epidermal development (Koster et al., 2004; Laurikkala et al., 2006), different reports suggest that DNp63 can directly induce K14 expression (Candi et al., 2006; Romano et al., 2007; Shalom-Feuerstein et al., 2011). In addition, p63-mediated expression of the desmosome component Perp is related to epidermal fate onset (Ihrie et al., 2005).

1.3.2 Early keratinocyte differentiation during Epidermal Stratification

Initiation of the epidermal stratification process is mediated by asymmetric cell divisions (ACD) of E14.5 basal cells to produce one basal and one suprabasal cell. In the absence of p63, apical localization of the spindle orientation machinery required to produce ACD does not occur, and epidermal stratification fails to occur (Terry Lechler & Elaine Fuchs, 2005). Some of the factors influencing ACD are discussed further in a later section. Equally important is the commitment of the cell placed away from the basement membrane to start undergoing the differentiation process to eventually die and form part of the epidermal barrier. At the heart of this decision-making process are p63 and the Notch signaling pathway. Several studies suggest that p63 is critical in maintaining the progenitor pool in different epithelia (Koster et al., 2004; Mills et al., 1999; Senoo et al., 2007; Yang et al., 1999), and for suppressing Notch-mediated keratinocyte differentiation (Nguyen et al., 2006; Rangarajan, 2001).

A clear sign of differentiation is the expression of K1/10 in keratinocytes, and later in epidermal development, cell-cycle exit is characteristic of differentiated keratinocytes. Apart from playing a role in regulating epithelial stemness, there is also evidence of p63's role in epidermal differentiation (Li et al., 2023). For example, DNp63 and Notch synergize to induce the differentiation marker K1 in cultured mouse keratinocytes (Nguyen et al., 2006), and knocking down DNp63 in neonate mice reduced K1 expression in the epidermis (Koster et al., 2007). Furthermore, IκB kinase-α (Ikkα), a DNp63 target gene, is the most abundant in the embryonic epidermis at E15.5, when spinous cells start to appear. Interestingly, knocking out Ikkα produced suprabasal layers that, although expressing K1, were BrdU positive at E16.5 (Koster et al., 2007). This suggests that Ikkα is necessary for cell-cycle exist of suprabasal cells, which normally occurs in post-mitotic spinous cells (Hu et al., 1999; Koster et al., 2007). Other factors important for cell cycle exist in suprabasal layers during epidermal development are Irf6 (Ingraham et al., 2006; Richardson et al., 2006) and Ovol1 (Nair et al., 2006). However, both

Ovol1 and Irf6 protein levels were already expressed in cycling intermediate cells (Dai et al., 1998; Knight et al., 2006).

A series of loss and gain of function studies *in vivo* were performed to understand the mechanism underlying the role in epidermal development. Upon ligand binding, the Notch receptor is cleaved, releasing its intracellular domain (NICD), which binds to the transcriptional repressor RBP-J, allowing the expression of target genes such as Hes and Hey (Lai, 2004). During development, Notch 1-3 are expressed in suprabasal layers (Powell et al., 1998). Inhibiting Notch signaling by conditionally ablating Notch1 and Notch2 or RBP-J in the developing epidermis resulted in a decreased number of K1-expressing suprabasal layers, including both spinous and granular layers (Blanpain et al., 2006; Moriyama et al., 2008). On the other hand, epidermal Notch activation through NICD overexpression resulted in extended spinous layers and impaired basal layers with reduced levels of K14 and integrin expression (Blanpain et al., 2006; Moriyama et al., 2008; Uyttendaele et al., 2004); while mice lacking Notch's target gene Hes1 presented expanded granular layers and few or no spinous cells. Thus, Notch signaling is able to both suppress basal cell fate and induce keratinocyte terminal differentiation in a mechanism independent of Hes1.

Notch signaling induces keratinocyte differentiation to granular fate through Ascl2; however, this can be repressed by Hes1 expression (Moriyama et al., 2008). Consistently, endogenous Hes1 expression is present in suprabasal cells starting at E14.5, and it stayed restricted to the first layers of spinous cells later in development (Blanpain et al., 2006; Moriyama et al., 2008). Therefore, Hes1 restricts premature terminal differentiation in the epidermis. Interestingly, Hes1 knockout did not alter p63 expression in suprabasal or basal layers at E14.5, while at E15.5, p63 was dramatically reduced in knockout mice compared to controls (Moriyama et al., 2008).

1.3.3 Terminal differentiation during epidermal development

Terminal keratinocyte differentiation implicates the adoption of granular cell fate, including lipid metabolism and secretion, followed by programmed cell death leading to cell cornification. Keratinocyte differentiation is largely regulated by an increase in extracellular Ca^{2+} concentration. Elevated Ca^{2+} in the exterior leads to an increase of intracellular free Ca^{2+}, creating an increasing epidermal Ca^{2+} gradient from basal to granular layers (Bikle et al., 1996; Menon et al., 1985; Sharpe et al., 1989). Keratinocytes can sense extracellular Ca^{2+} by the Ca^{2+} sensory receptor (CaSR), a member of the family C G-protein–coupled receptor that initiates intracellular responses. CaSR regulates Ca2+-mediated keratinocyte differentiation by activation of Rho GTPase, which facilitates actin remodeling (Tu et al., 2011; Tu & You, 2014). Ca2+ sensing also plays a key role in epidermal development. Epidermis-specific ablation of CaSR during development led to a loss of epidermal Ca2+ gradient, abnormal sphingolipid metabolism, decreased expression of terminal markers such as loricrin, filaggrin, and Tgm1, and delayed epidermal barrier formation (Tu et al., 2012).

A variety of transcription factors involved in the proper formation of a functional epidermal barrier have been reported. Grainyhead-like 3 (Grhl3) is an important transcription factor in keratinocyte terminal differentiation. Grhl3 is expressed in the epidermis during development, and it becomes restricted to the outermost differentiated layers at P0. Loss of function studies of Grhl3 revealed a decreased expression of cell adhesion molecules, lipid metabolic enzymes, structural and crosslinking proteins, like Tgm1, and defective epidermal barrier (Ting, Caddy, Hislop, et al., 2005; Yu et al., 2006). In addition, Grhl3-null mice exhibited defective lamellar bodies and altered lipid lamellae architecture (Ting, Caddy, Wilanowski, et al., 2005).

Another important factor for terminal differentiation in the developing epidermis is the receptor-interacting protein kinase 4 (RIPK4), a member of the RIPK/serine-threonine kinase

family, which functions as a downstream target of different signaling pathways (Holland et al., 2002). Epidermis-specific loss of RIPK4 displayed delayed keratinocyte differentiation, although cornification was still present. Mutants also showed aberrant distribution of polar lipids, defective inside-out barrier, lack of the tight junction claudin-1, and decreased F-actin (Urwyler-Rösselet et al., 2018). Therefore, RIPK4 is important for proper cortical actin localization and normal lipid organization for a functional epidermal barrier (De Groote et al., 2015; Urwyler-Rösselet et al., 2018).

Catalytically inactive RIPK4 displays similar epidermal defects to those observed in epidermis lacking IRF6 (Ingraham et al., 2006; Richardson et al., 2006). Loss of the kinase domain of RIPK4 showed proliferative suprabasal layers, a lack of non-polar lipid lamellar membranes, and reduced different classes of lipids. Similarly, IRF6 epidermal knockout mice had reduced expression of genes involved in lipid metabolism and tight junction formation (N. Oberbeck et al., 2019). This is congruent with biochemical and genetic assays demonstrating that RIPK4 directly phosphorylates IRF6, resulting in the expression of previously identified major transcriptional factors important for keratinocyte differentiation like Grhl3 and Ovol 1 (Kwa et al., 2014; Nina Oberbeck et al., 2019). Thus, the RIPK4-IRF6 signaling axis is essential for epidermal differentiation and proper epidermal barrier function, in part by mediating the regulation of transcriptional programs important for the lipidic composition of the stratum corneum (Flora & Ezhkova, 2020).

A knockout model of the transcription factor COUP-TF-interacting protein 1 (CTIP1) showed aberrant epidermal differentiation, reduced lamellar bodies, and altered lipid composition. This data was supported by the demonstration that CTIP1 binds to promoter regions of Fosl2, a differentiation-associated gene, and Fatty acid elongase 4 (Elvol4), a lipid metabolism related gene. Interestingly, CTIP1 was mainly restricted to the basal layers during development, except at E14.5, when it was also expressed in some suprabasal layers (Li et al., 2017). This data

suggests that CTIP1 might play a role in barrier formation by predisposing progeny to eventually terminally differentiate. Other factors described as relevant for epidermal barrier formation include Gata3, Klf4 and Fosl2 (de Guzman Strong et al., 2006; Segre et al., 1999; Wurm et al., 2015).

However, the aspects that allow the formation of a functional epidermal barrier on time to protect a newborn and prevent dehydration is still unclear. My dissertation work focuses on understanding the role of molecular and mechanical factors that play a role in terminal differentiation in the epidermis. Here, I uncovered that intermediate cells do not mature into spinous cells as previously believed. Instead, intermediate cells are granular precursors. My data suggests that mechanical cues might be playing a role in this direct transition from intermediate to granular cell fate. In addition, I developed an *in vivo* tool that allows inducible degradation of GFP-tagged proteins in a tissue-specific manner. This is a promising tool that could be used to study previously challenging-to-target cell populations, such as intermediate cells.

1.4 Author contributions

Parts of this chapter are from the Review "Polarity in skin development and cancer" by Alexandra Prado and Terry Lecher (Prado-Mantilla & Lechler, 2023b).

2 Molecular and Mechanical Signatures Contributing to Epidermal Differentiation and Barrier Formation

2.1 Introduction

Development of many tissues is characterized by rapid proliferation coupled with morphogenesis and differentiation. This process often uses specialized and transient cell types that are not found in homeostatic tissue, necessitating distinct pathways for differentiation (Singh & Tiwari, 2023). During the embryonic development of the epidermis, an initial single layer of progenitor cells gives rise to a multi-layered and differentiated tissue that acts as a chemical and mechanical barrier at birth (Moreci & Lechler, 2020; Sumigray & Lechler, 2015). This process begins at embryonic day (E) 14.5 in the mouse back skin when basal progenitor cells start to give rise to a suprabasal cell layer of intermediate cells (Damen et al., 2021; T. Lechler & E. Fuchs, 2005; Smart, 1970). Subsequently, basal cells divide to generate spinous cells, which are post-mitotic. These cells then further differentiate into granular cells, the last living cell types in the epidermis which are integral to forming the epidermal barrier. Intermediate cells are a transient cell type that expresses differentiation markers like Keratin 1 and 10 but remain mitotically active (Weiss & Zelickson, 1975). At this time point, the proliferation rate of intermediate cells is comparable to basal cells, suggesting that they are a significant contributor to tissue expansion (Damen et al., 2021; Smart, 1970). These cells lack basement membrane attachment, and thus, they proliferate in a tissue environment that is normally quiescent in the adult. Currently, we do not understand if they play functional roles outside of proliferation, their cell fate trajectory, or how they compare to later generated spinous cells at a molecular level. Further, we lack specific markers for intermediate cells despite recent scRNA-Seq data that has characterized the transcriptomes of these cells (Jacob et al., 2023). Generation of intermediate cells is transient (E14-15.5), and by E16.5, basal cells give rise to post-mitotic spinous cells (Figure 1.2). It is not known whether this switch in progeny type is driven by intrinsic changes in basal progenitors,

changes in signals from the surrounding periderm, and/or by systemic signals like circulating factors or amniotic fluid (Huebner et al., 2012).

In addition to chemical cues, mechanical information is assessed by cells and can instruct proliferation and differentiation decisions (Vining & Mooney, 2017). This has been most clearly demonstrated by substrates of differential elasticity/stiffness eliciting altered differentiation pathways in mesenchymal stem cells (Engler et al., 2006). Whether intra-tissue mechanical information is also instructive in differentiation has not been as thoroughly addressed. That said, in many tissues, differentiation can lead to changes in contractility and or stiffness. For example, in the epidermis, there is increased contractility in the granular cell layer, and this contractility is important for the formation of tight junctions in this cell layer (Miroshnikova et al., 2018; Rubsam et al., 2017; Sumigray et al., 2012a). While this flow of information from transcriptome to contractility has largely been assumed to be unidirectional, some works have demonstrated bidirectional interactions (Le et al., 2016; Meyer-ter-Vehn et al., 2006). When physical linkages between the cytoskeleton and nucleus were removed, there was a premature differentiation of keratinocytes and this was hypothesized to involve alterations in the transcription of the epidermal differentiation complex (EDC), a genetic locus that undergoes a change in localization in response to differentiation (Carley et al., 2021). Further, increased contractility in differentiated cells of the epidermis results in a non-cell autonomous effect on proliferation of their progenitors (Ning et al., 2021). However, we lack clear evidence that contractility can directly affect differentiation in the epidermis.

Here, we used bulk sequencing to characterize intermediate and spinous cell transcriptomes with great depth, as well as their progenitors. We defined markers that are specific for intermediate and spinous cells and showed marked transcriptomic differences in the basal cell progenitors that give rise to these distinct cell types. Further, our data demonstrate that intermediate cells express many genes associated with granular cells – a cell type that emerges

days later and is responsible for secreting lipids that constitute part of the epidermal barrier. Rather than moving through a spinous state, as has long been assumed (Koster & Roop, 2005), intermediate cells appear to directly transition to granular cells. Intermediate cells also show similarity to granular cells in having increased apparent actomyosin contractility. Using genetic models to induce contractility in spinous cells, we demonstrate that contractility is sufficient to induce a granular-like state. Together this work reveals the lineage pathways and the influences of contractility on epidermal barrier formation.

2.2 Results

2.2.1 Transcriptomic analysis of embryonic epidermal differentiation

During early epidermal stratification at E14.5, intermediate cells (ICs) are the first layer of suprabasal cells that express the differentiation marker keratin 10 (K10) and proliferate at a rate similar to basal cells (Figure 2.1A, B) (Damen et al., 2021; Smart, 1970). The proliferation rate of suprabasal cells decreases over the next 48 hours, and these cells are largely postmitotic by E16.5 (Figure 2.1A, B). To further validate these suprabasal cell dynamics during epidermal stratification, we performed live imaging of back skin explants from K10-rtTA; TRE-H2B-GFP embryos, which express H2B-GFP in K10-positive suprabasal cells. Consistent with data from fixed embryos, we observed numerous suprabasal mitotic events in explants collected from E14.5 embryos, while suprabasal cells in explants from E16.5 embryos were mitotically inactive (Figure 2.2). All divisions visualized were planar to the epithelium.

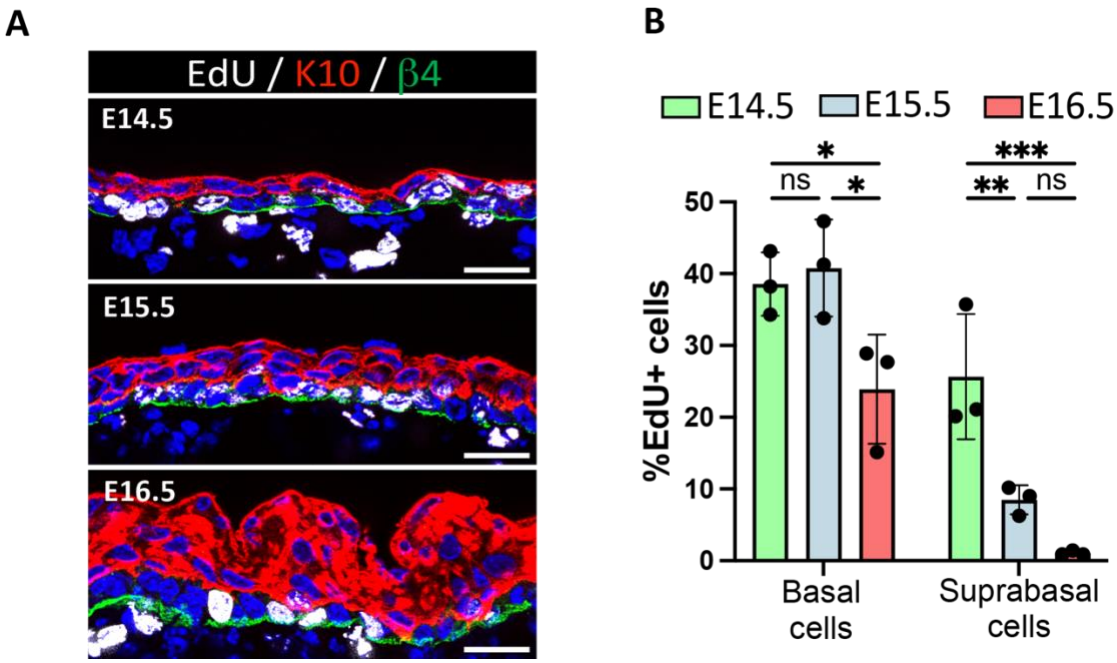

Figure 2.1: Proliferation of basal and suprabasal cells in early epidermal stratification

A) Image of EdU staining of proliferative cells in white. Immunofluorescence of suprabasal cells marked was labeled with K10 in red and the basement membrane, with b4 in green. Scale bars, 20 μm.
(B) Quantification of the percentage of EdU+ cells in the basal and the first two layers of suprabasal cells at E14.5, E15.5 and E16.5. Total number of mice analyzed was three mice per time point. Data are presented as mean ± standard deviation (SD). ANOVA,*: $p < 0.5$, ***: $p < 0.001$.

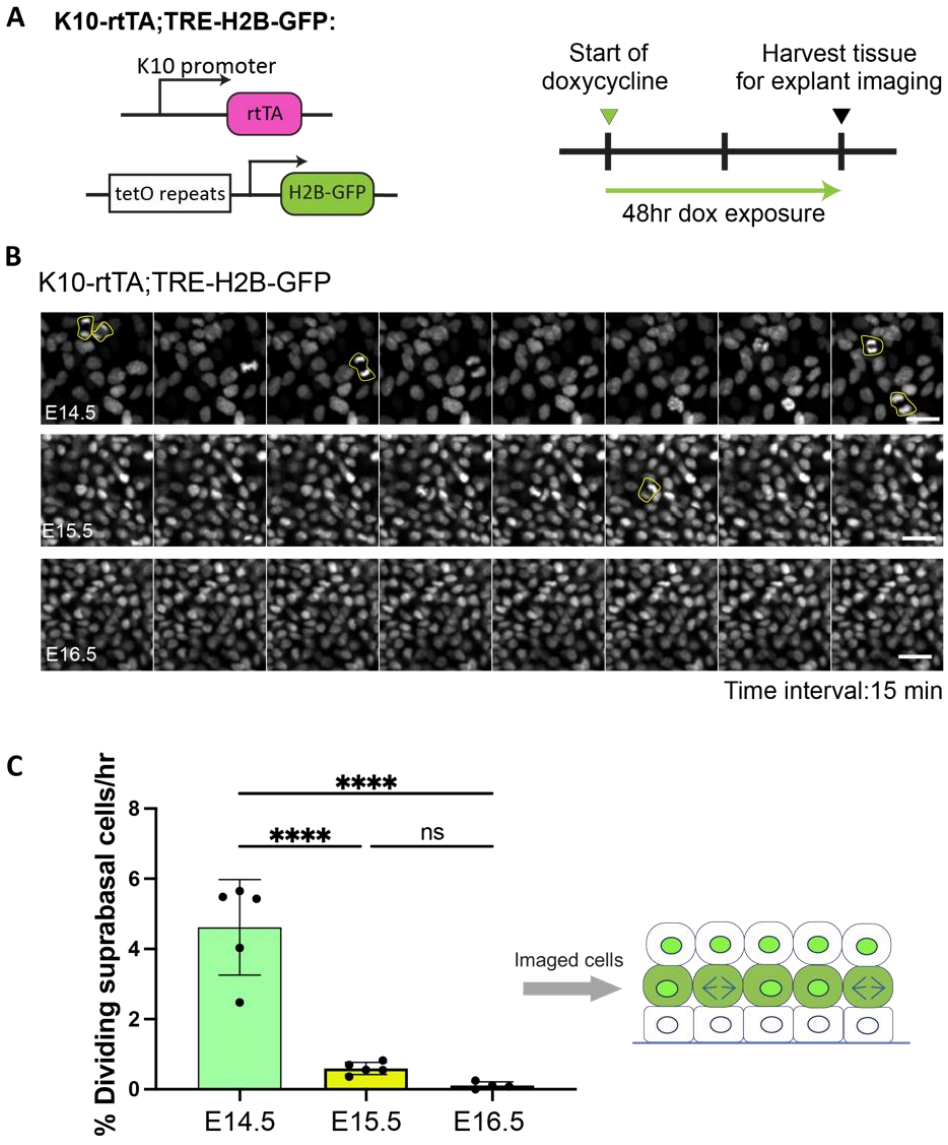

Figure 2.2: Live imaging of mitotic suprabasal cells during early epidermal stratification

(A) Diagram depicting alleles used for live imaging of suprabasal cells, and the timeline for doxycycline treatment.
(B) Snapshots from live imaging of back skin explants from E14.5, E15.5 and E16.5 K10-rtTA;Tre-H2B-GFP embryos, which express H2B-GFP in suprabasal cells. Images are from the first plane of H2B-GFP+ cells, corresponding to the suprabasal layer immediately on top of basal cells from E14.5, E15.5 and E16.5 explants. Time interval between snapshots: 15min.
(C) Percentage of mitotic events counted during 2hrs of live imaging. Only suprabasal cells from layers on top of basal cells were quantified. n=quantifications from at least 4 different fields from explants at each time point.

To understand the differences between suprabasal cells at E14.5 and E16.5, we explored the transcriptomic changes occurring between these two time points. We used K14-RFP;K10-rtTA;TRE-H2B-GFP mice and FACS to purify H2B-GFP$^+$ suprabasal cells and RFP$^+$ basal cells at E14.5 and E16.5 and performed bulk RNA sequencing of each of these cell populations (Figure 2.3A). Given that granular cells also form part of the suprabasal compartment at E16.5, we excluded the more superficial cells that bind *Ulex europaeus* agglutinin I lectin from E16.5 samples in order to uniquely compare suprabasal cells that lie immediately above the basal layer (ICs and spinous cells) (Brabec et al., 1980).

Principal component analysis (PCA) of the sequenced cell populations revealed that biological replicates grouped together and that samples were segregated by cell type (basal vs suprabasal) in the first component, and by age in the second component (E14.5 vs. E16.5). Notably, ICs at E14.5 and spinous cells at E16.5 were not clustered together, indicating that they are distinct populations, as are their corresponding basal cells (Figure 2.3B). Though not addressed further in this manuscript, the developmental transition in suprabasal cells from E14.5 to E16.5 may reflect the very different states of basal cells at these time points.

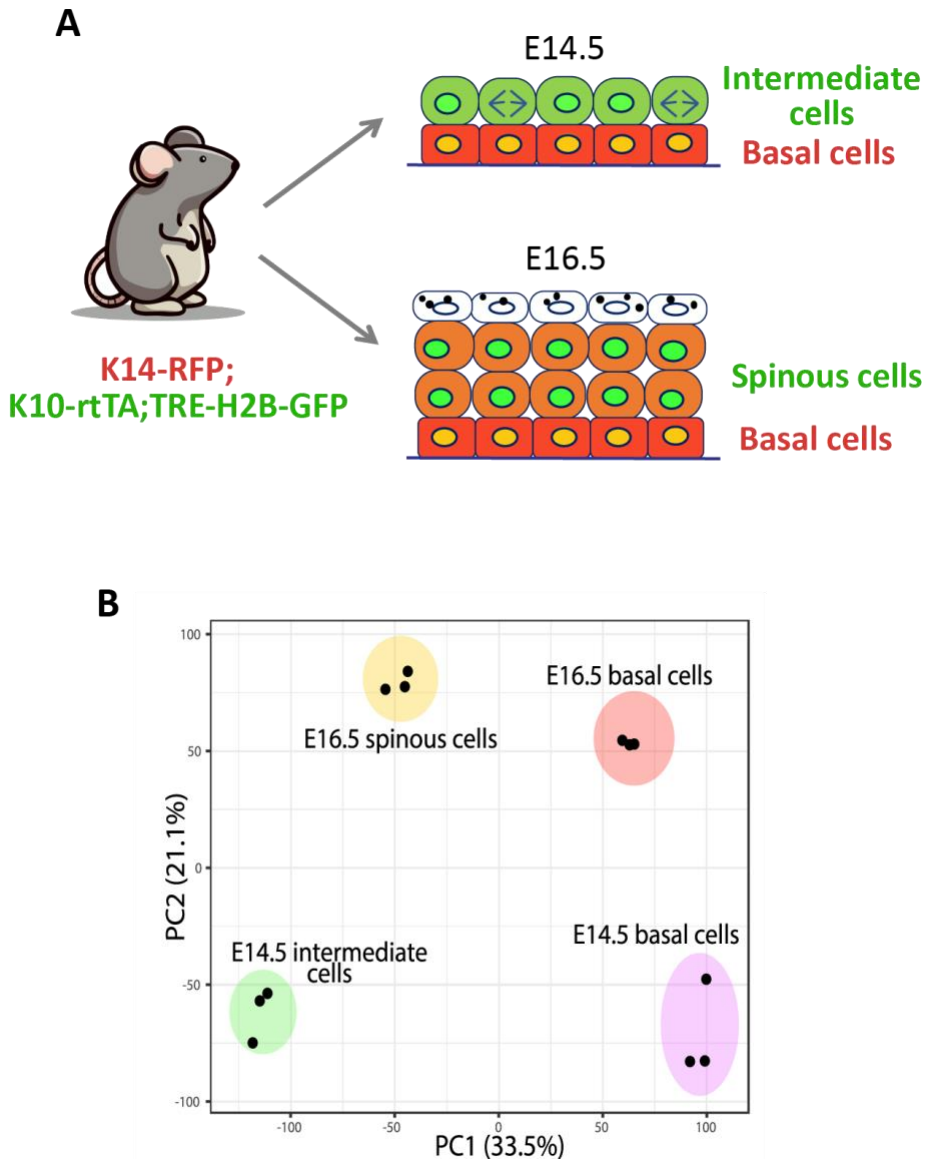

Figure 2.3: Transcriptomic analysis of embryonic epidermal cell populations

(A) Schematic showing basal and suprabasal cell populations collected for RNA sequencing: K14-RFP;K10-rtTA;TreH2B-GFP pregnant dams were all fed with doxycycline at E12.5, and then sacrificed at either E14.5 or E16.5. The E14.5 intermediate cells (Krt10GFP+;K14-RFP-), E16.5 spinous cells (Krt10GFP+;K14RFP-), and basal cells at E14.5 and E16.5 (Krt10GFP-;K14RFP+) cells were collected separately and sent for RNA sequencing.
(B) Principal component analysis of all four cell populations (n=3 embryos/cell population).

To identify specific molecular markers for ICs and spinous cells, we filtered the genes that were uniquely enriched in ICs (at E14.5 compared to both E16.5 spinous cells and E14.5 basal cells) and in spinous cells (compared to both E14.5 ICs and E16.5 basal cells). The IC gene

signature consisted of 610 genes and included Scara5, a scavenger receptor, St8sia6, which encodes a sialyltransferase enzyme, and Tgm1 (transglutaminase 1), an enzyme involved in covalent cross-linking of proteins (Figure 2.4A). To validate these candidates, we performed RNAScope and detected mRNA of Scara5 and St8sia6 in ICs but not in suprabasal cells at E16.5 (Figure 2.4B-E). It is worthwhile to note that Scara5 expression was specific to ICs, while St8sia6 mRNA was also present in granular cells at E16.5 (Figure 2.4B, C). This was also reflected in the presence of Loricrin and St8sia6 protein in the granular layers at E16.5 by antibody staining; however, we did not detect their fluorescence signal in ICs at E14.5 (Figure 2.5). This suggests that some granular genes are transcriptionally enriched in ICs but not yet appreciably expressed at the protein level. On the contrary, we found Tgm1 protein expression in intermediate cells, as described in more detail below (Figure 2.11).

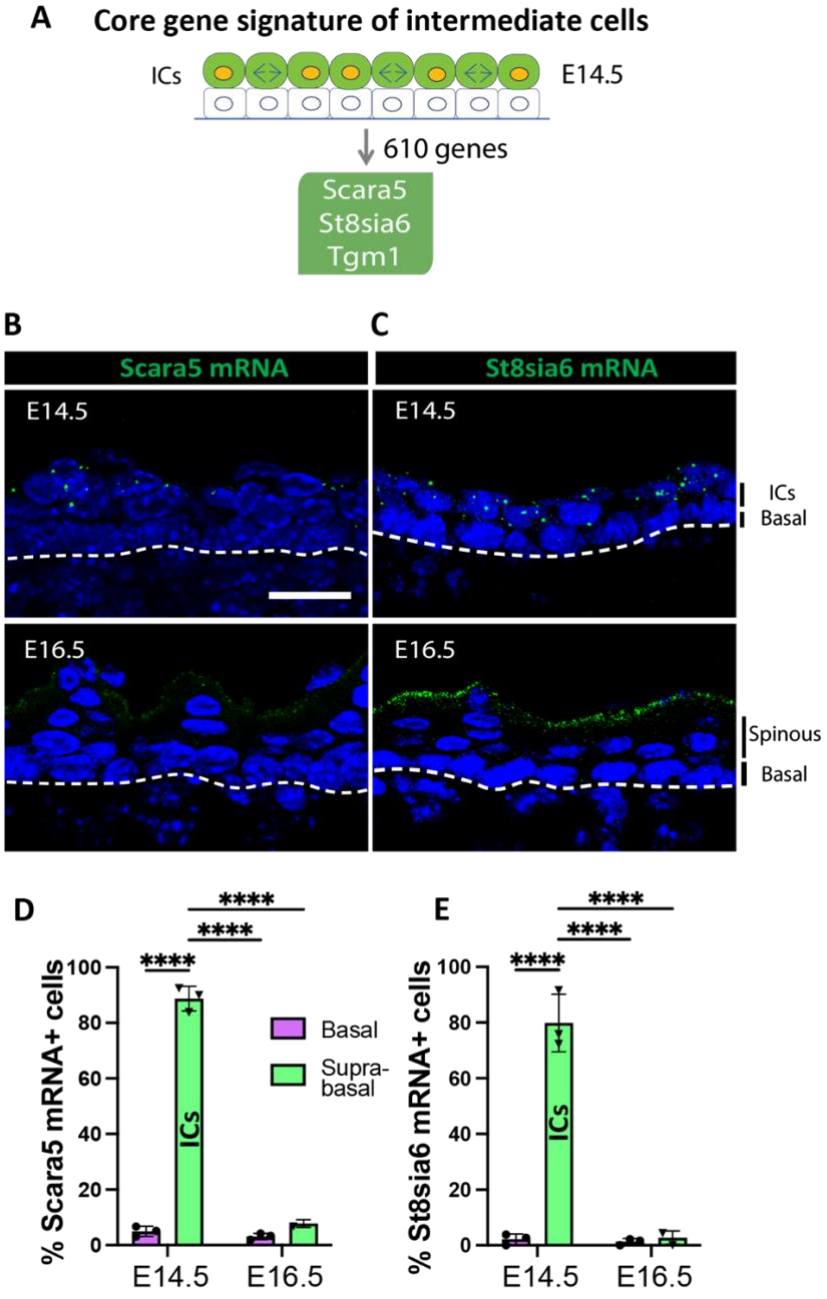

Figure 2.4: Identifying markers for intermediate cells

(A) The core gene signature of intermediate cells was obtained from the list of genes only upregulated in ICs (log2fold>1, p< 0.05; as compared with both basal cells at E14.5 and spinous cells at E16.5). Total genes in the IC signature were 610. From this list, Scara5 and St8sia6 were two of the most highly upregulated genes compared to spinous cells at E16.5.
(B and C) RNAscope of Scara5 (B) and St8sia6 (C) in WT embryos at E14.5 and E16.5. Basement membrane is indicated as a dotted line. Scale bar, 20 μm.
(D and E) Quantification of the percentage of Scara5+ (C) and St8sia6+ (D) basal and suprabasal cells at E14.5 and E16.5. Total number of mice analyzed was three mice per time point. Data are presented as the mean ± SD. **: $p < 0.01$, ***: $p < 0.001$, ANOVA.

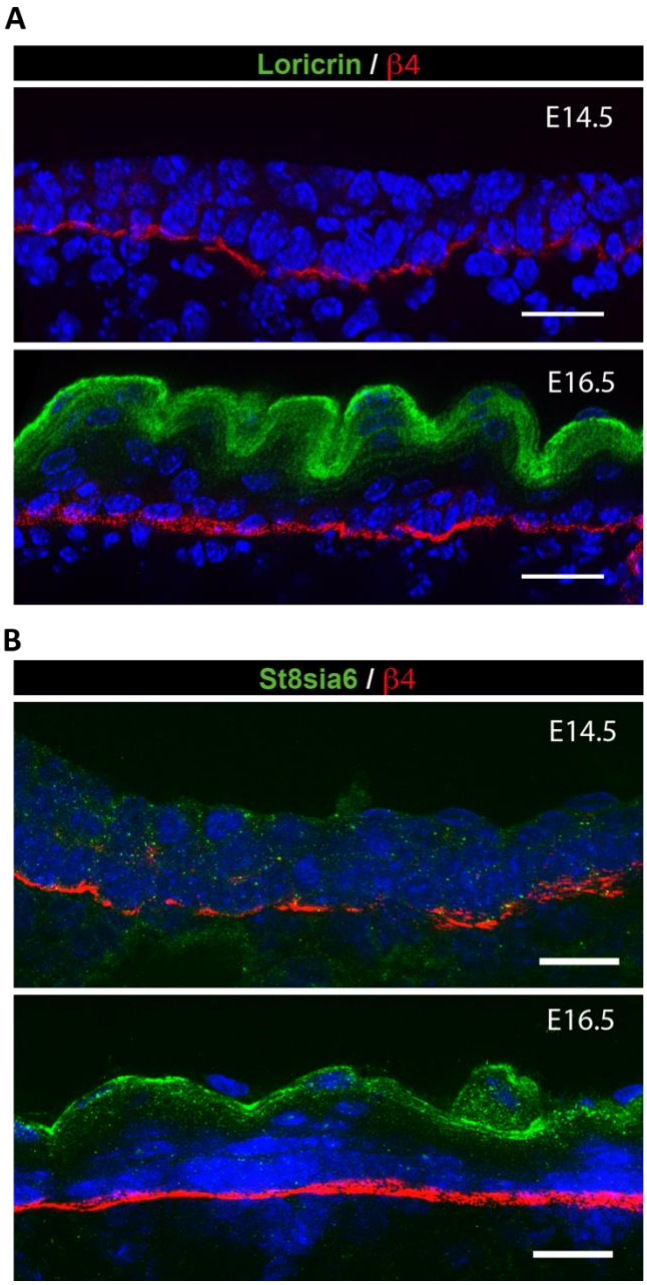

Figure 2.5: Intermediate cells do not express some granular markers at the protein level

(A and B) Immunofluorescence staining of Loricrin(A) or St8sia6 (B) in green labeling granular cells at E16.5 but not in intermediate cells at E14.5. Basement membrane is marked with β4 in red. Images representative of at least two animals per time point. Scale bars, 20 μm.

There were 163 genes whose transcripts were specifically upregulated in spinous cells at E16.5 (Figure 2.6A). Among this list, the transcription factor MafB was a prominent candidate since it has been implicated in epidermal differentiation in cultured human epidermal cells (Lopez-Pajares et al., 2015), and it is expressed in suprabasal cells *in vivo* during development (Miyai et al., 2016b). Consistent with our transcriptional data, immunofluorescence staining of MafB at E16.5 revealed that it was present in the first suprabasal cell layers in the epidermis but was excluded from granular cells (Figure 2.6B, D), and it was undetectable in ICs at E14.5. Another highly upregulated gene in this list, *Ptgs1*, that encodes the enzyme Cox1, was also observed to be enriched in spinous cells but not in ICs at the protein level (Figure 2.6C, E). Therefore, MafB and Cox1 are specific markers for spinous cells in the embryonic epidermis.

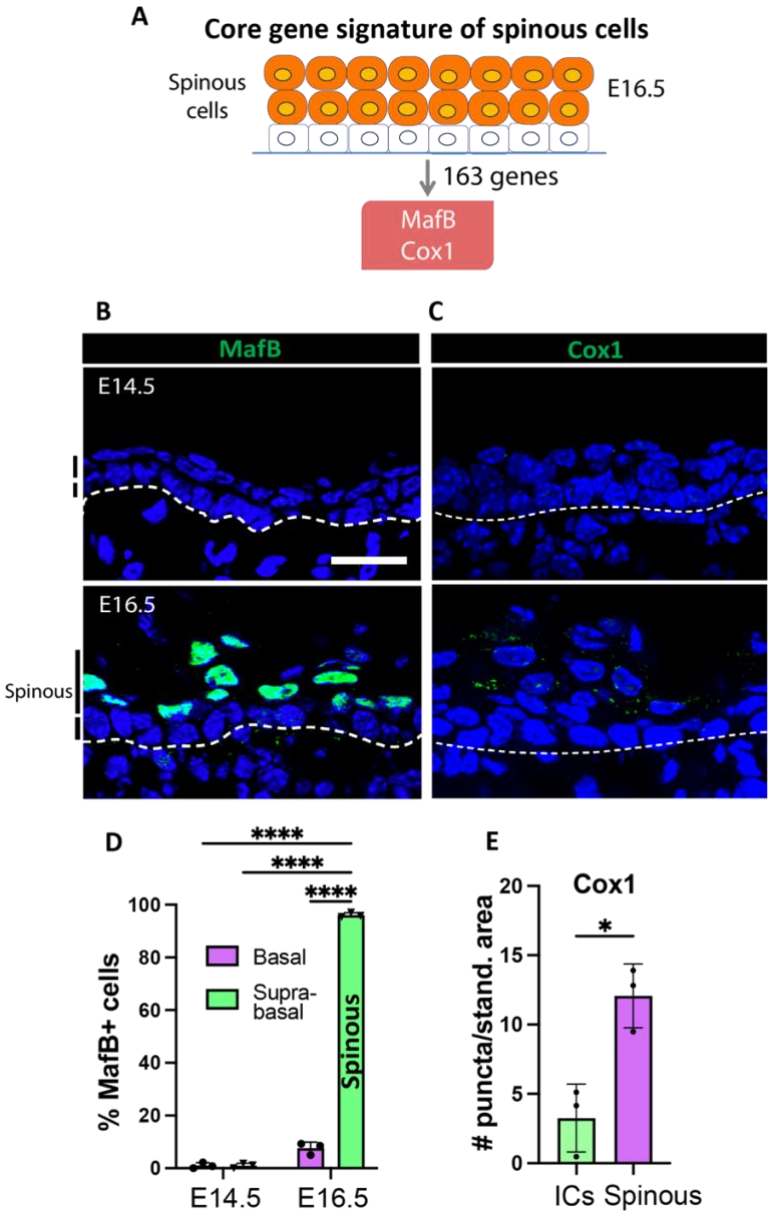

Figure 2.6: Identifying markers for spinous cells

(A) The core gene signature of spinous cells was obtained from the list of genes only upregulated in spinous cells (log2fold > 1, $p < 0.05$ compared with both basal cells at E16.5 and intermediate cells at E14.5). Total genes in the spinous cell signature were 163.
(B and C) Immunofluorescence staining of MafB (B) and Cox1 (C) in WT embryos at E14.5 and E16.5. Basement membrane is indicated as a dotted line. Scale bars, 20 μm.
(D) Quantification of the percentage of MafB+ (B) basal and suprabasal cells at E14.5 and E16.5. Total number of mice analyzed was three mice per time point. Data are presented as the mean ± SD. ****: $p < 0.0001$, ANOVA.
(C) Quantification of Cox1 puncta/standardized area in intermediate cells was compared to the first two layers of spinous cells at E16.5. Total number of mice analyzed was three mice per time point. Data are presented as the mean. *: $p < 0.05$, two-tailed unpaired t-test.

2.2.2 MafB inhibits proliferation of intermediate cells

To test the functional role of Maf transcription factors in determining spinous cell fate, we prematurely induced MafB expression in ICs. For this, we collected K10-rtTA;TRE-MafB-HA (here after called K10-MafB) embryos that were collected at E14.5, when suprabasal cells are ICs (Figure 2.7A). In these embryos, MafB-HA was expressed in about 30% of all suprabasal cells (Figure 2.7B). Examination of EdU incorporation revealed that HA+ cells had a significantly lower rate of incorporation than ICs in controls, demonstrating that MafB expression is sufficient to decrease cell proliferation (Figure 2.7C, D). Notably, however, we found that there was increased proliferation of surrounding MafB-negative cells in mutant embryos (Figure 2.7C, D); while the overall suprabasal proliferation rate was not significantly different in mutants vs controls (Figure 2.7E). This suggests a potential homeostatic mechanism for maintaining total proliferation during the epidermal stratification process.

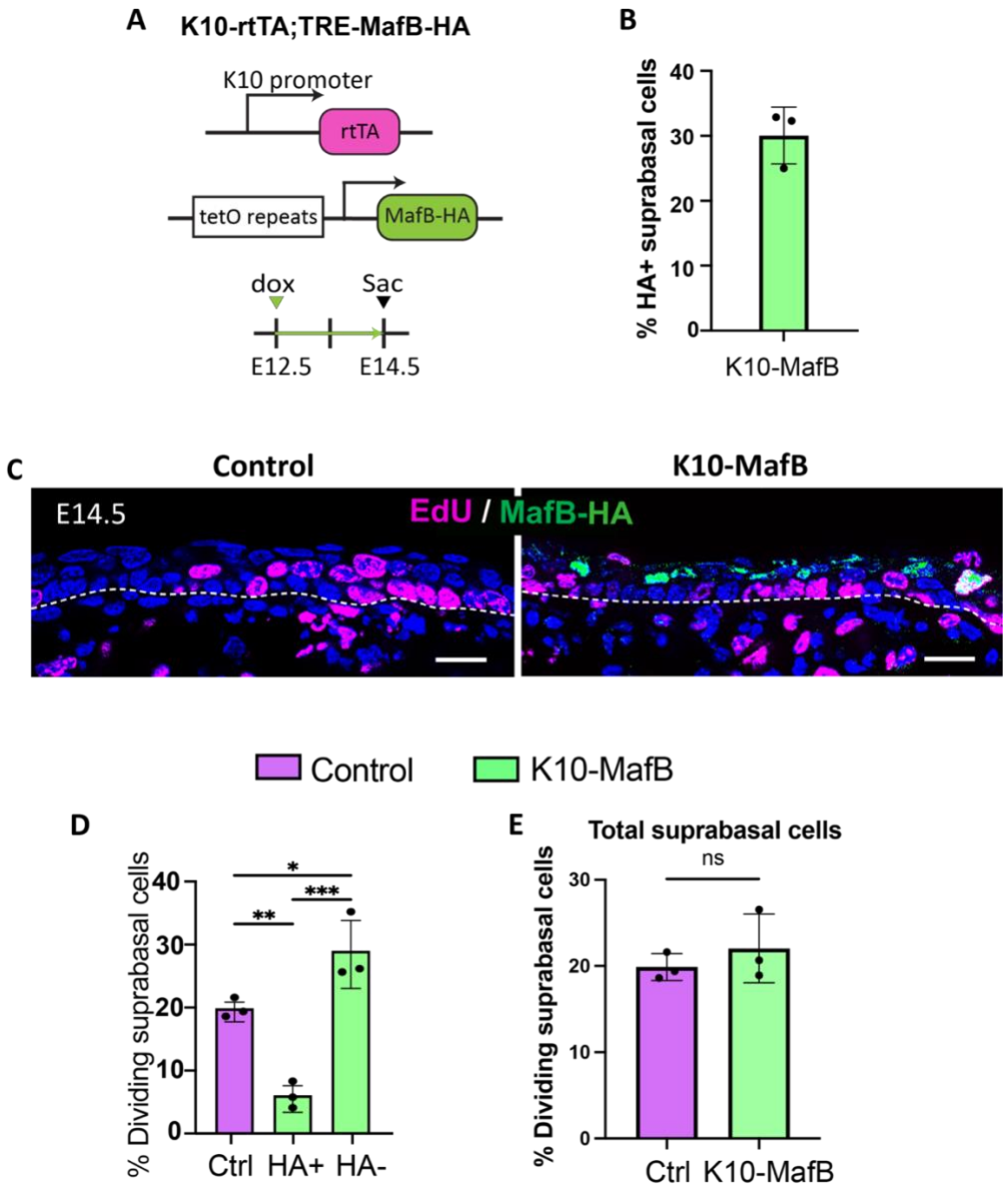

Figure 2.7: Mis-expression of MafB in intermediate cells is sufficient to decrease proliferation

(A) Diagram depicting alleles used to induce MAFB expression in intermediate cells. Pregnant K10rtTA;Tre-MafB-HA mice were fed with doxycycline chow at E12.5 and sacrificed at E14.5.
(B) Percentage of suprabasal cells expressing MafB (HA+) in K10-MafB mice at E14.5.
(C) Image of EdU staining (magenta) and MafB expressing ICs immunolabeled with HA (green) in K10-rtTA;Tre-MafB and control mice at E14.5. Scale bars, 20 μm.
(D) Percentage of dividing suprabasal cells (EdU+) in control, and HA+ and HA- cells in K10-MafB mice at E14.5 (n=3 embryos/genotype). Data are presented as the mean ± SD. *: $p < 0.05$, **: $p < 0.01$, ***: $p < 0.001$, ANOVA.
(E) Overall percentage of dividing cells among all suprabasal cells at E14.5 in K10-MafB vs controls is not significantly different.

To determine whether MafB expression was sufficient to repress IC-specific gene expression, we examined IC markers, including Tgm1 and Scara5. While we found a decrease in the levels of Tgm1 protein (Figure 2.8A, D,), Scara5 mRNA levels were unchanged (Figure 2.8B, E). These data demonstrate that MafB may repress parts of the IC signature but does not globally repress all markers. Given that it altered the mitotic status of ICs into a spinous-like state, we also examined whether MafB expression was sufficient for the induction of spinous markers. However, we found that the spinous marker Cox1 was not induced by MafB (Figure 2.8C, F). Therefore, MafB is sufficient for some aspects of spinous fate (like loss of proliferation), but not for the expression of all spinous marker genes.

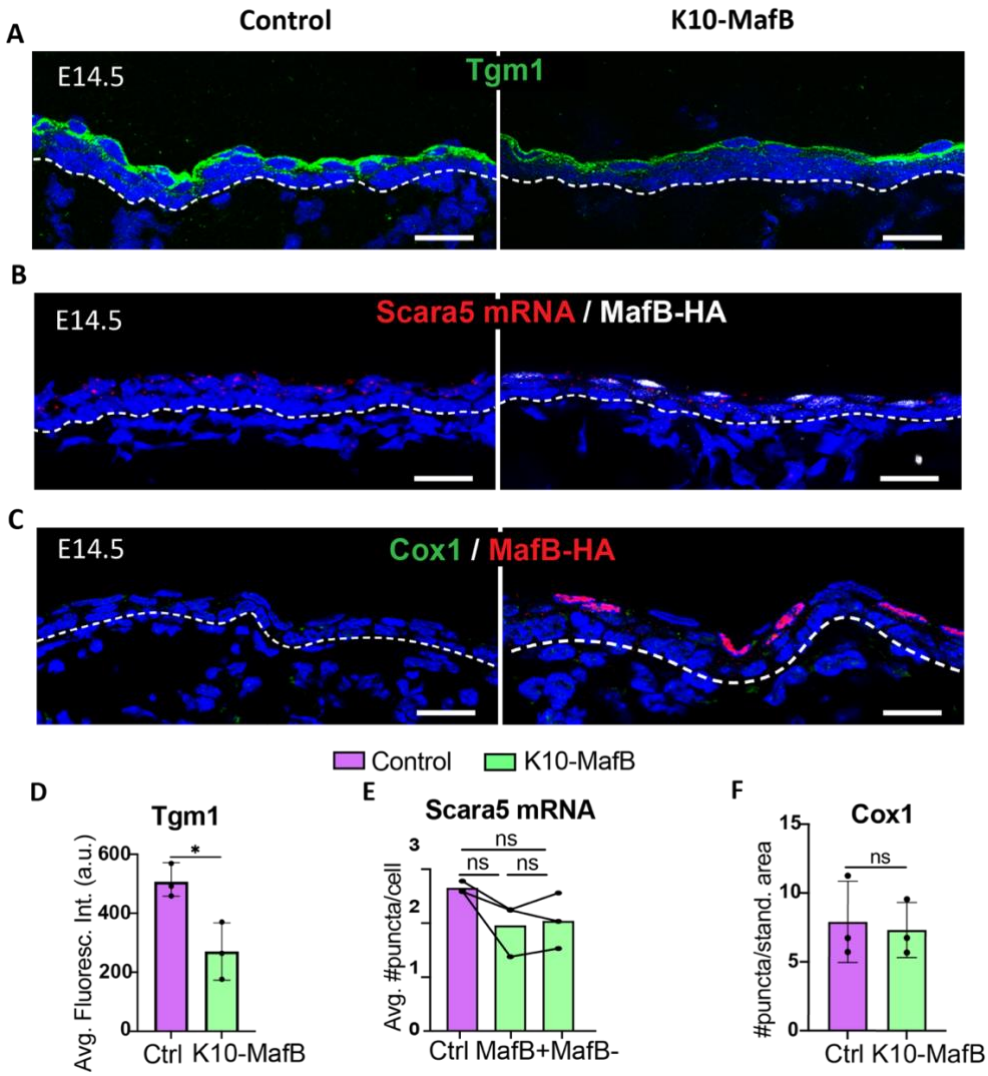

Figure 2.8: MafB induction is not sufficient for the expression of all spinous marker genes

(A) Immunofluorescence staining of reduced Tgm1 fluorescence in K10-MafB vs control mice at E14.5.
(B) RNAScope of Scara5 in red and immunostaining with MafB in white.
(C) Immunofluorescence staining of Cox1 in K10-MafB vs control mice at E14.5.
(D) Quantification of Tgm1 average fluorescence in suprabasal cells of control vs K10-MafB at E14.5 (n=3 embryos/genotype). Data are presented as the mean ± SD. *: $p < 0.05$, two-tailed unpaired t-test.
(E) Quantification of the average number of Scara5 RNAScope puncta per cell in suprabasal layers of control, and MafB+ and MafB- cells of K10-MafB mice at E14.5 (n=3 embryos/genotype). Data are presented as the mean. ns = not significant, ANOVA.
(F) Quantification of number of Cox1 puncta per standardized area of suprabasal layer in K10-MafB vs control mice at E14.5. (n=3 embryos/genotype). Data are presented as the mean. ns = not significant, two-tailed unpaired t-test.

2.2.3 Intermediate cells are granular cell precursors

Using the IC-specific gene signature we identified above; we turned to Gene Ontology (GO) analysis to determine biological pathways characteristic of these cells. Categories that were uniquely enriched in ICs at E14.5 included pathways involved in lipid metabolic processes and establishment of the skin barrier (Figure 2.9A). These pathways are hallmarks of granular cells, which produce and secrete lipids that contribute to the formation of the watertight cornified layer that acts as the epidermal barrier. These findings were unexpected since granular cells have not formed yet at E14.5. Comparing the IC gene signature to a granular gene signature that we generated from published data ((Matsui et al., 2021) GSE168011) revealed a striking overlap with over 1/3 of the genes in the IC signature also being part of the granular cell signature (Figure 2.9B). GO analysis of these shared genes revealed pathways such as keratinocyte differentiation, endomembrane system (reminiscent of lamellar bodies), and lipid processes (Figure 2.10A). Notably, both Grhl3 and Hopx, two transcription factors that control late epidermal differentiation were upregulated in both of these cell types (Chalmers et al., 2006; Chen et al., 2019; Obarzanek-Fojt et al., 2011; Ting, Caddy, Hislop, et al., 2005; Ting, Caddy, Wilanowski, et al., 2005; Yu et al., 2006).

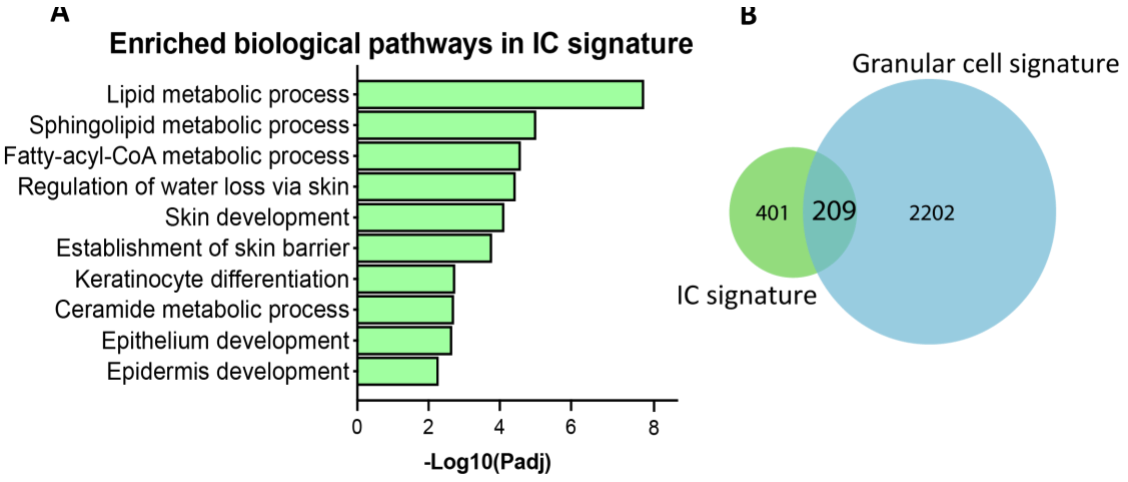

Figure 2.9: Intermediate cells are transcriptionally similar to granular cells

(A) Gene Ontology (GO) term enrichment analysis of genes in the intermediate cell signature.

(B) Venn diagram illustrating the number of genes in the intermediate cell signature compared with the granular signature (log2fold>1, $p < 0.05$) for each cell population. A total of 209 genes were commonly enriched in ICs and granular cells, which represents 34% of the total IC signature.

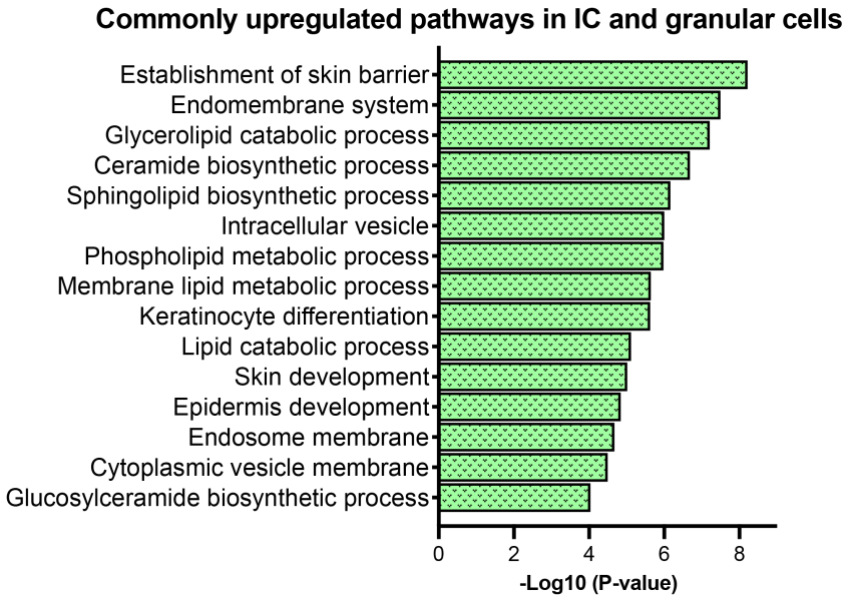

Figure 2.10: Intermediate and granular cells shared pathways

GO analysis from commonly enriched genes in intermediate and granular cell signatures show pathways related to lipid biosynthetic processes and endomembrane systems.

To validate the expression of canonical granular markers in ICs, we performed immunofluorescence staining of Tgm1 (Figure 2.11A, C), an enzyme that performs protein cross-linking of structural proteins for cornified envelope formation, and Abca12 (Figure 2.11B, D), which plays a role in transporting lipids into lamellar bodies and is disrupted in Harlequin Ichthyosis (Akiyama, 2010; Thomas et al., 2006). Both proteins were already expressed at the protein level in ICs, but not in spinous cells.

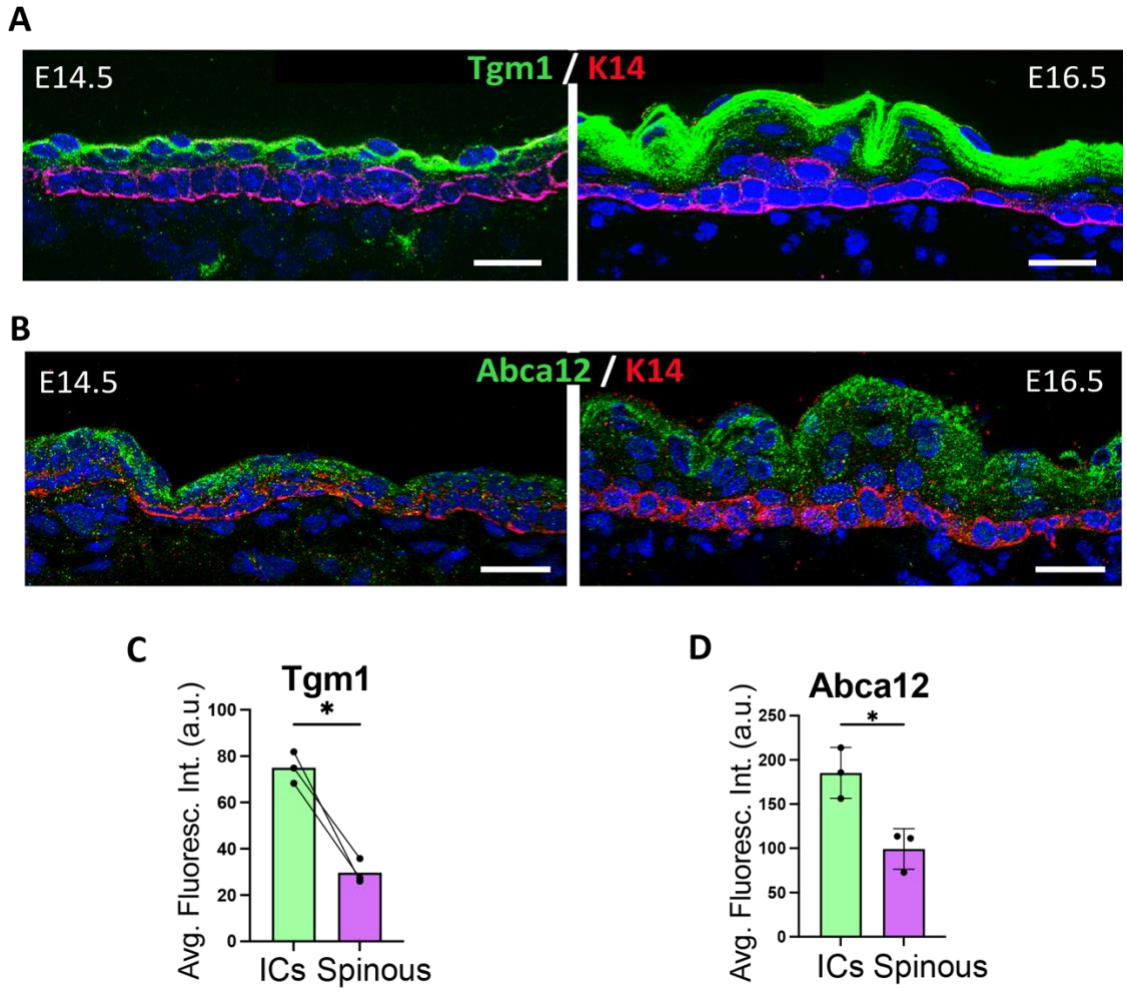

Figure 2.11: Intermediate cells express some granular markers

(A and B) Immunofluorescence staining of Tgm1 (A) and Abca12 (B) in green and K14 (red) to mark basal cells in WT embryos at E14.5 vs E16.5. Scale bars, 20 μm.
(C) Quantification of Tgm1 average fluorescence intensity at suprabasal cells at E14.5 (IC) vs the first two layers of suprabasal cells at E16.5 (spinous cells). Bar represents the mean. *$p < 0.05$, two-tailed paired t-test. Total number of mice analyzed was three mice per time point.
(D) Quantification of Abca12 average fluorescence intensity at suprabasal cells at E14.5 (ICs) vs the first two layers of suprabasal cells at E16.5 (spinous cells). Data are presented as the mean ± SD. *: $p < 0.05$, two-tailed unpaired t-test. Total number of mice analyzed was three mice per time point.

Together, these data suggested that in addition to promoting rapid amplification of keratinocytes, intermediate cells may serve as progenitors for the first granular cells that form during development. To test this hypothesis, we performed a pulse-chase experiment in K10-rtTA;TRE-H2B-GFP embryos by injecting a low dose of doxycycline to induce the expression of

H2B-GFP in K10-positive cells at E14.5 (i.e. only ICs) (Figure 2.13A). We followed the H2B-GFP+ cells over time, and we found that at E15.5, these cells were already more superficial, separated from basal cells by a layer of H2B-GFP negative cells (Figure 2.12A). Based on their expression of MafB, these cells are the first spinous cells produced (Figure 2.12A). Strikingly, about 95% of H2B-GFP+ cells did not stain for MafB (Figure 2.12D). Thus, rather than converting to a spinous cell fate, they are displaced upwards. When we chased these cells until E16.5, they were located in the uppermost layers of the epidermis (Figure 2.12B, E), and they co-stained with loricrin, a granular cell marker (Figure 2.13B). This indicates that most ICs transition into granular cells without going through a MafB+ state. When labeled cells were chased until E18.5, GFP signal was clearly present in the cornified layer, demonstrating that the traced ICs had terminally differentiated before birth (Figure 2.12C).

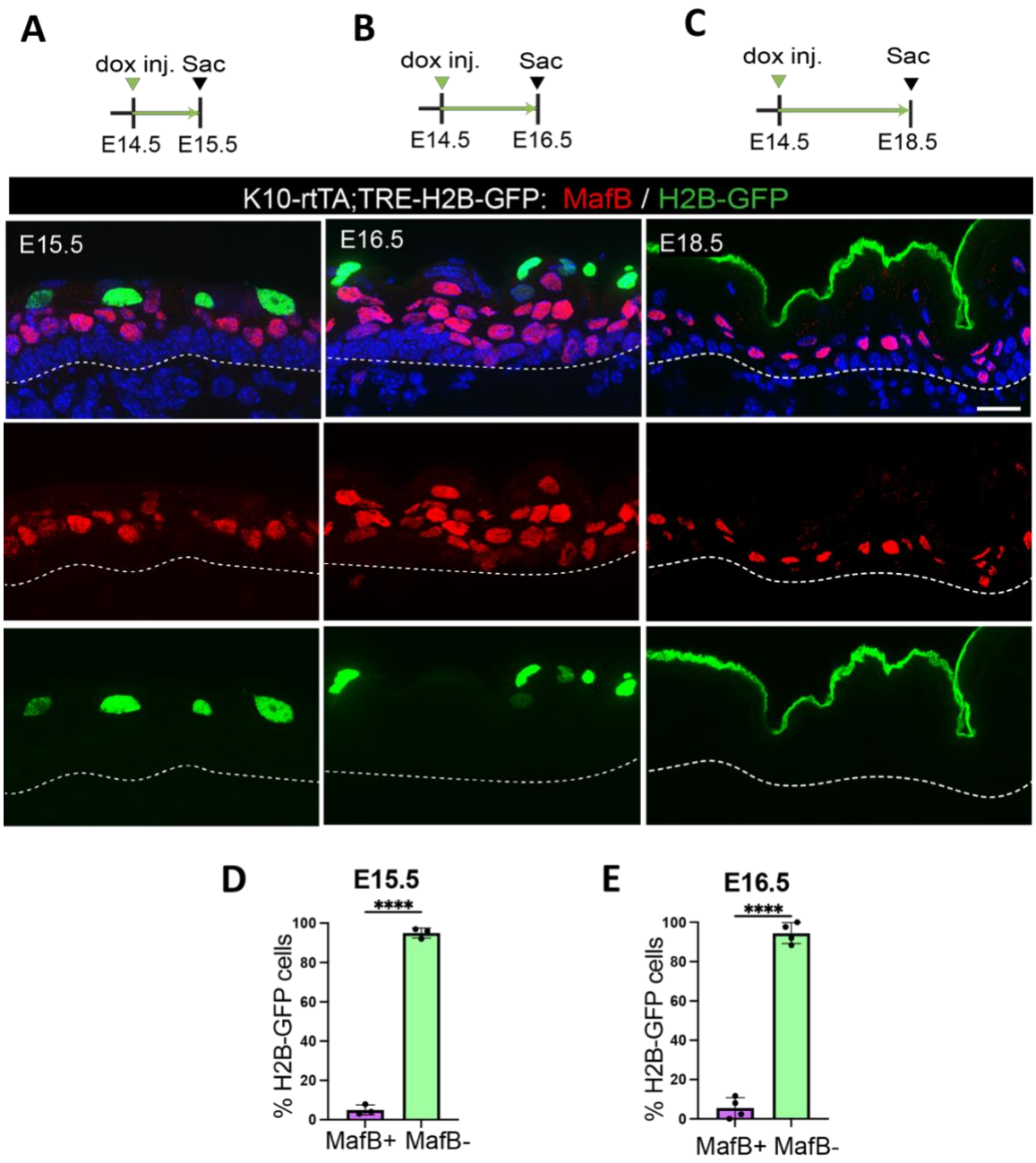

Figure 2.12: Intermediate cells do not differentiate into spinous cells

(A, B and C) Immunofluorescence staining of spinous cells with MafB in red and labeled cells with H2B-GFP from K10-rtTA;TRE-H2B-GFP mice that were injected with a low dose of doxycycline at E14.5 to label only ICs and sacrificed at E15.5 (A), E16.5 (B) or E18.5 (C).Basement membrane is indicated as a dotted line. Scale bars: 20 µm.
(D and E) Percentage of MafB+ and MafB-suprabasal cells expressing H2B-GFP at E15.5 (n= 3 embryos) (A) and E16.5 (n= 4 embryos) (B). Data are presented as the mean ± SD. ****: $p < 0.0001$, two-tailed unpaired t-test.

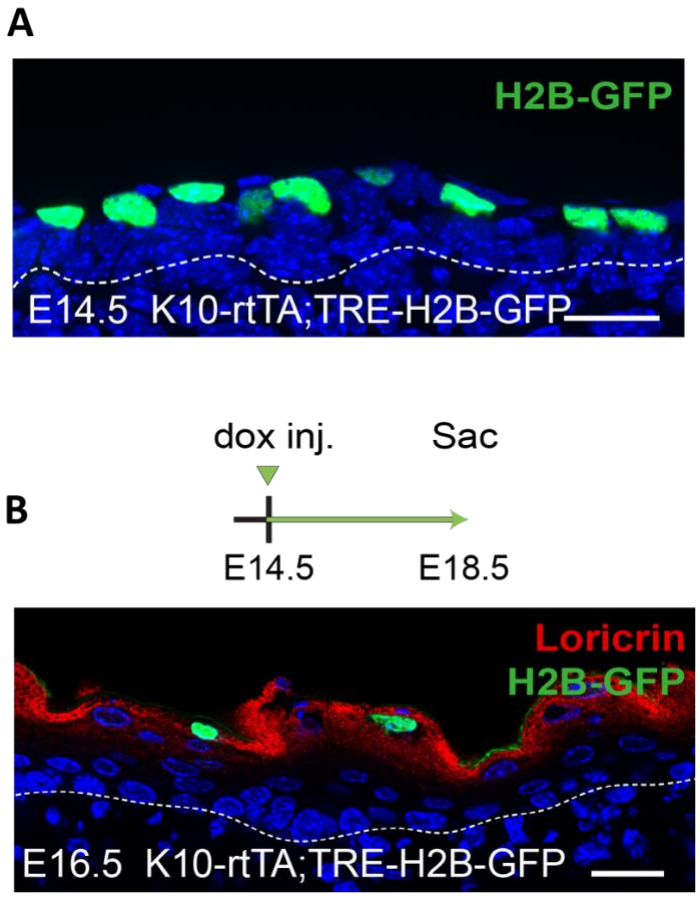

Figure 2.13: Intermediate cells differentiate into granular cells

(A) Image showing H2B-GFP expression in intermediate cells in a E14.5 K10-rtTA;TRE-H2B-GFP mouse fed with doxycycline from E12.5. Basement membrane is indicated as a dotted line. Scale bars: 20 μm.
(B) Immunofluorescence staining of Loricrin in red colocalizing with H2B-GFP labeled cells in K10-rtTA;TRE-H2B-GFP mice injected with a low dose of doxycycline at E14.5 and sacrificed at E16.5. Scale bars: 20 μm.

The above data suggest that the first spinous cells arise from basal cells and not from differentiation of ICs. To test this, we generated K14-rtTA;TRE-H2B-GFP mice and pulsed them with low levels of doxycycline at E14.5. With these conditions, we specifically labeled basal cells at E14.5 and followed their progeny. In embryos chased to E15.5, we observed that 80% of basal cells and 70% of all MafB+ cells were H2B-GFP+, demonstrating that most spinous cells arise from basal divisions (Figure 2.14). Altogether, these data demonstrate that most ICs are direct precursors for granular cells and do not pass through a MafB+ spinous intermediate.

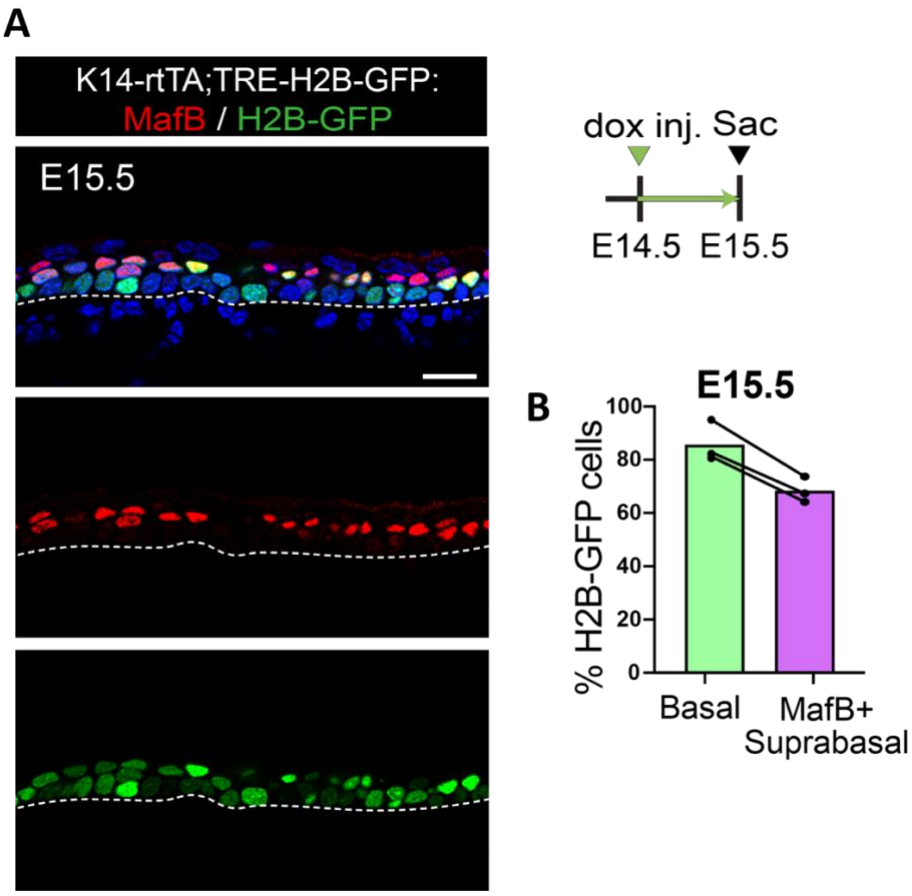

Figure 2.14: Most spinous cells arise from basal cells

(A) Immunofluorescence staining of spinous cells with MafB in red and labeled cells with H2B-GFP in K14rtTA;TreH2B-GFP mice that were injected with a low dose of doxycycline at E14.5 and sacrificed at E15.5.
(B) Percentage of basal cells and MafB+ suprabasal cells expressing H2B-GFP. Paired samples are quantifications from the same mouse (n=3 embryos).

2.2.4 Contractility status changes through epidermal development and is sufficient to drive aspects of granular cell fate

Further analysis of our RNA-Seq dataset suggested that intermediate cells may be mechanically as well as molecularly distinct from spinous cells. We examined the list of genes that were upregulated in ICs versus spinous cells, regardless of their expression levels in basal cells. GO term analysis revealed that regulation of cell morphogenesis and the actin cytoskeleton were among the most highly upregulated pathways in ICs (Figure 2.15A). Heat map analysis of

the contractome gene set (Zaidel-Bar et al., 2015), demonstrated clear differences in suprabasal cell expression at E14.5 and E16.5 (Figure 2.15B). To validate these findings, we stained for markers that indicate contractility status. We observed that F-actin levels were higher in basal and suprabasal cells at E14.5, as well as in granular cells at E16.5. However, they were low in spinous cells at this later time point (Figure 2.15C-C''). Myosin IIA, a major contributor to actomyosin contractility in the epidermis (Miroshnikova et al., 2018; Sumigray et al., 2012a), was also higher in ICs than spinous cells (Figure 2.15D-D''). Similarly, a18, an antibody that recognizes an epitope of a-catenin that is exposed when adherens junctions are under tension (Yonemura et al., 2010), was also higher in basal and suprabasal cells at E14.5 vs E16.5 (Figure 2.15E-E'').

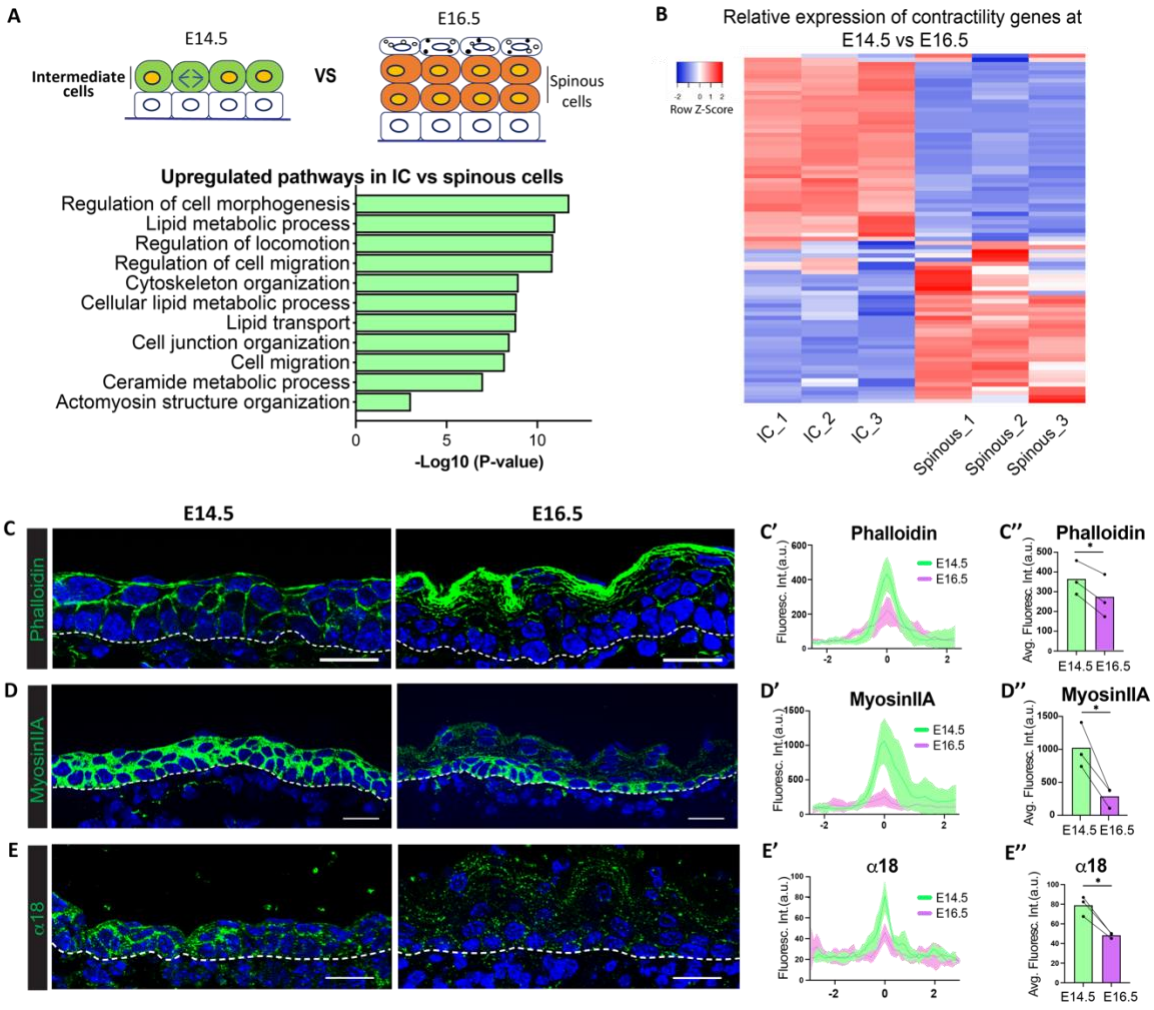

Figure 2.15: Intermediate cells show upregulation of contractility markers as compared to spinous cells

A) Diagram showing the cell populations compared to obtain the list of genes analyzed in (B and C).
(B) Gene Ontology (GO) term enrichment analysis of genes upregulated in intermediate cells vs spinous cells at E16.5, regardless of their expression in basal cells (log2fold>1, p< 0.05) reveals upregulation of biological processes related to cytoskeleton organization.
(C) RNA-Seq heatmap depicting differential expression of contractome genes in intermediate and spinous cells at E16.5. Gene expression by FPKM was log2-transformed.
(D, G and J) Immunofluorescence staining of Phalloidin (D), MyosinIIA (G) and alpha18 (J) in green at E14.5 vs E16.5. Scale bars, 20 μm.
(E, H and K) Fluorescence intensity of suprabasal-suprabasal cell boundaries in the first two layers of suprabasal cells. Line scans were performed in WT embryos at E14.5 (between intermediate cells) and E16.5 (between spinous cells). Line scan graphs show centered measurements across six cell-cell boundaries at each time point, data are presented as the mean ± SD.
(F, I and L) Quantification of average fluorescence intensity from the line scan maximum values at suprabasal-suprabasal cell boundaries in WT E14.5 and E16.5. For bar plots, bars represent the

mean, joined dots are paired samples from each time point. n= 3 embryos per time point, average maximum values of at least 15 line scans at suprabasal cell boundaries in each embryo were calculated. *p < 0.05, two-tailed paired t-test.

Furthermore, active nuclear YAP, a mechanoresponsive transcriptional co-activator, was present in ICs and granular cells at E16.5, but not in spinous cells. Similarly, the percentage of basal cells at E14.5 with active YAP was significantly higher than basal cells at E16.5 (Figure 2.16). Apart from its role in mechanotransduction, the active form of YAP is an important driver of proliferation in the basal layers of the epidermis (Aragona et al., 2020; Schlegelmilch et al., 2011; H. Zhang et al., 2011). To test a potential role of YAP in IC proliferation, we used K10-rtTA;TRE-Yap1^{S112A}-GFP (hereafter called K10-YAP^{CA}) mice to induce an active form of YAP, marked by H2B-GFP, in suprabasal cells at E16.5 (Figure 2.17A). Active YAP was not sufficient to induce proliferation in spinous cells; however, it resulted in a non-cell autonomous increase in proliferation of basal cells (Figure 2.17B).

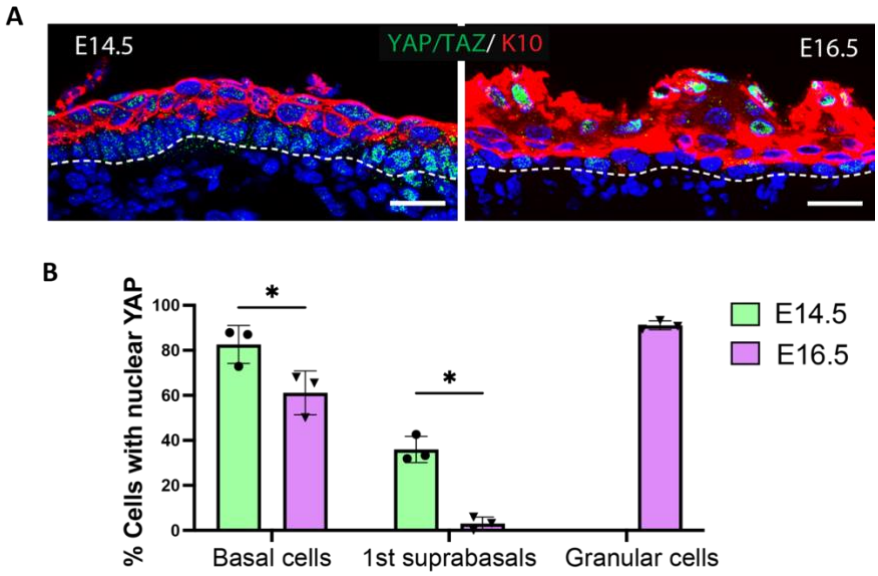

Figure 2.16: Like granular cells, more intermediate cells have nuclear YAP than spinous cells

(A) Immunofluorescence staining of YAP/TAZ at E14.5 and E16.5. Scale bars, 20 μm.
(B) Percentage of nuclear active YAP in basal cells and in the first two suprabasal layers at E14.5 and E16.5. Active YAP was also quantified in granular cells at E16.5. *:p < 0.05, multiple unpaired t-test. n= 3 embryos/time point.

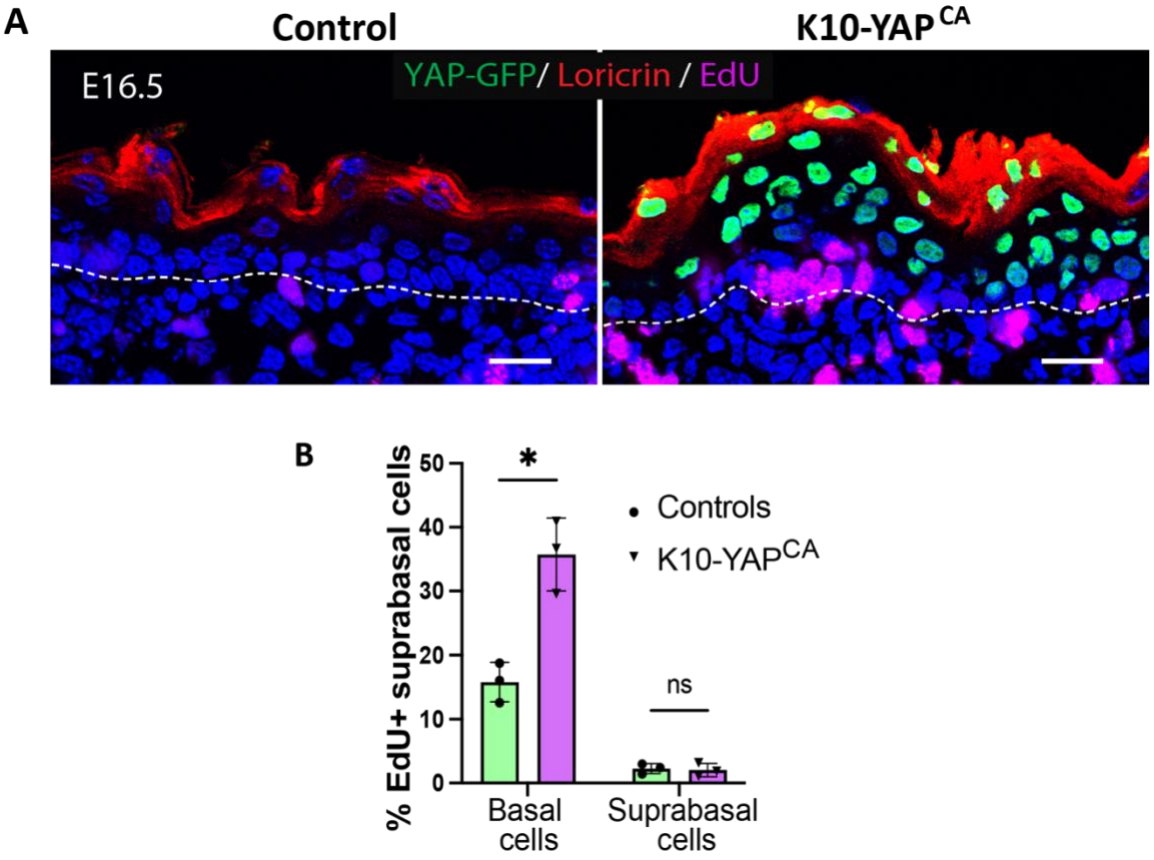

Figure 2.17: Inducing constituvely active YAP in spinous cells does not increase their proliferation

(A) Image of EdU staining in magenta and immunofluorescence of Loricrin in red from control and K10-YAPCA embryos at E16.5. Cells expressing constitutively active nuclear YAP are labeled with H2B-GFP in green. Mice were fed with doxycycline from E13.5. Scale bars: 20 μm. (B) Percentage of dividing suprabasal cells in control vs K10-YAPCA. n= 3 embryos/genotype. For all plots in this panel, cells located in the first two layers of suprabasal cells immediately above the basal layer were considered for quantification. *: $p < 0.05$, ns: not significant, two-tailed unpaired t-test.

The apparent changes in contractility through epidermal development raised the question of whether the shared contractility between ICs and granular cells lies downstream of differentiation, or if it contributes to their similar gene expression. To test the effects of heightened contractility in the suprabasal cells, we turned to mouse models we previously developed that allow doxycycline-induced actomyosin contractility: K10-rtTA; TRE-Spastin and

K10-rtTA, TRE-Arhgef11^{CA}, hereafter referred as K10-Spastin and K10-Arhgef11^{CA}, respectively (Hinnant et al., 2024; Muroyama & Lechler, 2017; Muroyama et al., 2018; Ning et al., 2021).In both cases this expression is confined to suprabasal cells. K10-Spastin expresses the active form of the microtubule severing protein Spastin which increases contractility (Ning et al., 2021); and K10-Arhgef11^{CA} induces expression of a constitutively active Rho-GEF that activates RhoA GTPase, a key positive regulator of actomyosin contractility (Ning et al., 2021).

We started by examining the transcriptomic changes that are induced by contractility (from K10-Spastin vs controls at E16.5, log2 fold change >=1; GEO: GSE158786) and compared it with the intermediate and granular cell signatures. Remarkably, we found that 47% of contractility-induced genes overlapped with the granular gene signature (Figure 2.18A)– demonstrating a major change in gene expression and differentiation state by intracellular contractility (hypergeometric test representation factor 3.4, $p=2X10^{-101}$). GO analysis revealed that the common signature was highly enriched in keratinocyte differentiation, cornified envelope, lamellar bodies and lipid processes – all hallmarks of granular cells (Figure 2.18C). When comparing with the IC signature, there was still significant overlap - 80 of the 610 genes in the IC signature (13%) were also found in the contractile signature, though less than that found in the granular cells (Figure 2.18B). These included the late epidermal differentiation transcriptional regulars Grhl3 and Hopx. The most enriched terms for the overlapping genes between ICs and the contractile gene signature were lipid processing and transport (Figure 2.18D). In addition, mainly lipid metabolic genes were upregulated in the shared ICs, granular cell, and contractility signatures (Figure 2.18E), suggesting that these were the pathways commonly upregulated in IC and granular cells as a consequence of contractility. Notably, many EDC genes were enriched in the contractile and granular signatures (30/61), but many fewer in the IC signature (5/61). This demonstrates specific differentiation pathways are enriched in ICs, while the contractile gene signature is much more similar to the full granular gene expression program.

In contrast to an upregulation of granular gene markers in hypercontractile skin, we noted that about 1/3 of all the spinous signature genes were downregulated in this mutant (55/163) genes, demonstrating a partial suppression of the spinous cell fate.

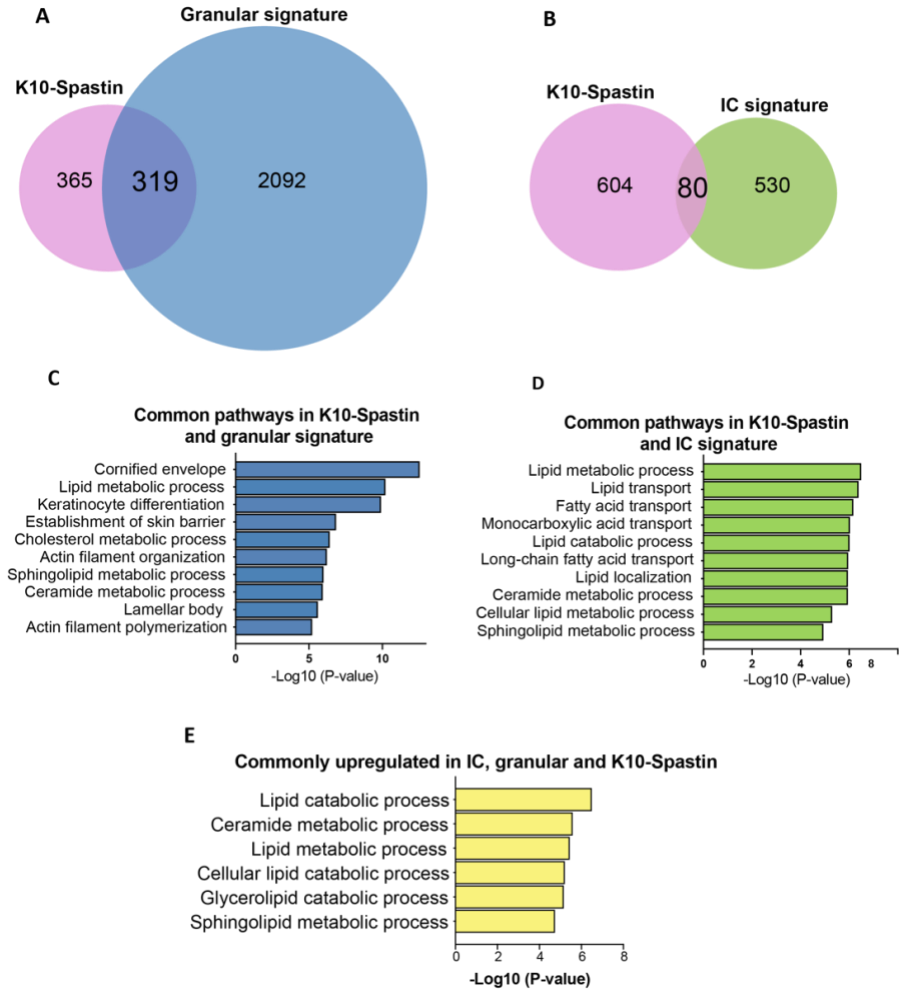

Figure 2.18: K10Spastin cells are more granular like than intermediate like

(A and B) Size proportional-Venn Diagrams depicting that K10Spastin cells are more granular-like (46.6% similarity) than intermediate-like (11.7% similarity). Pink: list of genes enriched in K10Spastin vs WT embryos at E16.5, blue: genes in granular signature, green: genes in intermediate cell signature.
(C and D) GO term analysis of the list of genes commonly upregulated in suprabasal K10-Spastin (vs control spinous cells at E16.5, log 2-fold > 1, $p < 0.05$) and granular cell signature (C) or intermediate cell signature (D).
(E) GO term analysis of genes commonly upregulated in ICs, granular cells and K10-Spastin (total: 50 genes) are lipid metabolic processes: lipid metabolic processes are commonly upregulated among K10Spastin, IC and granular.

We next examined the effects of increased contractility through analysis of specific markers for spinous cells we identified earlier in this study. We used both models of increased contractility in suprabasal cells: K10-Spastin and K10-Arhgef11^{CA}, where expression of the transgene for both is detectable by HA staining. In both mouse models, suprabasal cells with increased contractility (at E16.5 and later) did not express the spinous marker MafB (Figure 2.19A, C), even when they were positioned in the first layers on top of basal cells, where they should clearly be spinous cells. In contrast, these cells precociously expressed the granular marker Tgm1 (Figure 2.19B, D). Similar results were obtained in back and glabrous skin of K10-Arhgef11^{CA} adult mice (Figure 2.20), and at E17.5, when suprabasal contractility was induced after there were already spinous cells (Figure 2.21). These latter results suggest that the effects of increased suprabasal contractility are the same regardless of the time of its induction.

Analysis of the IC marker Scara5 revealed that increasing suprabasal contractility did not alter Scara5 mRNA levels in HA+ cells compared to controls; suggesting again that contractility induces a granular-like rather than intermediate-like cell type in mutant mice (Figure 2.19E).

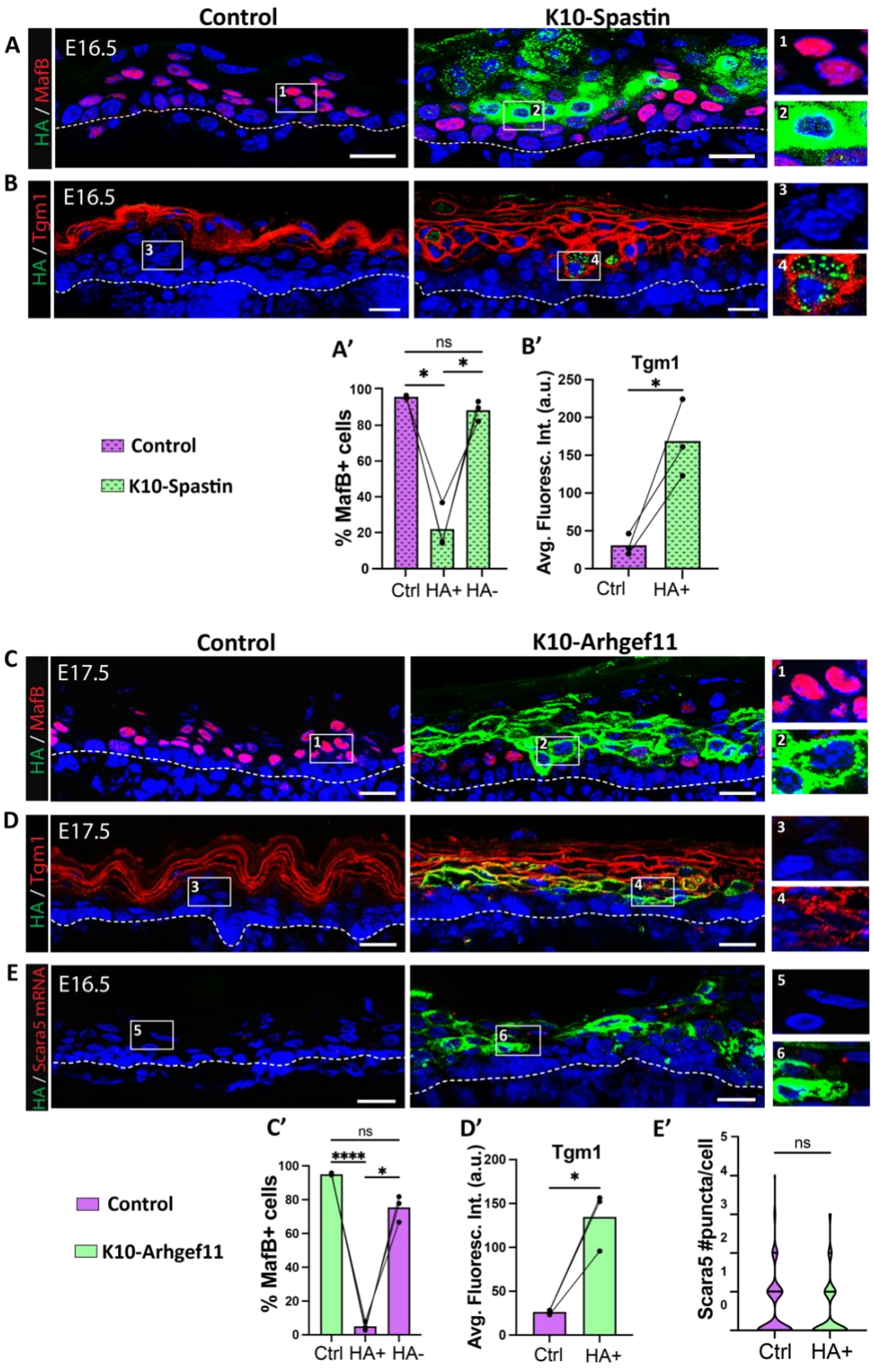
Control
K10-Spastin
A
E16.5
HA / MafB
B
E16.5
HA / Tgm1
A'
B'
Control
K10-Spastin
% MafB+ cells
Ctrl HA+ HA-
Tgm1
Avg. Fluoresc. Int. (a.u.)
Ctrl HA+
Control
K10-Arhgef11
C
E17.5
HA / MafB
D
E17.5
HA / Tgm1
E
E16.5
HA / Scara5 mRNA
C'
D'
E'
Scara5 #puncta/cell
ns

Figure 2.19: Increased contractility in spinous cells is sufficient to induce many granular genes

(A and B) Immunofluorescence staining of MafB (A) or Tgm1 (B) in red, and suprabasal cells expressing Spastin marked by HA (green) in K10-Spastin and controls. Images of E16.5 embryos, doxycycline fed starting at E14.5. Insets to the left of all images in this panel show close-ups of HA+ cells in suprabasal layers adjacent to basal cells. Scale bars: 20 μm.
(C and D) Immunofluorescence staining of MafB (C) or Tgm1 (D) in red, and suprabasal cells expressing Arhgef11^{CA} marked by HA (green) in K10-Arhgef11 and controls. Images of E17.5 embryos, doxycycline fed from E10.5. Scale bars: 20 μm.
(A' and C') Percentage of MafB+ suprabasal cells in controls, and in HA+ and HA-cells in K10-Spastin at E16.5 (C') or K10-Arhgef11^{CA} at E17.5 (E'). Total number of mice analyzed was three embryos per genotype. Data are presented as the mean ± SD. *: $p < 0.05$, ****: $p < 0.0001$, repeated-measures one-way ANOVA, Tukey's multiple comparisons test. For all plots in this panel, cells located in the first two layers of suprabasal cells immediately above the basal layer were considered for quantification.
(B' and D') Quantification of average fluorescence intensity of Tgm1 in suprabasal cells of control and HA+ cells in K10-Spastin at E16.5 (B') or K10-Arhgef at E17.5 (D'). Total number of mice analyzed was three embryos per genotype. *: $p < 0.05$, two-tailed paired t-test.
(E) RNAScope of *Scara5* in red and immunostaining with HA in green in control and K10-Arhgef11. Images of E16.5 embryos, doxycycline fed starting at E14.5. Scale bars: 20 μm. (E') Violin plot of number of Scara5 puncta per suprabasal cell in control, and HA+ cells and neighbor HA-cells in K10-Spastin at E16.5. n= 224 HA+ cells and 160 WT cells from 2 embryos per genotype. ns: not significant, two-tailed unpaired t-test.

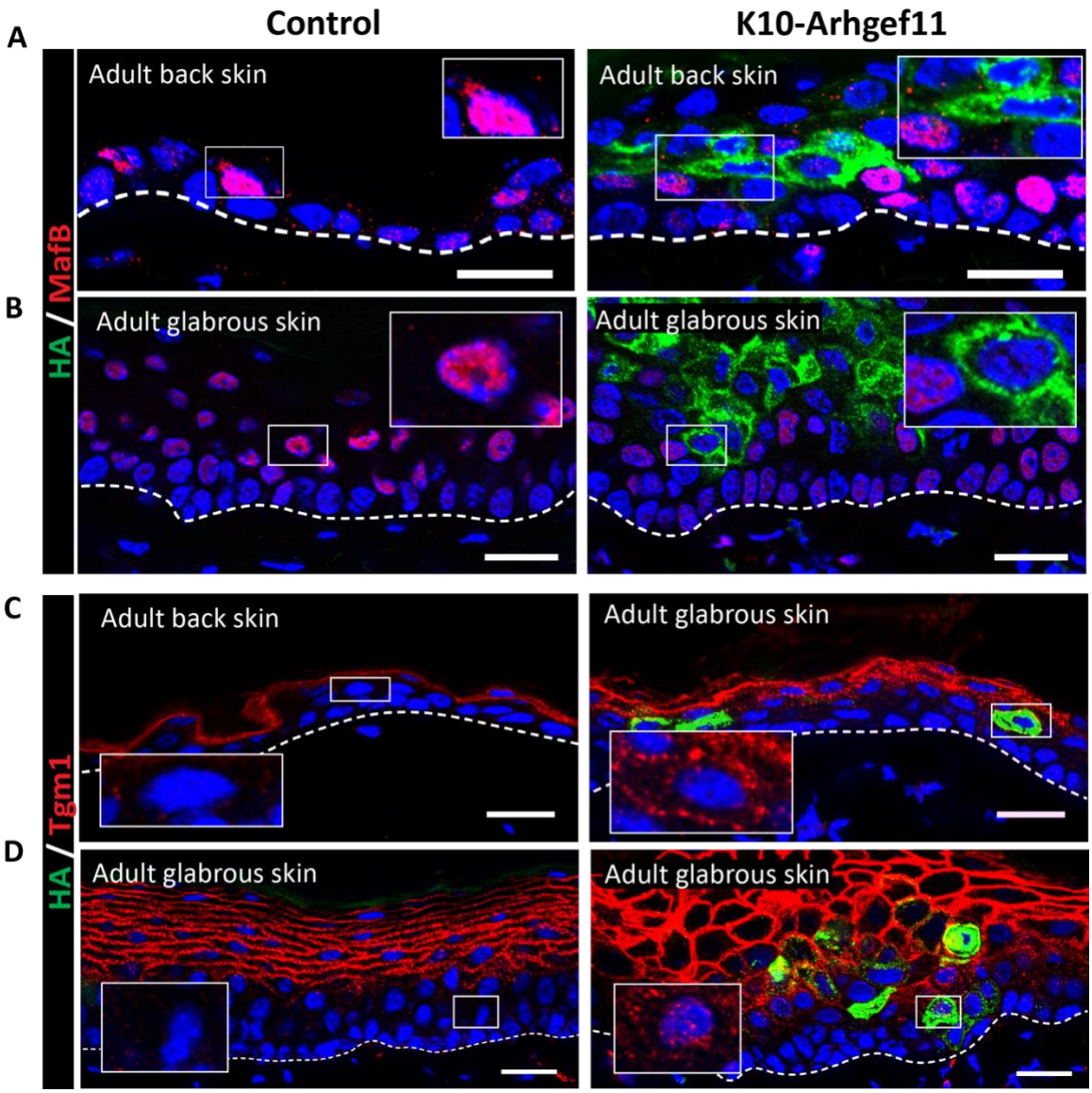

Figure 2.20: Increased contractility in spinous cells of adult epidermis induces some granular markers in adult epidermis

(A and B) Immunofluorescence staining of MafB in back skin (A) or glabrous skin (B) in red, and suprabasal cells expressing Arhgef11CA marked by HA (green) in adult K10-Arhgef11 and controls. Mice were fed with doxycycline since adulthood. Scale bars, 20 μm.
(C and D) Immunofluorescence staining of Tgm1 in back skin (C) or glabrous skin (D) in red, and suprabasal cells expressing Arhgef11CA marked by HA (green) in adult K10-Arhgef11 and controls. Mice were fed with doxycycline since adulthood. Scale bars, 20 μm.

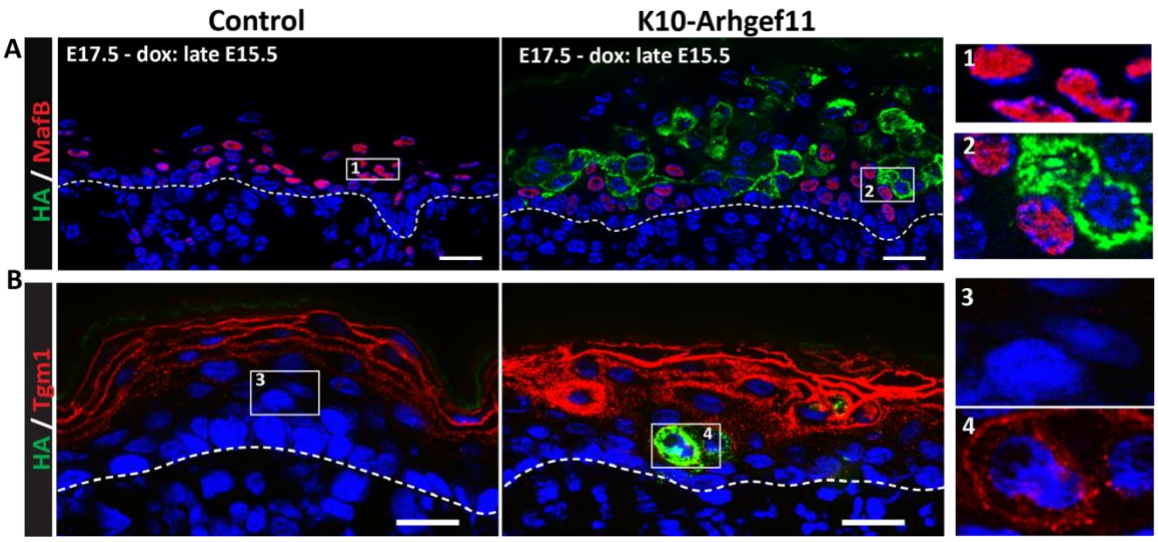

Figure 2.21: Increased contractility in spinous cells accelerates acquisition of granular markers

(A and B) Immunofluorescence staining of MafB (A) or Tgm1 (B) in red, and suprabasal cells expressing Arhgef11CA marked by HA (green) in adult K10-Arhgef11 and controls. Images from E17.5 embryos, fed with doxycycline starting at E15.5. Scale bars, 20 μm.

Nuclear YAP signaling has been shown to be downstream of increased contractility in both of our contractility mouse models previously tested (Ning et al., 2021), and YAP is localized to the nucleus in granular cells (Figure 2.16B). To test the role of YAP in inducing a granular-like state, we again used the mouse model K10-YAP^{CA}. We observed that inducing active YAP did not induce Tgm1 in spinous cells (Figure 2.22A, C), and did not suppress the expression of MafB, the spinous cell marker (Figure 2.22B, D). These data suggest that YAP activation lies downstream of contractility but is not sufficient to induce the effects observed by increased contractility in spinous cells. In addition to YAP activation, stretching of keratinocytes results in epigenetic changes, including an increase in H3K27me3 levels (Le et al., 2016). However, inducing contractility did not cause a significant change in nuclear levels of this epigenetic mark (Figure 2.23).

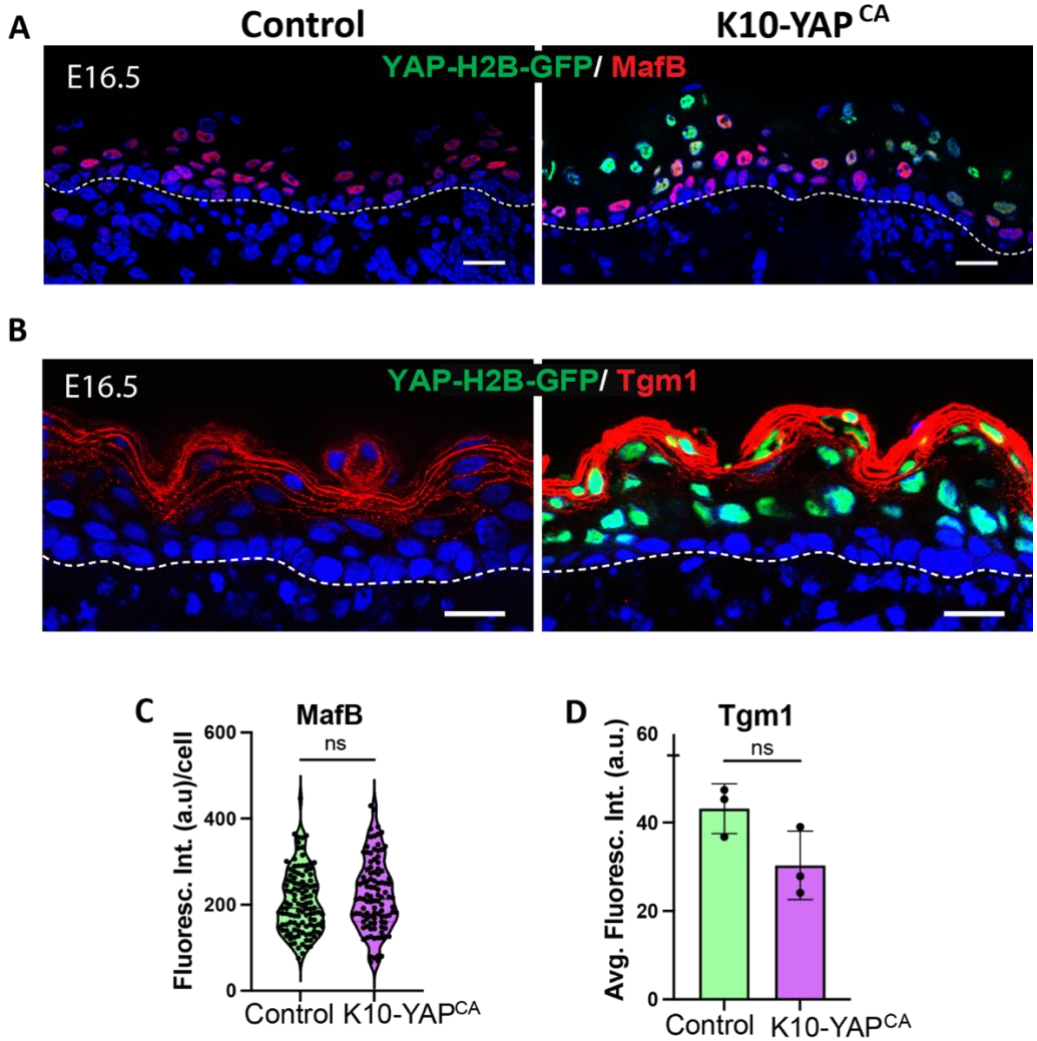

Figure 2.22: Inducing constitutively active YAP in spinous cells does not induce granular markers

(A and C) Immunofluorescence of MafB (A) or Tgm1 (C) in red, active YAP in green (YAP-H2B-GFP) in control, and K10-YAP^{CA} at E16.5. Scale bars: 20 μm.
(B) Average MafB fluorescence intensity per cell in control and K10-YAP^{CA}. n=113 suprabasal cells from 3 control embryos, and 103 from 3 K10-YAP^{CA} embryos. ns: not significant, two-tailed unpaired t-test.
(D) Average fluorescence intensity of suprabasal cells, area above basal cells in control and K10-YAP^{CA} embryos at E16.5 were measured. n= 3 embryos/genotype. ns: not significant, two-tailed unpaired t-test.

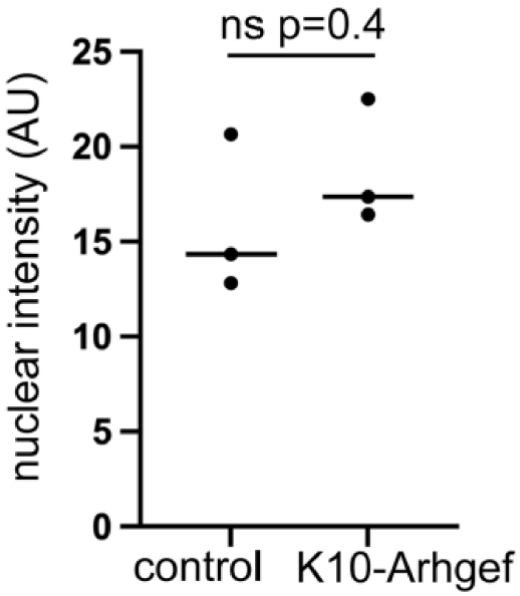

Figure 2.23: Increased contractility does not alter H3K27me3 levels

Quantifications of nuclear H3K27me3 levels in control spinous and K10-Arhgef-expressing spinous cells.

2.3 Discussion

Embryonic epidermal cells coordinate their growth and differentiation to allow rapid stratification and barrier formation. Our data here characterize intermediate cells in epidermal development, revealing novel trajectories of cell differentiation. Further, our data directly demonstrate that actomyosin contractility in the developing epidermis can play an instructive role in differentiation – promoting granular-like gene expression and suppressing spinous markers.

Bulk RNA-Seq analysis has allowed us to characterize embryonic epidermal cells in greater depth. This revealed that basal cells undergo significant changes between E14.5 and E16.5, consistent with the fact that they generate distinct cell progeny at these time points (intermediate vs spinous cells). In addition, like suprabasal cells, basal cells at these time points also show differences in mechanical properties. Whether this is in response to changes in their physical environment or is mediated by internal timers remains unknown. That said,

understanding specific markers and transcriptional regulators of these maturing basal cells may allow us to manipulate these transitions to maintain or bypass distinct stages of epidermal development.

Analysis of the intermediate cell transcriptome revealed an unexpected expression of granular genes in these transient cells. This gene expression program was especially enriched for lipid-modifying enzymes that play a key role in barrier formation. In contrast, few EDC genes were upregulated in intermediate cells, suggesting that only parts of the granular program are expressed early in these cells, and many of the structural components of the eventual barrier are expressed only later. Further, our short-term lineage tracing suggests that most intermediate cells transition into granular cells without going through a MafB+ (a spinous cell marker) stage. This reveals two distinct differentiation pathways leading to the granular cell state, one through intermediate cells during development and one through spinous cells post-natally. This raises questions about whether each route will require distinct regulatory and transcriptional pathways (Figure 2.24).

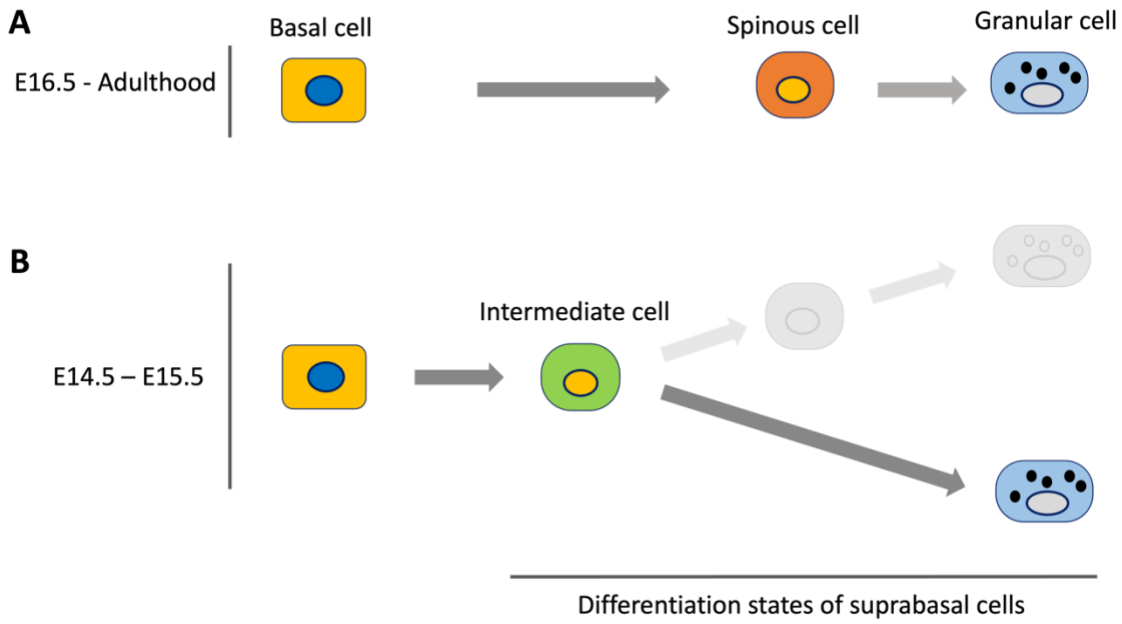

Figure 2.24: Different paths to granular fate

(A) Starting at E16.5, suprabasal cells start as spinous cells before differentiating into granular cells.
(B) Between E14.5 and E15.5, intermediate cells directly mature into granular cells without first transitioning through a MafB+ spinous fate.

Finally, our data revealed mechanical similarities between intermediate and granular cells, in addition to their similarities at the transcriptomic level. Actomyosin regulators were transcriptionally upregulated in both of these cell types as compared to spinous cells, and we were able to validate these findings in intact skin. Importantly, we found that contractility was sufficient to induce granular-like gene expression and to repress some spinous cell markers. This reveals a rather direct effect of contractility lying upstream, as well as presumably downstream, of differentiation pathways. It also explains the observation that increased contractility results in premature formation of the epidermal barrier (Muroyama & Lechler, 2017). It has been appreciated for some time that granular cells have increased actomyosin contractility, which is important for the function and placement of tight junctions specifically in this layer of the epidermis (Itoh et al., 2012; Prado-Mantilla & Lechler, 2023b; Rubsam et al., 2017; Sumigray et

al., 2012b). There are many intriguing possibilities for how contractility may affect cell fates, such as mechanosensitive transcriptional regulators that mediate this effect. We tested a possible role for YAP1, a transcriptional regulator whose activation is induced by contractility in the epidermis. We found that active YAP1 was insufficient to drive these gene expression changes. Future work is required to determine the mechanism of mechanosensitive differentiation in the epidermis. The epidermis increases contractility in response to externally applied forces that result in stretch, and in response to perturbation of cell adhesions (Aragona et al., 2020; Sumigray et al., 2014). It will be important to test whether these stimuli alter differentiation pathways through their effects on contractility.

Of note, we found that contractility had a strong effect on the EDC, whose positioning within the nucleus changes with differentiation (Gdula et al., 2013; Mardaryev et al., 2014; Williams et al., 2002). This suggests that aspects of epigenetics and chromatin organization may be downstream of contractility, as shown by external forces directly stretching chromatin (Tajik et al., 2016) and extrinsic topographical cues constricting the nucleus to induce chromatin reprogramming (Wang et al., 2023). Notably, we found that there is a decrease in mRNA levels of Sun1 and Nesprin1/3, parts of a complex that tether the actin cytoskeleton in the cytoplasm to chromatin in the nucleus when contractility is increased, in hypercontractile cells. Loss of Sun1/2 also leads to precocious differentiation in the epidermis (Carley et al., 2021) through effects on integrin-mediated mechanical integration, though whether regulation of these connections mediates the contractility effect seen in suprabasal cells will require further investigation.

The lipid lamellar, which binds together corneocytes in the cornified layer, is mainly composed of about 50% ceramides, 25% free fatty acids, and 10% cholesterol. These lipids are synthesized in the granular cells and stored in lamellar bodies, before secreting them to the intercellular spaces through lamellar bodies (Prado-Mantilla & Lechler, 2023a; Vietri Rudan & Watt, 2021). Increased contractility and lipid metabolic pathways are enriched in both

intermediate and granular cells. Comparing the commonly upregulated genes in these cell populations with the signature of heightened contractility in suprabasal cells revealed pathways related to ceramide metabolism and lipid catabolism. This is an interesting finding that suggests that contractility is a regulator of lipid metabolism. Therefore, increased contractility in granular cells may play a role in lipid synthesis for epidermal barrier function and may be the factor partially inducing IC similarities with granular cells. However, we cannot rule out a potential role of contractility in modifying lipids for intracellular lipid signaling in keratinocytes that induces differentiation (Vietri Rudan & Watt, 2021).

2.4 Materials and Methods

Mice

All animal work was approved by Duke University's Institutional Animal Care and Use Committee and performed in accordance with their committee guidelines. Mice were genotyped by PCR, and both male and female mice were analyzed in this study. All mice were maintained in a barrier facility with 12-hour light/dark cycles. Mouse strains used in this study include: K14-RFP (L. Zhang et al., 2011), K10-rtTA and TRE-Spastin (Muroyama & Lechler, 2017), TRE-Arhgef11^{CA} (Ning et al., 2021), CD1 (Charles River, strain code: 022). Other mice were from the Jackson Laboratories, and their stock numbers are as follows: TRE-H2B-GFP (005104), TRE-Yap1^{S112A}-GFP (031279, (Gao et al., 2013)).

Generation of the TRE-MafB-HA mouse line

MafB with an HA tag on the C-terminus followed by a stop codon was synthesized by GenScript and ligated into the pTRE2 vector. To verify the proper doxycycline-dependent expression of the TRE-MafB-HA cassette, the vector was co-transfected with a K14-rtTA plasmid into cultured keratinocytes and placed in doxycycline-containing media. TRE-MafB-HA plasmid was linearized, purified, and used by the Duke Transgenic Core to generate transgenic TRE-MafB-HA mice via pronuclear injection.

Skin explant preparation

Back skin of embryonic mouse skin was dissected, rinsed, and gently unfolded in sterile PBS, then placed on a 2% agarose pad diluted in a 1:1 sterile water:media mixture (10% FBS in DMEM, doxycycline (2 μg/ml, to induce H2B-GFP expression) and 1:100 Penicillin/Streptomycin). Note that the dermis of the skin explant faces the agarose pad. The skin explants on agarose were gently placed into a 6 cm dish containing 1 mL 10% FBS in DMEM (Gibco, 11965). The explants were cultured at 37°C and 7.5% CO2 for at least 2 hours for recovery before live imaging.

Sample preparation for RNA-Seq

K10-rtTA;TRE-H2B-GFP;K14-RFP pregnant dams were all fed with doxycycline chow at E12.5, and then sacrificed at either E14.5 or E16.5. Embryos were checked under a dissecting microscope for GFP and RFP expression before use, and their tails were taken to confirm genotypes. E16.5 back skins were cut off and treated with 1.4 U/ml dispase II (Roche, 4942078001) in HBSS at room temperature for 1 hour, then peeled off the epidermis from the dermis. The epidermis of E14.5 back skin was not peeled off due to its low thickness. Both E16.5 epidermis and E14.5 skin samples were digested in 1:1 trypsin (GIBCO, 25200-056) with versene (GIBCO, 15040-066) at 37°C and rotated for 20 minutes. Samples were then mixed 1:1 with FACS buffer (HBSS with 2.5% FBS and 10 μg/ml DNAaseI) and centrifuged at low speed. The cell pellet was diluted into FACS buffer with propidium iodide solution (Sigma, P4864, to exclude dead cells), and filtered using sterile Celltrics 30 μm filters (Sysmex, 04-004-2326). The lectin UEA1 (Ulex europaeus agglutinin I) binds to carbohydrates in cell surfaces present in uppermost keratinocytes. To exclude them, we used biotinylated UEA1 (Vector Laboratories, B-1065) and detected them with APC-streptavidin (BioLegend, 405207). The E14.5 intermediate cells (K10-GFP^{+};K14-RFP^{-};APC-UEA1^{-}), E16.5 spinous cells (K10-GFP^{+};K14-RFP^{-};APC-UEA1^{-}), and basal cells at E14.5 and E16.5 (K10-GFP^{-};K14-RFP^{+}) cells were FACS sorted

separately. RNA was extracted using a QIAGEN RNAeasy Mini kit (QIAGEN, 74104) following the manufacturer's protocols, with DNA digested using RNase-Free DNase (QIAGEN, 79254). Biological replicates, three independent RNA samples from each cell population, were collected and sent for sequencing and analysis by Novogene.

RNA-Seq analysis

Differential expression analysis between two time points or cell types (three biological replicates per group) was performed using the DESeq2 R package. The gene signature of a cell population was obtained by the overlapping genes that were enriched compared to the suprabasal cells at a different time point and enriched compared to the basal cells at its corresponding time point. A significance threshold of adj p-value < 0.05, log2 fold change≥ 1 and FPKM≥ 1 was used for defining marker genes of each cell population.

GO term analysis for differentially expressed genes and gene signatures was performed using the Gene Ontology enrichment analysis (Ashburner et al., 2000; Gene Ontology et al., 2023; Thomas et al., 2022).

FPKM of differentially expressed genes in the contractome list were log2-transformed and used for heatmaps. Heatmaps were generated using the online resource Heatmapper (Babicki et al., 2016), using the average linkage clustering method and Pearson's distance measurement methods.

PCA plot of all cell population data was generated using the web tool Clustvis: https://biit.cs.ut.ee/clustvis/ (Metsalu & Vilo, 2015).

Granular cell signature was determined from genes significantly upregulated in ETA sheets vs epidermal sheets (p-value < 0.05, log2 fold change≥ 1) obtained from the previously published dataset: GSE168011 (Matsui et al., 2021).

Immunofluorescence

Fresh tissue was embedded in OCT (Sakura), frozen, and sectioned at 10 μm using a cryostat. Sections were fixed with 4% paraformaldehyde (PFA) in PBS for 8 minutes at room temperature or ice-cold acetone (for Tgm1 and St8sia6 staining) for 2 minutes, washed with PBS containing 0.2% Triton (PBST) for 5 minutes, then blocked with blocking buffer (3% bovine serum albumin with 5% normal goat serum (Gibco, 16210064), and 5% normal donkey serum (Sigma-Aldrich, D9663) in PBST) for 15 minutes. Sections were incubated with primary antibodies diluted in blocking buffer for 1h at room temperature (α18 antibody was incubated for 15 minutes), then three times washed with PBST, and incubated in secondary antibodies and stains, such as Hoechst 34580 or Phalloidin, for 15 minutes at room temperature. After three washes with PBST, sections were finally mounted in the anti-fade buffer (90% glycerol in PBS plus 2.5 mg/ml p-Phenylenediamine (Thermo Fisher, 417481000)) and sealed using clear nail polish in the borders.

Primary antibodies used in this study: rat anti-HA (Sigma-Aldrich, 11867423001), chicken anti-keratin 5/14 (generated in the Lechler lab), rabbit anti-keratin 10 (Covance, 905401), guinea pig anti-keratin 10 (Progen, GP-K10), rat anti-β4 integrin (BD Biosciences, 553745), rabbit anti-MyosinIIA (Biolegend, PRB-440P), rat anti-α18 (gift from Akira Nagafuchi, Kumamoto University), rabbit anti-YAP/TAZ (Cell Signaling Technology, 8418S), rabbit anti-Tgm1(Proteintech,12912-3-AP), rabbit anti-MafB (Novus, NBP1-81342), rabbit anti-St8sia6 (Sigma, HPA011635), rabbit anti-Abca12 (gift from Dr. Wong, University of Michigan). F-actin was stained with phalloidin-488 (Invitrogen, A12379).

EdU labeling

Pregnant dams were intraperitoneally injected with 10 mg/kg of EdU and sacrificed after 1 hour for tissue dissection. Back skins of embryos were collected, and tails were taken for genotyping. Tissue sections were fixed with 4% PFA and stained with primary and secondary

antibodies, and then EdU was detected following the Click-iT EdU (Thermo Fisher, C10337) protocol.

Lineage tracing/pulse-chase

K10-rtTA;TRE-H2B-GFP pregnant dams were intraperitoneally injected with a low dose of doxycycline (1mg/kg) at E14.5 to label only intermediate cells. Dams were sacrificed, and their embryos were collected after 1 day (E15.5), 2 days (E16.5), or 4 days (E18.5) for tissue dissection. Their tails were kept for genotyping and K10-rtTA;TRE-H2B-GFP embryos were sectioned and analyzed.

RNA-Scope

RNAScope was performed using the Multiplex Fluorescent v1 and v2 systems (ACD, 323100) followed by antibody co-staining. Back skins from mouse embryos were freshly frozen in OCT and sectioned at 10 μm. Tissue sections were fixed for 1 hour with 4% PFA at 4°C. After fixation, standard RNAScope protocols were used according to manufacturer's instructions. The following probes were used: St8sia6 (ACD, 887831-C1) and Scara5 (ACD, 522301-C1). TSA Vivid Fluorophore 570 (ACD, 323272) was used to develop probe signal. Then, antibody staining was performed to quantify the probe signal in suprabasal cells, using guinea pig anti-keratin 10 antibody, and in basal cells, using chicken anti-keratin 5/14. HA+ cells were marked with rat anti-HA or rabbit anti-MafB (for K10-MafB samples). Coverslips were mounted using Prolong Gold (Invitrogen, P10144).

Imaging

For live imaging of K10+ cell division, prepared skin explants were placed upside down in a Lumox dish 35 (Sarstedt, 94.6077.331) with the epidermal side facing toward the membrane. Samples were imaged at 15 minute-intervals overnight using the MetaMorph software on an Andor XD revolution spinning disc confocal microscope at 37°C and 5% CO_2 using a 20x/0.5 UplanFl N dry objective.

For immunofluorescence staining, tissue sections were imaged on a Zeiss AxioImager Z1 microscope with Apotome.2 attachment, Plan-APOCHROMAT 20X/0.8 objective, Plan-NEOFLUAR 40X/1.3 oil objective, or Plan-NEOFLUAR 63X/1.4 oil objective, Axiocam 506 mono camera, and acquired using Zen software (Zeiss). When making intensity measurement comparisons, all images within one experiment were taken with identical exposure times.

Image quantification and statistics

All image quantifications were done using FIJI software. Quantifications of fluorescence intensity of cortical F-actin, Myosin IIA and α18 were measured by drawing 10-pixel wide lines across cell-cell boundaries. Maximum values from plot profiles were aligned to yield the final line scan plots. The mean of the maximum values of each line scan was calculated per mouse and compared between conditions or time points to determine statistical significance.

EdU, Scara5, St8sia6, YAP and MafB measurements were determined by calculating the percentage of the number of positive cells in the total number of suprabasal cells in the first two suprabasal layers adjacent to basal cells. Quantifications are from at least three fields per mouse.

Tgm1 average fluorescence intensity was calculated by measuring the mean value of suprabasal cells above basal cells. This area was defined by drawing 50-pixel width lines in the suprabasal area, along the labeled basal layer, using the Freehand line tool in FIJI.

All statistical analyses were performed using GraphPad Prism 10 software. Data shown in bar plots was presented as mean ± standard deviation (SD), and significance was determined using two-tailed Student's t-test, or, for multiple comparisons, one-way or two-way ANOVA, followed by Tukey's or Sidak tests. Further details in statistical analysis were specified in figure legends. Data were determined to be statistically significant when p value < 0.05. Asterisks denote statistical significance (ns = not significant, *: $p < 0.05$, **: $p < 0.01$, ***: $p < 0.001$, ****: $p < 0.0001$).

2.5 Author contributions

This chapter is based on my first-author publication, “Molecular and Mechanical Signatures Contributing to Epidermal Differentiation and Barrier Formation” (Prado-Mantilla et al., 2024): Wenxiu Ning contributed to the data production of part of Figure 1, data production and analysis in Fig1-supplement1 and part of Figure 5. Terry Lechler contributed to data acquisition and analysis of Figure 2.23. The rest of all data was acquired, analyzed and plotted. Manuscript was written in collaboration with Terry Lechler.

3 Degradation system to conditionally knockdown GFP-tagged proteins in mice

3.1 Introduction

Understanding the role of a gene is usually assisted by the disruption of its resulting protein's function and the analysis of resulting phenotypes. To this end, genome editing tools such as recombinases, transcription activator-like effector nuclease (TALEN), Zn finger nuclease, and CRISPR-Cas9 are used to generate permanent changes to the genome resulting in protein loss or alterations (Cong et al., 2013; Gaj et al., 2016; Le & Sauer, 2000; Mali et al., 2013; Miller et al., 2011; Pickar-Oliver & Gersbach, 2019; Porteus, 2008). There are numerous genes whose encoded protein expression is essential for cell viability and the development of an organism. Genetic knockouts of these genes *in vivo* may result in embryonic lethality and deter the ability to examine their role in later stages of life. To study these genes, it is crucial to employ technologies that conditionally deplete the protein of interest (POI). Conditional protein perturbation *in vivo* is typically performed at the pre-translational level, targeting the mRNA, like using RNA interference methods, or the genome (Elbashir et al., 2001; Gilbert et al., 2013; Gossen & Bujard, 1992; Housden et al., 2017; Le & Sauer, 2000; Sauer & Henderson, 1988). Most commonly, conditional genetic manipulations that delete or truncate a gene use site-specific recombinase (SSR) technologies such as the Cre/lox and FLP/FRT systems (Branda & Dymecki, 2004; Gronostajski & Sadowski, 1985; Kos, 2004; Zhu & Sadowski, 1995).

Although SSR-based systems have tremendously advanced the understanding of gene function in mice, they have some deficiencies that have limited their utility. These genetic alterations are generally irreversible and preclude the ability to easily restore protein function later to better pinpoint where and when the protein is needed. In addition, targeting the stem cell/progenitor cells causes a permanent lack of protein expression in them and all their progeny. This is problematic when studying gene function in stem cells because differentiated daughter

cells also constitute part of their progenitor stem cell niche (Ning et al., 2021). Thus, conventional methods for protein disruption make it difficult to determine whether the POI has cell-autonomous effects in stem cells and or whether there are non-cell-autonomous effects resulting from changes in their differentiated progeny cells.

Another disadvantage of using conventional methods for studying gene function is that they are indirect, where protein depletion depends on the half-life of the preexisting POI and its mRNA. Thus, making these technologies problematic to use during rapidly-ocurring developmental processes. While technologies targeting the mRNA can be relatively quicker than genome-editing recombinase approaches, the limiting factor is still the protein turnover rate (Schwanhäusser et al., 2011). Protein half-lives vary widely, spanning from less than a day to hundreds of days in mouse tissues. Even though most proteins are degraded within a few days, the half-life of long-lived proteins ranges from months to years (Fornasiero & Savas, 2023; Rolfs et al., 2021). These long-lived proteins are relevant for aging and degenerative diseases (D'Angelo et al., 2009; Heo et al., 2018; Lambeth et al., 2019; Savas et al., 2012; Toyama et al., 2013), and are present in all mouse tissues, especially in cartilage, where they are implicated in morphogenesis, cell adhesions and the extracellular matrix (Rolfs et al., 2021). Long protein half-lives can be a problem in assessing protein function in the context of fast biological processes. For example, it’s hard to target the differentiated cell pool in highly dynamic tissues such as the skin and the intestine. These tissues have quick cell turnover rates that are likely faster than the time required for POI depletion when using conventional technologies. Thus, newly generated cells would still express the POI. Similarly, targeting transient cell populations that exist for short periods of time, such as intermediate cells during epidermal development, can be extremely challenging.

These problems can be circumvented by directly targeting protein degradation. The major proteolytic system in cells is the ubiquitin-proteasome system (UPS) that rapidly degrades

proteins sent to the 26S proteasome (Hochstrasser, 1995; Navon & Ciechanover, 2009). The UPS targets proteins by polyubiquitination through a cascade reaction consisting of E1 ubiquitin-activating enzyme, E2 ubiquitin-conjugating enzymes and E3 ubiquitin ligase. Briefly, E1 activates ubiquitin, which is then transferred to E2. Finally, E2 cooperates with one of the hundreds of E3 to transfer the activated ubiquitin to the substrate to be degraded (Ciechanover et al., 1980; Hershko et al., 1982; Hershko et al., 1983; Varshavsky, 2006). Substrate recognition elements within the E3 complex provide the specificity of the target protein to be ubiquitinated (Figure 3.1). The peptide sequences in substrate proteins that are recognized by E3 are denominated degron (Natsume et al., 2016; Varshavsky, 1991; Verma et al., 2020).

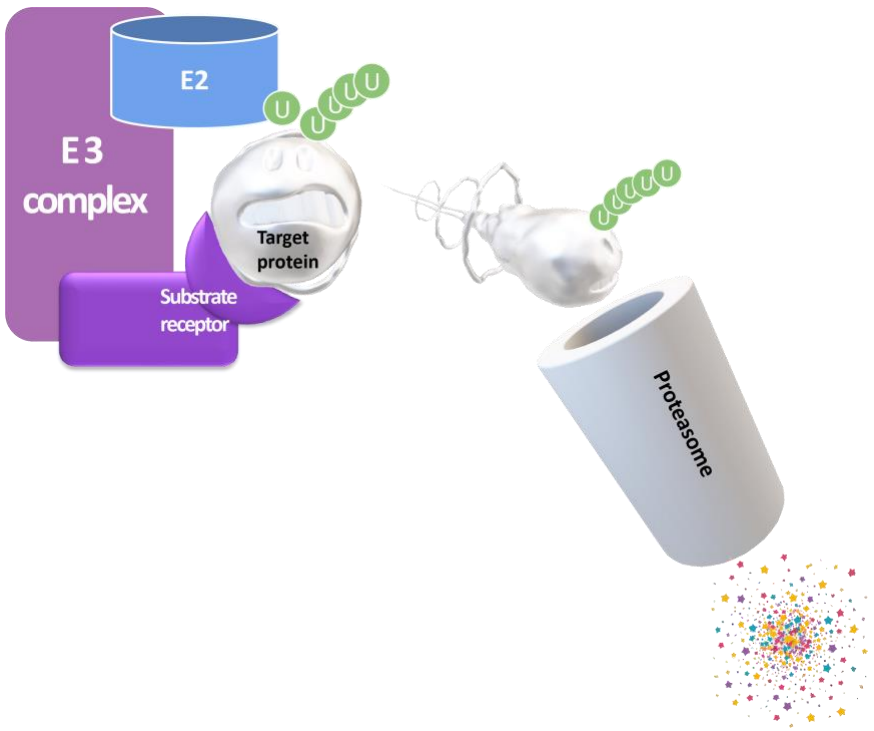

Figure 3.1: Schematic of the Ubiquitin Proteasome System

Numerous *in vitro* studies have demonstrated that by attaching these degron domains to POI, they function as tags that bring them into proximity with an E3 ubiquitin ligase, leading to

their rapid proteasomal degradation (Verma et al., 2020). Degron-fused proteins can be conditionally regulated by different factors like light, temperature, expression of another protein, or a small molecule ligand (Natsume et al., 2016). Examples of tools using chemically controlled degrons are the Auxin-Inducible Degradation (AID) and dTAG technologies. AID utilizes a plant degradation pathway that is induced by auxin, a family of plant hormones, in non-plant cells. In this system, the degron domain of IAA17 (AID domain) is fused to the POI, which binds to the exogenously expressed plant-derived protein TIR1 to recruit the E3 ubiquitin ligase upon auxin exposure (Nishimura et al., 2009; Tan et al., 2007). The dTAG technology uses a mutant version of the protein FKBP12 to tag a POI. To induce this system, heterobifunctional molecules (e.g., dTAG-v1 and v13) that bind to both the protein tag and an E3 ubiquitin ligase are administered (Clackson et al., 1998; Nabet et al., 2020; Nabet et al., 2018).

These degron tools have proven useful in Drosophila and C. elegans, though their use in mouse models has been limited (Phanindhar & Mishra, 2023). In the last few years, a number of groups have reported genome-engineered mouse models that conditionally induce acute protein depletion using AID (L. Macdonald et al., 2022; Suski et al., 2022; Yesbolatova et al., 2020) and dTAG technologies (Bisia et al., 2023; Bondeson et al., 2022; Nabet et al., 2020; Olsen et al., 2022). However, none of these allowed tissue-specific targeting of proteins. Furthermore, these approaches require the creation of new mouse lines with specific degron tags for each gene of interest, which can be time-consuming and costly. Thus, mouse tools that allow to more generally target any POI in specific tissues are needed.

Another direct protein degradation technology is the affinity-directed protein missile (AdPROM) system, which uses a Cullin 2-based E3 ligase complex. One of the substrate receptors of this E3 complex is VHL (Cai & Yang, 2016). Under normal oxygen conditions, VHL binds to the hydroxy-proline modified HIFα and brings it to close proximity to E2 to be polyubiquitinated and subsequently degraded (Kamura et al., 2004; Yu et al., 2001). Fulcher et al.

modified VHL by attaching a nanobody anti-GFP (Fulcher et al., 2016) in the C-terminus to degrade GFP-tagged proteins (Figure 3.2). AdPROM has been shown to work *in vitro* to degrade GFP-tagged PAWS1 and VPS34 in human cells (Fulcher et al., 2016).

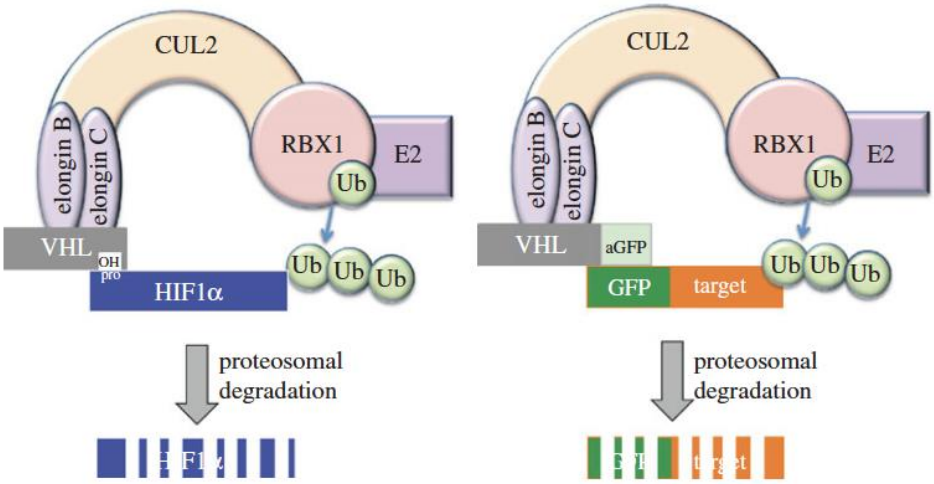

Figure 3.2: Schematic of the affinity-directed protein missile system for targeted proteolysis

(A) Diagram illustrating the structure of the CUL2-E3 ligase complex, demonstrating VHL-mediated degradation of HIF1α in normoxic conditions.
(B) AdPROM system: VHL attached to a nanobody anti-GFP to target and degrade GFP-fused proteins. Figure adapted from (Fulcher et al., 2016).

In this study, we generated mAdPROM, an inducible mouse tool that knocks down endogenous proteins in a temporally and spatially controlled manner. We took advantage of the AdPROM technology and combined it with the Tet-ON system to achieve tissue specificity and temporal control. Employing this tool, we were able to degrade endogenous GFP-tagged proteins in different tissues and cell compartments in adult mice. In addition, we tested mAdPROM's functionality by knocking down the glucocorticoid receptor (GR) protein in the epidermis and observed similar phenotypes than already-known GR epidermal knockouts. Furthermore, due to The time and costs associated with generating knock-in/knock-out mouse lines, the ability to generate one GFP knock-in strain that allows both imaging and loss-of-function abilities will be advantageous.

3.2 Materials and Methods

Mice

All mouse work was approved by Duke University's Institutional Animal Care and Use Committee and performed in accordance with committee guidelines. Mice were genotyped by PCR, and both male and female mice were analyzed in this study. All mice were maintained in a barrier facility with 12-hour light/dark cycles. Mouse strains used in this study include: K10-rtTA (Muroyama & Lechler, 2017), ZO1-GFP (Foote et al., 2013), K14- H2BGFP (Tumbar et al., 2004), GR-GFP (from Dr. Diana Laird, (Brewer et al., 2002)). Other mice were from the Jackson Laboratories, and their stock numbers are as follows: K14-rtTA (008099), Villin-rtTA (031283/ 031285), mGFP was generated by mating Rosa-mT/mG (007576) mice with a CMV-Cre-deleter strain (006054) (Ning et al., 2021).

Generation of mAdPROM mouse line

To generate the mAdPROM line, we used the pBABED Hygro Tet-on VHL aGFP plasmid (MRC PPU, DU 54221). To verify the proper doxycycline dependent expression of the previously generated the vector was co-transfected with a K14-rtTA plasmid (Ning et al., 2021) into cultured keratinocytes and placed in doxycycline-containing media. The plasmid was linearized, purified, and used by the Duke Transgenic Core to generate transgenic mice via pronuclear injection. Genotyping to identify founders and following mAdPROM genotyping was performed using forward primer: CTGCCCGTATGGCTCAACTTC, and reverse primer: CTAGAAACCGTCACCTGGG. Two mAdPROM lines were kept: Lines 17 and 41, which have robust transgene expression in the intestine and the epidermis, respectively.

Immunofluorescence staining

Fresh tissue was embedded in OCT (Sakura), frozen, and sectioned at 10 μm using a Cryostat. Sections were fixed with 4% paraformaldehyde (PFA) in PBS for 8 minutes at room temperature, washed with PBS containing 0.2% Triton (PBST) for 5 minutes, then blocked with

blocking buffer (3% bovine serum albumin with 5% normal goat serum (Gibco,16210064), and 5% normal donkey serum (Sigma-Aldrich, D9663) in PBST for 15minutes. Sections were incubated with primary antibodies diluted in blocking buffer for overnight at 4C (or at room temperature for: 1hr Loricrin, 2hrs GR), then three times washed with PBST, and incubated in secondary antibodies and Hoechstv34580 for 15 minutes at room temperature. After three washes with PBST, sections were mounted in the anti-fade buffer (90% glycerol in PBS plus 2.5 mg/ml p-Phenylenediamine (Thermo Fisher, 417481000) and sealed using clear nail polish in the borders.

Primary antibodies used in this study: mAb Rb anti VHH- iFluor555 (1:500, GenScript, A01863), Ch anti GFP (1:2000, Abcam, ab13970), Rb anti Loricrin (1:100, gift from Colin Jamera), mAb Rb anti GR (1:100, Cell Signaling, 12041T).

EdU labeling

Pregnant dams were intraperitoneally injected with 10 mg/kg of EdU and sacrificed after 1 hour for tissue dissection. Back skins of embryos were collected and fresh frozen, and tails were taken for genotyping. Tissue sections were fixed with 4% PFA and stained with primary and secondary antibodies, then EdU was detected following Click-iT EdU (Thermo Fisher,C10337) protocol.

3.3 Results

To assess the use of the AdPROM system *in vivo*, we generated mAdPROM, a transgenic mouse containing a cassette encoding the E3 ligase VHL attached to a nanobody anti-GFP (VHL-aGFP) under the tetracycline-responsive promoter element (TRE) (Fulcher et al., 2016). Using the Tet-ON system, tissue specificity can be achieved in mouse lines by directly controlling the expression of the reverse Tet-regulated transactivator (rtTA) under a tissue-specific promoter (Urlinger et al., 2000) or by crossing any tissue-specific Cre line with the ubiquitous Rosa-rtTA line (Hochedlinger et al., 2005). Only after doxycycline (dox) exposure, rtTA binds to the TRE

promoter allowing expression of its downstream transgene. In this way, pairing mAdPROM with a tissue-specific rtTA line, VHL-aGFP (hereafter called degron) expression can be controlled both spatially and temporally.

To assess the ability of degron to knock down GFP-tagged proteins in different cell compartments *in vivo*, I used mouse lines expressing GFP in different locations of the cell. First, I tested whether degron can deplete proteins in the cortex of the cell. For this, we used a mouse line we previously generated, a knock-in ZO1-GFP (Foote et al., 2013). We measured the ZO1-GFP levels in the cell-cell junctions of the adult tail epidermis, where, conveniently, there was a mosaic expression of degron (Figure 3.3A). We were able to detect cells expressing degron by immunofluorescence staining utilizing an antibody that recognizes camelid nanobodies (VHH). This allowed us to observe that the GFP levels in junctions between two adjacent cells expressing degron ($degron^{Pos}$) was drastically reduced compared to two adjacent degron-negative ($degron^{Neg}$) cells. Accordingly, GFP intensity was decreased to about half between $degron^{Pos}$/$degron^{Neg}$ junctions (Figure 3.3A-C). These results suggest that degron efficiently depletes cortical proteins like ZO1.

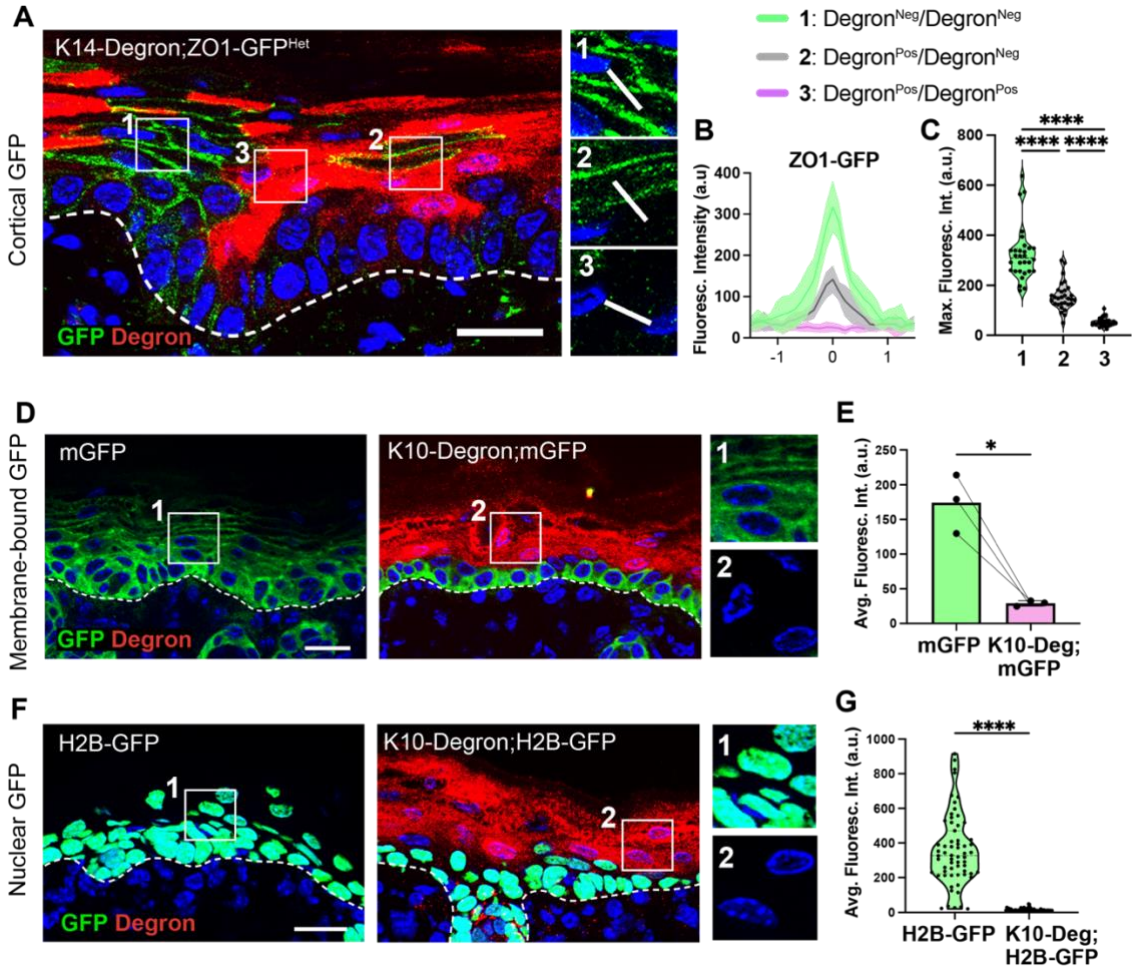

Figure 3.3: mAdPROM degrades GFP-tagged proteins located in different cell compartments

(A) Immunofluorescence staining of degron (red) in epidermis of K10-Degron;H2B-GFP neonates and control H2B-GFP littermate. Insets show only GFP in control (1) or in K10-Degron;H2B-GFP (2).
(B) Quantification of average H2B-GFP fluorescence intensity per nucleus in controls vs degron+ cells in experimental mice. n=49 cells for control and 63 degron+ cells for experimental from 2 animals per genotype. $p < 0.0001$, two-tailed unpaired t-test.
(C) Immunofluorescence staining of GFP and degron in epidermis of K10-Degron;mGFP neonates and control mGFP littermate. Insets show only GFP in control (1) or in K10-Degron;mGFP (2).
(D) Quantification of average fluorescence intensity per mouse from all suprabasal areas in controls or degron+ suprabasal areas in experimentals (n=3 experimental mice per genotype). $p = 0.0298$, two-tailed paired t-test.
(E) Immunofluorescence staining of GFP and degron in the tail epidermis of a K14-Degron;ZO1-GFP adult mouse. Insets show areas across cell-cell junctions between: (1) two cells not expressing degron (DegronNeg), (2) DegronNeg and a cell expressing degron (DegronPos), or (3) two DegronPos cells.

(F) Plot of line scans across ten cell-cell junctions for each category, as represented with white lines in E insets (1, 2 and 3).
(G) Violin plots of the maximum fluorescence values across each line scan for categories described in E (n = 30 measurements across 10 cell-cell junctions in each category). $p < 0.0001$, ordinary one-way ANOVA, multiple comparisons.

To test whether mAdPROM can be useful for targeted protein degradation in specific cell populations, we crossed it with cell-type specific rtTA lines. First, we assessed degron expression in the suprabasal cell compartment of the epidermis. In the epidermis, the suprabasal layers are composed of differentiated keratinocytes that express keratin 10 (K10). Therefore, we used the K10-rtTA line that directs the expression of rtTA under the promoter K10 (Muroyama & Lechler, 2017). Crossing this line with mAdPROM, we generated K10rtTA;mAdPROM (hereafter, K10-Degron) and used ZO1-GFP neonates to test it. Heterozygous ZO1-GFP (ZO1-GFP^{Het}) neonates showed GFP across all epidermal layers, but it was stronger in the cortex of suprabasal cells. K10-Degron;ZO1-GFP^{Het} mice exhibited strong degron expression across suprabasal layers of the epidermis, and as expected, GFP was efficiently depleted only in this compartment of the epidermis (Figure 3.4A, D, G).

We also induced degron in the epidermal stem cells that constitute the basal layer of the epidermis. These cells express keratin 14 (K14), so we generated K14-rtTA;mAdPROM (hereafter called K14-Degron) to determine whether degron can target only stem cells but not their progeny. To test this line, we paired it with homozygous GR-GFP, a knock-in GFP fused to the C-terminus of the endogenous GR (Brewer et al., 2002). As expected, embryonic skin of K14-Deg;GR-GFP^{Hom} animals had degron expression mainly restricted to the basal layer. Unlike control GR-GFP^{Hom} embryos that express GR-GFP in the entire epidermis, K14-Deg;GR-GFP^{Hom} showed GR-GFP only in suprabasal cells for the most part. This means that while basal cells had depleted GFP, its progeny (suprabasal cells on top) still expressed it (Figure 3.4B, E). Importantly, in this case, we also demonstrated that degron can produce a significant protein decrease even when both alleles of the gene are tagged with GFP. It's worthwhile to notice that

even though using K14rTA we could specifically target the embryonic stem cells, this was not the case in the adult epidermis, as shown in Figure 1A. Here, there was mosaic K14rtTA expression in basal and suprabasal layers, potentially due to problems in the transgene line or the nature of epidermal differentiation in adults, when basal cells move up to differentiate, instead of producing new differentiated keratinocytes like during development.

Besides the epidermis, we tested this tool in a different epithelial tissue with a high-turnover rate, the intestine. Using the Villin-rtTA line, we were able to induce degron mainly in the absorptive epithelial cells that populate the villi of the intestine, although we observed it in crypts on some occasions. Interestingly, ZO1-GFP that is normally located in the tip of epithelial cell borders in controls, was drastically decreased in parts of the villi were degron was expressed in Villin-Degron;ZO1-GFP^{Het} of adult intestines (Figure 3.4C, F, H). We observed the same in Villin-Degron;ZO1-GFP^{Hom} mice (data not shown). Thus, degron is useful to deplete GFP-tagged proteins in the different epithelial tissues.

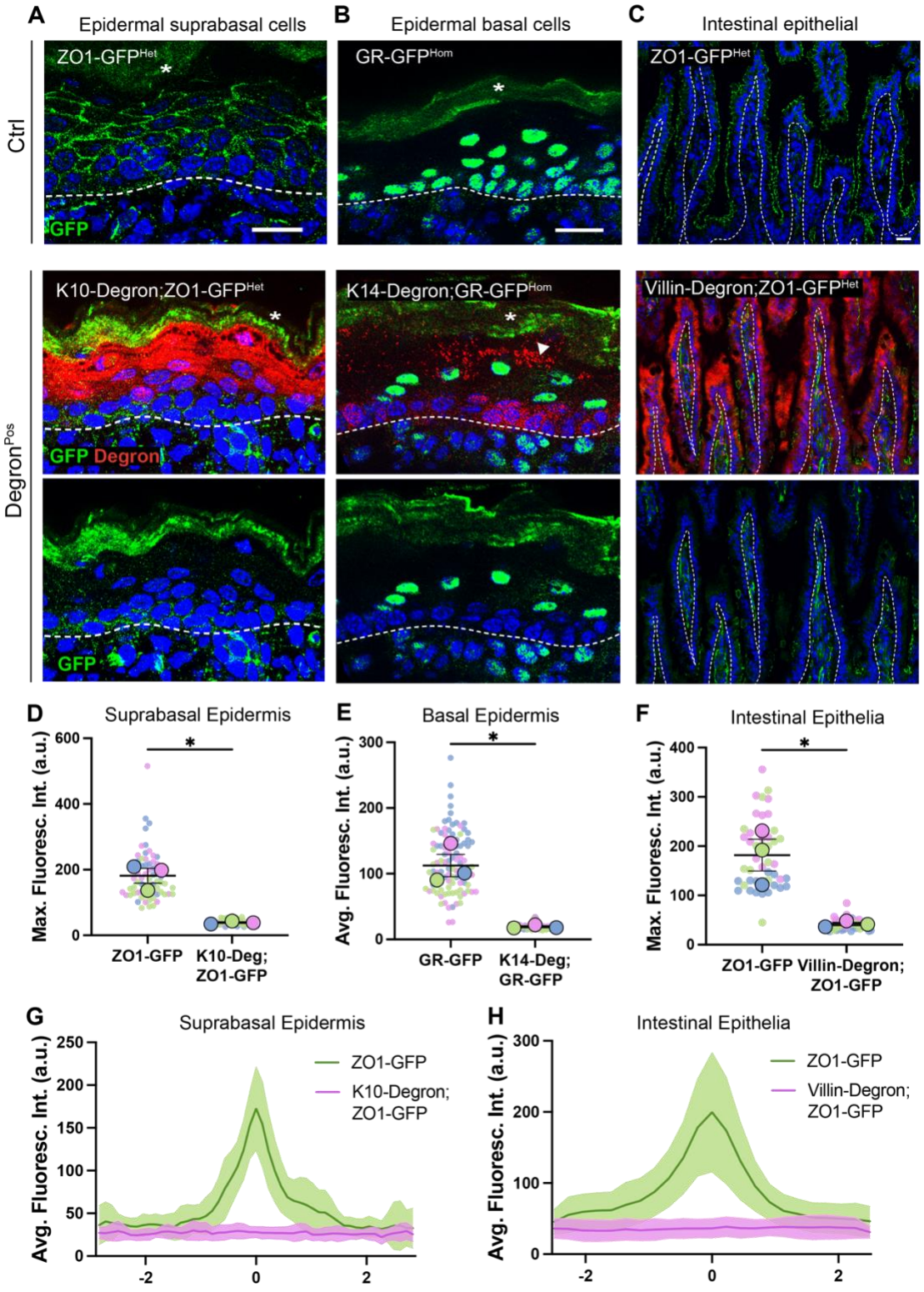

Figure 3.4: mAdPROM degrades GFP-tagged proteins in different cell populations

(A) Immunofluorescence staining of GFP (green) and degron (red) in back skin epidermis of K10-Degron;ZO1-GFP neonates and control ZO1-GFP littermate. The lowest panel shows only GFP in K10-Degron;ZO1-GFP. Dotted lines represent the basement membrane. * indicates auto-fluorescent cornified layer. All scales: 20μm.
(B) Immunofluorescence staining of GFP and degron in E18.5 back skin epidermis of K14-Degron;GR-GFP and control GR-GFP littermate. The lowest panel shows only GFP in K14-Degron;GR-GFP. White arrowhead indicates unspecific antibody staining.
(C) Immunofluorescence staining of GFP and degron in adult intestinal epithelia of Villin-Deg; ZO1-GFP and control ZO1-GFP littermate.
(D) Quantification of the maximum values of line scans across cell-cell junctions from epidermal suprabasal layers in ZO1-GFP (n=3 mice, at least 20 line scans per animal), and degron^{Pos} areas in ZO1-GFP (n=3 mice, at least 20 line scans per animal) neonates. Each dot represents the maximum value of a line scan, and lines show the mean±SEM. p=0.0294, paired two-tailed t-test.
(E) Quantification of the average fluorescence intensity of nuclei in the basal layers in GR-GFP (n=3 mice, 98 nuclei total), or degron^{Pos} basal cells in K14-Degron;GR-GFP (n=3 mice, 110 nuclei total) embryos. Each dot represents each nucleus, and lines show the mean±SEM. p=0.0268, paired two-tailed t-test.
(F) Quantification of the maximum values of line scans across apical cell-cell junctions from villi epithelial cells in ZO1-GFP (n=3 mice, 15 line scans per animal), and degron^{Pos} areas in Villin-Degron;ZO1-GFP (n=3 mice, 15 line scans per animal) adult mice. Each dot represents the maximum value of a line scan, and lines show the mean±SEM. p=0.0398, paired two-tailed t-test.
(G) Example of line scans across twelve cell-cell junctions in the epidermal suprabasal layers of ZO1-GFP or suprabasal degron^{Pos} areas of K10-Degron;ZO1-GFP mice. Plotted line scans are from 3 different mice per genotype. Line scans were measured using a 10μm-width line across cell borders or between two neighboring nuclei if junctions were not visible. Data are represented as mean±SD.
(H) Example of line scans across twelve epithelial cell-cell junctions in the intestinal villi of ZO1-GFP control or suprabasal degron^{Pos} areas of K10-Degron;ZO1-GFP mice. Plotted line scans are from 3 different mice per genotype. Line scans were measured using a 10μm-width line across cell borders or between two neighboring nuclei if junctions were not visible. Data are represented as mean±SD.

By using the Tet-ON system, we aimed to produce an inducible tool that could rapidly degrade proteins. We tested how quickly we could deplete ZO1-GFP in the suprabasal epidermis by exposing K10-Degron;ZO1-GFP^{Het} mice to dox for different durations. When E18.5 control and experimental embryos were exposed to dox for 1 day, we observed evident GFP reduction levels compared to GFP negative controls (Figure 3.5A,C), similar to what we observed in Figure 2A, when embryos were dox-treated for 5 days. Therefore, we decided to challenge the system by injecting a high dose of dox to a pregnant dam and collected embryos 6 hours after injection. To our surprise, degron was already present in suprabasal cells, where it had depleted GFP intensity levels, similar to dox-exposure for 24 hours and negative control that never expressed GFP

(Figure 3.5B, D). This data demonstrates that our degron tool can efficiently deplete GFP-fussed proteins as soon as 6 hours after dox-mediated induction *in vivo*.

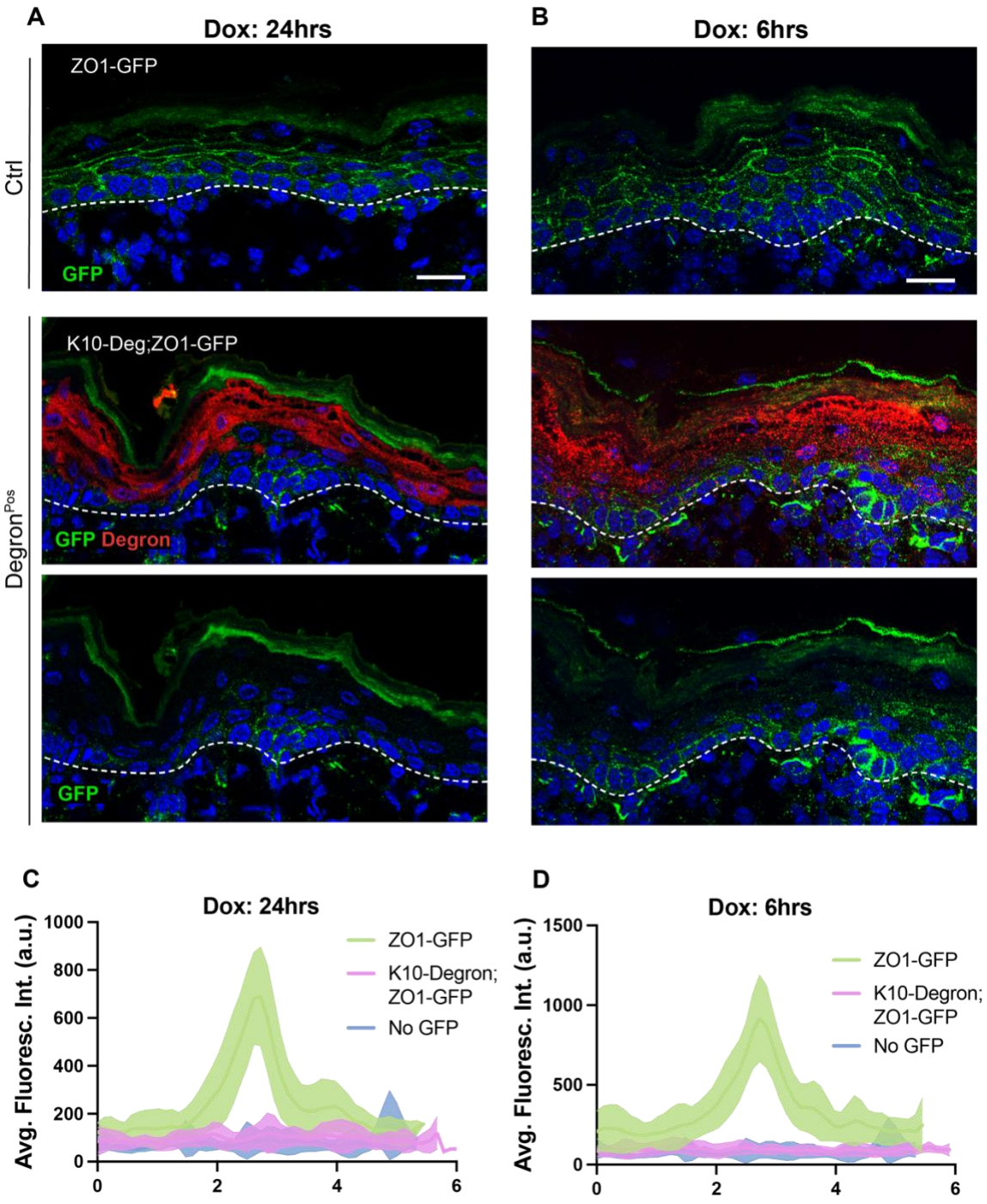

Figure 3.5: Kinetics of GFP degradation using mAdPROM

(A and B) Immunofluorescence staining of GFP (green) and degron (red) in E18.5 back skin epidermis of K10-Degron;ZO1-GFP and control ZO1-GFP 24 hrs (A) or 6hrs (B) after dox exposure. The lowest panel shows only GFP in K10-Degron;ZO1-GFP. Dotted lines represent the basement membrane. All scales: 20μm.
(C and D) Plot of line scans across nine cell-cell junctions in the epidermal suprabasal layers of ZO1-GFP, control no-GFP or suprabasal degron^{Pos} areas of K10-Degron;ZO1-GFP or mice 24 hrs (C) or 6hrs (D) after dox exposure. Plotted line scans are from 3 different mice per genotype. Line scans were measured using a 10μm-width line across cell borders or between two neighboring nuclei if junctions were not visible. Data are represented as mean±SD.

Next, we sought to assess whether this system could be useful for studying the role of a POI *in vivo*. Glucocorticoid receptor (GR) was a good candidate to test this tool since it is expressed throughout all layers of the epidermis and its knock-out has already been studied. GR is part of the nuclear receptor superfamily, and upon binding to its ligand (steroid hormones Glucocorticoids), GR acts as a transcription factor (Perez, 2011). Previous studies of null and epidermis-specific GR knockouts (GR^{eKO}) have reported differentiation defects during development, as well as aberrant epidermal proliferation and increased expression of inflammatory genes (Bayo et al., 2008; Latorre et al., 2013; Sevilla et al., 2010; Sevilla et al., 2013). These reports suggest multiple roles of GR in the epidermis. However, the role of GR in each cellular compartment of the epidermis and how they contribute to the aforementioned effects still remains unanswered. By knocking down GR-GFP using mAdPROM, we expect to potentially phenocopy the effects seen in knockouts. Even more, this tool could allow us to dissect the role of GR in different cell populations of the epidermis.

To address mAdPROM's functionality, we used homozygous GR-GFP to deplete all endogenous GR protein. We focused on the effects of GR during development. First, we used K14-Degron;GR-GFP^{Hom} to induce targeted GR degradation only in basal layers starting at E13.5 (before the start of epidermal stratification) or later in development, at E16.5. Tissues were collected at E18.5, a day before birth. Embryos with depleted basal GR-GFP had an increased proliferation rate of stem cells compared to control GR-GFP^{Hom} embryos, regardless of the time of dox-induction (Figure 3.6C, E), like the hyperproliferation observed in GR^{eKO} embryos

(Sevilla et al., 2013). However, we did not observe an apparent difference in the late epidermal differentiation marker Loricrin between experimental and control embryos at either dox-induction time (Figure 3.6A). On the other hand, depleting GR-GFP in the differentiated compartments of K10-Degron;GR-GFP^{Hom} embryos that were dox-treated starting at E13.5 (a day before K10 expression) did not have significant proliferation differences compared to littermate controls at E18.5 (Figure 3.6D, F). Yet, there was an obvious decrease in the thickness of Loricrin-positive and cornified layers in knockdown embryos compared to controls (Figure 3.6B), suggesting differentiation defects similar to phenotypes observed in GR^{eKO} mice during development (Bayo et al., 2008; Sevilla et al., 2010; Sevilla et al., 2013). Overall, mAdPROM was able to replicate some phenotypes observed in knockout studies. In addition, this tool allowed us to understand the role of GR in different compartments of the epidermis, suggesting that GR participates in suppressing hyperproliferation regardless of its expression in differentiated layers, while GR directly participated in terminal differentiation of keratinocytes. Importantly, these data show that mAdPROM is a useful tool for loss-of-function studies.

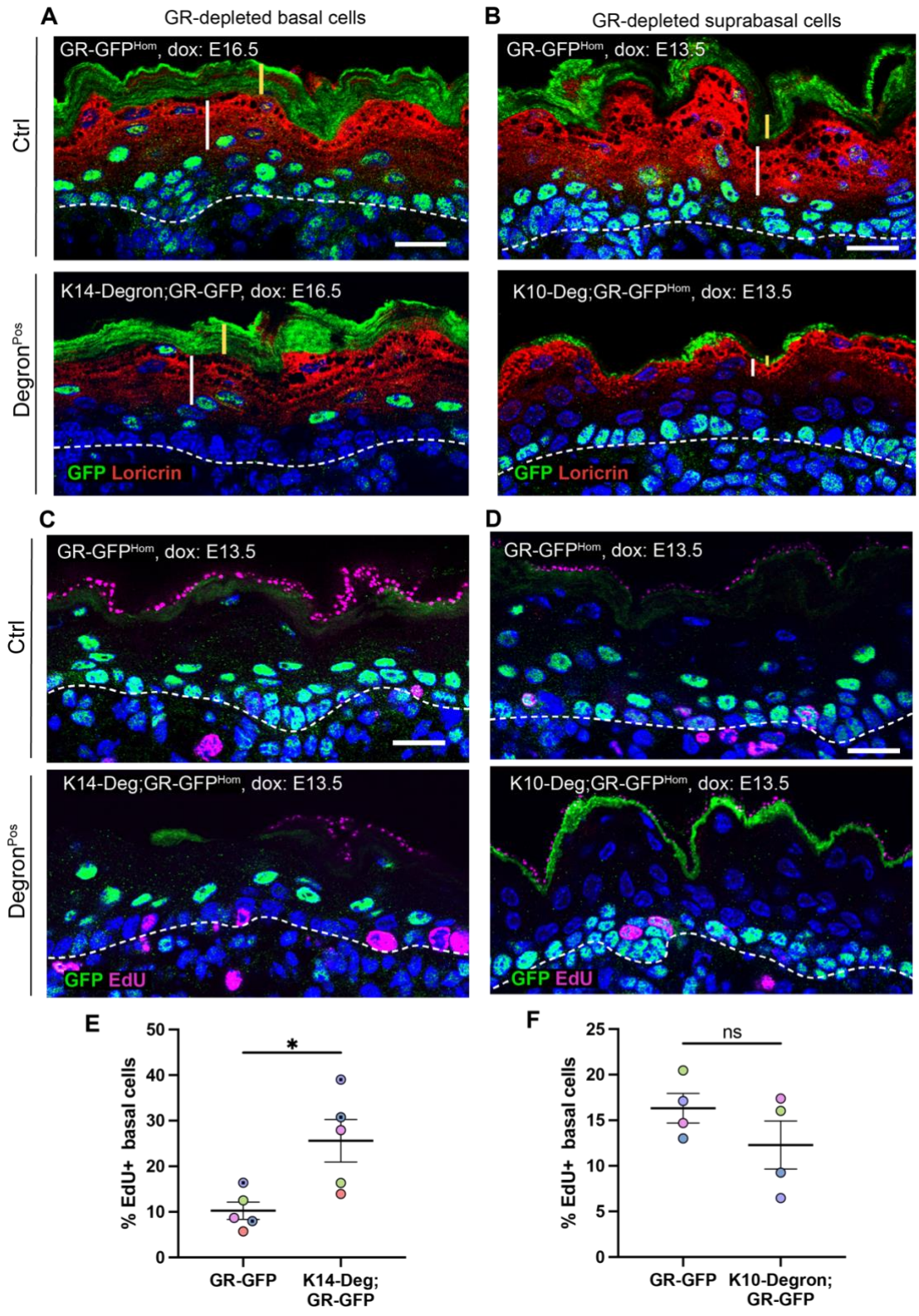

Figure 3.6: mAdPROM efficiently depletes GR-GFP and reproduces knockout phenotypes

(A and B) Immunofluorescence staining of GFP (green) and Loricrin (red) in E18.5 back skin epidermis of K14-Degron;GR-GFP (A) or K10-Degron;GR-GFP (B) and control GR-GFP littermates. White and yellow lines show granular and cornified layers thickness, respectively. Dotted lines represent the basement membrane. All scales: 20μm.
(C and D) Immunofluorescence staining of GFP (green) and EdU (magenta) in E18.5 back skin epidermis of K14-Degron;GR-GFP (C) or K10-Degron;GR-GFP (D) and littermate controls.
(E) Quantification of EdU positive cells in the basal layers of K14-Degron;GR-GFP (n=5 mice) and littermate controls (n=5). Each circle represents a mouse: solid color dots represent mice dox-exposed since E13.5, and circles with a dot represent mice dox-exposed since E16.5. Lines show the mean±SEM. p=0.0172, paired two-tailed t-test.
(F) Quantification of EdU positive cells in the basal layers of K10-Degron;GR-GFP (n=4 mice) and littermate controls (n=4). Each circle represents a mouse dox-exposed since E13.5. Lines show the meanSEM. p=0.0235, paired two-tailed t-test.

3.4 Discussion

For the first time, we developed a mouse tool that is temporally inducible and tissue-specific for quick targeted protein degradation. This system utilizes the Cul2-E3 ligase complex by altering its substrate recognition protein, enabling it to target proteins fused with GFP for proteasomal degradation through proximity-driven ubiquitylation. This process is mediated by the substrate recognition protein VHL, which is attached to a nanobody anti-GFP that allows specific recognition of GFP-tagged proteins for proteasomal degradation.

While earlier tools effectively degraded proteins after ligand administration, they lacked the ability to target proteins in specific tissues. dTAG technology uses an in-frame tag with a gene of interest; thereby, it is constitutively expressed throughout the whole system. Since the molecule that activates it is administered systemically, there is no way of restricting protein depletion to a specific tissue. On the other hand, the AID also tags the endogenous gene of interest, and it relies on the expression of the plant protein TIR1 to allow degradation. Hence, this technology could allow tissue-specific degron expression if TIR1 was conditionally expressed by crossing a lox-stop-lox TIR mouse line with a tissue-specific Cre line, instead of a constitutive line (Lewis Macdonald et al., 2022). However, tissue-specific protein knockdown has not yet been demonstrated to our knowledge.

We demonstrated that our tool is able to degrade proteins as fast as 6 hours after dox exposure. These results were comparable to those of other inducible *in vivo* protein degradation systems. Using the dTAG system in mouse adult tissue, they were able to completely deplete NELFB protein in 6 hours (Abuhashem et al., 2022). However, the only way of inducing this system is through intraperitoneal (IP) administration of heterobifunctional molecules. However, the drug duration in the animal's system is low and would require multiple IP injections that seem toxic for mice (L. Macdonald et al., 2022; Suski et al., 2022; Yesbolatova et al., 2020). This is not ideal when studying the effects of degradation over prolonged periods of time. Conversely, mAdPROM could be induced by administering dox-food to mice, which has been demonstrated not to be toxic and can be employed for protein degradation for longer periods of time. Furthermore, dTAG has been shown not to work in the brain, potentially due to the large molecular weight of its inducible molecules, unlike doxycycline, which can pass the blood-brain barrier. Thus, mAdPROM could be useful for studies in the brain.

The fact that mAdPROM employs a nanobody to target GFP-tagged proteins is a convenient feature of this tool. Nanobodies are single antigen binding domains that originate from camelid heavy-chain antibodies and have a molecular weight of around 15 kDa (Bever et al., 2016). This allows the degron to access the nucleus and potentially other organelles; however, this remains to be tested.

Lastly, mAdPROM was able to degrade GR fused to a GFP and partly produce effects similar to those in GR epidermal knockout models, such as hyperproliferation and aberrant expression of the late differentiation marker Loricrin. However, other differentiation markers and epidermal barrier integrity, as well as potential inflammatory responses in these mice need to be addressed in the future. Further exploring the effects of GR depletion in basal and suprabasal cells will enable us to distinguish the function of GR within the differentiated cell compartment from that in the progenitor compartment of the epidermis.

3.5 Author contributions

I (Alexandra Prado Mantilla) am the sole author of this chapter

4 Conclusions

4.1 Molecular and Mechanical Signatures Contributing to Epidermal Differentiation and Barrier Formation

4.1.1 Updated model of intermediate cell differentiation

The work presented in this dissertation expands our understanding of intermediate cells, a previously understudied cell population that exists only during epidermal development. Here, we debunk previous assumptions in the field about the differentiation path of the first K1/10 differentiated keratinocytes ever produced during epidermal stratification. In the adult epidermis, the series of differentiation steps that a keratinocyte undergoes on its path to terminal differentiation involve spinous fate prior to becoming granular cells. Considering this, along with the fact that suprabasal cells cease proliferating by E16.5, it has been widely accepted in the field that intermediate cells first mature into spinous cells before committing to a granular cell fate (Figure 1.2).

Using RNA sequencing of basal and first suprabasal cells at E14.5 and E16.5, we identified markers for intermediate and spinous cell populations during development. Surprisingly, lineage tracing experiments, combined with the expression of our previously identified markers, revealed that intermediate cells do not transition into spinous cells as previously thought. Instead, they directly differentiate into granular cells. This was supported by our transcriptional data and validation of granular markers expressed in intermediate cells, suggesting that these cells are granular cell precursors. These findings uncover a novel path of epidermal differentiation that is active in the early stages of epidermal stratification but not later, under normal conditions (Figure 2.24). Based on this evidence, I propose an updated model of epidermal development in which intermediate cells bypass the spinous stage and directly transition to a granular fate (Figure 4.1).

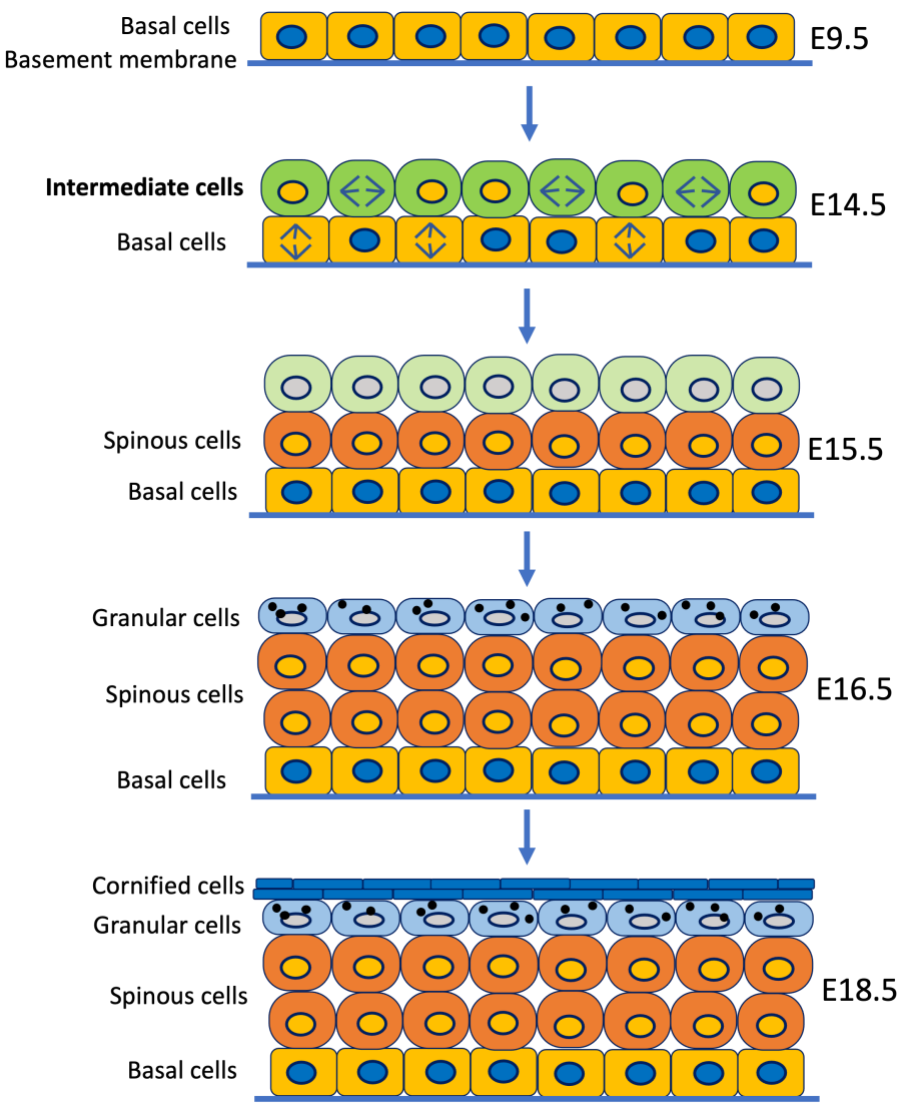

Figure 4.1: Updated model of intermediate cell differentiation during epidermal development

Intermediate cells bypass the spinous fate and directly differentiate into granular cells, then into corneocyte cells.

Supporting the idea that ICs are significantly different from spinous cells and follow a different path of differentiation, a study utilizing single-cell RNA sequencing revealed that at P0, a pseudo-temporal trajectory analysis demonstrated a linear differentiation trajectory from basal to terminally differentiated cells. In contrast, at E14.5, an outlying branch composed of

proliferative intermediate cells deviates from the linear trajectory (Lin et al., 2020). Whether this novel epidermal differentiation path occurs beyond development, such as during atypical skin conditions, remains to be elucidated.

4.1.2 Potential role of contractility in intermediate cell differentiation

Apart from transcriptional changes, I also observed tissue-level mechanical differences in the developing epidermis at E14.5 and E16.5, which included increased actomyosin contractility in both basal and suprabasal cells at the earlier time point. Increased contractility is a hallmark of granular cells, and it regulates tight junction formation and integrity (Itoh et al., 2012; Rubsam et al., 2017; Sumigray et al., 2012b). Thus, contractility is another similarity that intermediate cells share with granular cells. Surprisingly, ectopically increasing contractility in suprabasal cells is enough to induce the expression of granular markers in cells that, due to their proximity to the basal layer, would typically be expected to differentiate into spinous cells. These findings suggest that contractility regulates certain granular features, including lipid metabolic pathways, and may contribute to the granular-like characteristics of intermediate cells. This intriguing possibility needs to be directly tested. However, we cannot rule out whether the lipid-modifying enzymes increased in intermediate cells are instead playing a role in intracellular lipid signaling that induces keratinocyte differentiation (Vietri Rudan & Watt, 2021).

A previous study has shown that the LINC complex, which links the nucleoskeleton and the cytoskeleton, transmits integrin-dependent tension to the nuclear lamina in integrin-engaged basal cells. This process is necessary to repress premature epidermal differentiation by restricting chromatin accessibility of genes in the EDC locus (Carley et al., 2021). Given our hypothesis that intermediate cells are precursors to granular cells, we examined the expression of EDC genes in intermediate cells. Despite their departure from the basement membrane, intermediate cells expressed only a few EDC genes at the transcriptional level. Actomyosin contractility can also increase tension at the nuclear envelope through the LINC complex, which can influence

mechanosensitive responses (Lombardi & Lammerding, 2011). Increased actomyosin contractility in intermediate cells may help maintain chromatin accessibility and continue to repress the expression of EDC genes; however, whether this occurs remains to be explored.

Another reason for intermediate cells expressing some, but not all, granular markers just yet might be due to the presence of a key transcriptional regulator that blocks the expression of genes involved in the terminal steps of epidermal differentiation, such as genes important for cornified envelop formation located at the EDC locus. I proposed that his potential factor is Hes1, a transcription factor downstream of Notch signaling. Notch signaling has been proposed to induce terminal differentiation via Ascl2 activation, while also maintaining spinous fate via Hes1 by repressing premature granular differentiation. This was supported based on Hes1 knockout mouse models that exhibited extended Loricrin and Involucrin positive granular layers and few to no spinous layers (Moriyama et al., 2008).

Hes1 is already present in suprabasal layers at E14.5. Similar to our data, Moriyama *et al.* showed that the epidermis at E14.5 does not express cornified envelop structural components at the protein level. However, the Hes1 knockout epidermis at E14.5 visibly expressed Loricrin and Involucrin protein (Moriyama et al., 2008). Thus, I propose that instead of maintaining spinous fate, Hes1 is necessary to avoid premature terminal differentiation of the first suprabasal layers throughout epidermal development, including intermediate cells. Consistent with this idea, our genetic model of increased contractility (K10-Spastin) in the suprabasal layers had significantly reduced Hes1 levels and expressed almost half of EDC genes. This may partly explain why the gene expression in K10-Spastin is more similar to granular cells than intermediate cells. In addition, patients with psoriasis have decreased levels of Hes1 in the epidermis (Wang et al., 2022). Studies in mouse or human T-cell acute lymphoblastic leukemia cells suggested that decreasing MafB reduced Hes1 expression (Pajcini et al., 2017). Whether MafB expression influences Hes1 during epidermal development or the exact mechanism that turns off Hes1 to

allow granular fate would be an interesting direction to follow that could even have clinical implications for patients with psoriasis.

Another transcription factor that was upregulated in intermediate cells compared to spinous is Grhl3. This gene is crucial for barrier formation, lipid metabolism and regulates Tgm1 (Ting, Caddy, Hislop, et al., 2005; Yu et al., 2006). Grhl3 upregulation in intermediate cells may explain proteins found in intermediate but not spinous cells, like Tgm1 and Abca12. Interestingly, a recent study found that cytoplasmic localization of Grhl3 is important for the formation of actomyosin networks that increase cell stiffness (Kimura-Yoshida et al., 2018). Overall, Grhl3 appears to be an important factor possibly influencing intermediate cell characteristics. It would be interesting to closely study Grhl3 localization during epidermal stratification, and whether it is sufficient to induce increased contractility in the epidermis and other granular-like markers.

4.1.3 Temporal changes in basal cell populations

In addition to differences in the suprabasal layers, the transcriptional landscape of basal cells at E14.5 and E16.5 was considerably different. These findings show that the whole tissue, including the stem cell pool, undergoes significant changes over time during the stratification process. This raises the possibility that the differences in intermediate and spinous cells come from their progenitors and potential pre-determined factors that might inherit their differentiated progeny, resulting in distinct cell fates. But what is making basal cells different over time? One idea is that mechanical differences at the tissue level may influence chromatin changes in basal cells that are reflected in their different transcriptomes and, thus, the different fates of their progeny.

The increased contractility in the epidermis at E14.5 compared to E16.5 could be due to the tissue responding to mechanical changes in its environment. Potential external factors that might contribute to this include muscle development and changes in stiffness or composition of the underlying basement membrane or dermis. However, the extent to which the transcriptional

and mechanical differences in the developing epidermis over time are driven by external factors or by internal biological processes remains unclear. It would be important to investigate whether the differences observed in basal cells are enough to produce different types of cells, and whether these differences are caused by specific transcription factors or mechanical signals. Understanding these factors could have significant implications for skin grafting, especially when small amounts of basal cells are taken from patient biopsies. By manipulating epidermal stem cells to produce intermediate cells, we could potentially accelerate the growth of cultured keratinocytes and speed up the final stages of epidermal differentiation.

4.1.4 Role of Intermediate Cells in Epidermal Barrier Formation

During development, the rapid growth of the embryo requires all epidermal layers to expand swiftly to keep pace with the increasing size. A proposed role of intermediate cells is to expand the suprabasal cell numbers during a rapid growth period during development. In this study, we revealed that intermediate cells eventually become the epidermal barrier at birth. Also, we demonstrated that they have unique features beyond just being proliferative, suggesting that they must have another function during development. To address this, we intended to ablate this transient cell population by inducing Diphtheria toxin fragment A (DTA). However, DTA-induced cell death took too long and was not observed until intermediate cells were differentiated into granular cells. Naturally, inhibiting granular cells would cause problems during development, while specifically the role of intermediate cells was still unaddressed. Another way of studying their function could be by reducing their numbers. We showed that inducing MafB in intermediate cells led to their decreased proliferation but did not result in a decreased number of suprabasal cells at this time point since there was a compensation of hyperproliferating non-mutant surrounding cells, suggesting that epidermal homeostasis during development is difficult to perturb. Thus, depleting or reducing this cell population in our hands was challenging, highlighting the need for a tool that can target cell populations that exist only for a few days.

To this day, the role of intermediate cell during development remains an enigma. However, in this study, we advanced the understanding of these cells, such as the fact that they have a granular-like transcriptional profile, skip the spinous phase, and directly transition to a granular fate. Furthermore, a day before birth, they are already part of the cornified layer. Based on these observations, one can speculate that intermediate cells are necessary to quickly form a functional epidermal barrier that protects the newborn right before birth. Even though intermediate cells only exist during development, our hypothesis raised the possibility that intermediate cell-like states may be induced beyond development when the epidermal barrier is disrupted. Examples of this could be during wounding or other skin pathologies.

4.1.5 Implications for wound healing and skin pathologies

During wounding, there is a breach of the epidermal barrier, and cells at the leading edge migrate while trailing basal and suprabasal cells in the proliferative hub proliferate to help close the exposed area (Aragona et al., 2017). Besides its role in epidermal barrier formation during development, GRHL3 is expressed at the suprabasal cells at the wound front and is important for repairing the epidermal barrier in case of injury in adult mice (Gordon et al., 2014; Kashgari et al., 2021). However, it is dispensable for terminal differentiation in the adult epidermis during homeostasis (Gordon et al., 2014). This is consistent with the idea of activating an intermediate-like state when a new barrier needs to be formed. In addition, all cells throughout the epidermis at the wound edge express Myosin 1b, a tension-sensitive myosin that suggests high levels of cytoskeleton reorganization for cell migration and contractility in this area (Aragona et al., 2017), similar to intermediate states. It would be interesting to compare the intermediate cell signature with the molecular signature at the leading edge and proliferative hub to see if any of these cells are intermediate-like or are undergoing differentiation through our discovered novel path for terminal differentiation. Thus, understanding the factors that influence ICs could help patients with large or chronic wounds to more quickly re-establish the epidermal barrier.

Other situations where the epidermal barrier is compromised in adults are in skin disorders. In these conditions, immune responses that respond to barrier disruption provide feedback signaling to the epidermis, which further complicates this scenario (Zhang et al., 2022; Zhou et al., 2022). However, the possibility of activating intermediate-like cells in attempts to form an effective barrier is intriguing. Evidence for this includes GRHL3 upregulation in psoriasis lesions, which does not occur in non-leasional areas (Goldie et al., 2018; Zhou et al., 2022). Also, high throughput transcriptome analysis revealed altered lipid metabolism in the skin of patients with psoriasis compared to those with healthy skin (Yu et al., 2020). Additionally, our spinous marker MafB is expressed in suprabasal cells of normal human epidermis, but it was significantly reduced in patients with atopic dermatitis and psoriatic lesions (Miyai et al., 2016a). Further analysis of human skin samples in these pathologies could help us understand if they present other characteristics of intermediate cells, like high expression of lipid metabolism-related genes or higher contractility in suprabasal layers. If true, understanding the biology of intermediate cells could further help the treatment of patients with skin pathologies involving a defective epidermal barrier.

4.1.6 Concluding remarks and future directions:

In conclusion, intermediate cells undergo a novel path of terminal differentiation, where they differentiate into granular cells without previously becoming spinous cells, as was previously believed in the field. The mechanisms behind the expression of just certain aspects of granular cells are still unknown. I propose that increased contractility, potentially induced by enriched Grhl3, induces genes involved in lipid metabolism. This was aligned with common pathways enriched in our genetically induced increased contractility. In addition, EDC genes involved with late differentiation and formation of the cornified layer are likely repressed by expression of the Notch target Hes1. These hypotheses need to be tested, and the factors that make intermediate cells proliferative need further study.

My dissertation work shed light on mechanisms of epidermal differentiation during development. This study helped us recognize the uniqueness of intermediate cells and only scratch the surface of their complexity. Continuing to study and understand intermediate cell biology is important in the skin field, and discovering the exact underlying mechanism of their characteristics could even have clinical applications.

Future directions for this project include directly assessing whether contractility is upstream of granular-like fate. This could be done by conditionally reducing actomyosin contractility, specifically in differentiated compartments. Reducing contractility in intermediate or granular cells may allow us to determine whether contractility is necessary for keratinocyte differentiation other than regulating tight junction localization and integrity. Also, it could clarify what are the specific mechanisms induced by a high-contractile environment in the epidermis. Additionally, exploring the mechanosensitive mechanisms involved in late epidermal differentiation presents an interesting route for future investigation.

In the future, it would be interesting to have a tool that allows rapid and reversible protein manipulation in suprabasal cells. This would enable us to temporarily decrease actomyosin contractility solely when intermediate cells are present, allowing us to assess the role of contractility specifically in these cells, without the potential confounding influences from granular cells. Similarly, such inducible tool could allow us to understand the function of intermediate cells during epidermal developing by assisting intermediate cells ablation, either by degrading cell-cycle required proteins to stop their proliferation, or by inducing cell death uniquely of these cells.

Another intriguing question raised during this study is whether intermediate and spinous cell fates come from their progenitors. The interfollicular epidermis was previously assumed to be homogeneous during development. However, our RNA sequencing data shined a light on the significant transcriptomic differences in basal cells over a period of two days. Studying the cues

that induce these differences in basal cells could be crucial to determine whether manipulating them could alter the fate of their progeny. For example, inducing cues that expand the E14.5 basal-like state in the epidermal progenitors until E16.5—when new keratinocyte progeny are supposed to have spinous fate—would continue to produce progeny that are intermediate cells.

This may help answer a crucial question in stem cell biology: Are factors inherited asymmetrically from the progenitor responsible for the fate of progeny cells, or do transcription factors activated after cell division by environmental signals or internal cues determine differentiated cell fate? In the case that basal-cell manipulations are sufficient for changes in cell progeny, it may suggest that cellular fate decisions could be "pre-determined" by their progeny. Conversely, if alterations in cytoskeletal contraction can effectively alter the fate of progeny cells, this might support the latter hypothesis.

This could help address an important question still unanswered in the field of stem cell biology: whether asymmetrically inherited factors from the progenitor are responsible for progeny cell fate or whether transcription factors activated after cell division in response to environmental signals or intrinsic cues are responsible for differentiated cell fate. On the other hand, if changes in cytoskeletal contraction are sufficient for altering progeny's cell fate, could be an indication of the latter hypothesis.

4.2 Degradation system to conditionally knockdown GFP-tagged proteins in mice

In the second part of my dissertation work, I generated the mouse line mAdPROM, which works as tool for quick conditionally degrading GFP-fused proteins in a spatially and temporally controlled manner. Traditionally, *in vivo,* loss-of-function studies employ genome editing tools like recombinases, in which the effects of lack of POI can only be observed after the pre-existing mRNA and protein have been degraded. However, due to the long half-lives of proteins, the use

of these tools is limited for studying many quick biological events such as cell cycle, cell signaling, and rapid developmental processes. Furthermore, due to the irreversible nature of conventional recombinase-based tools, targeting uniquely stem cell compartments in a tissue or assessing the role of a protein in a determined period of time in an organism's life is impossible to do with these technologies.

Numerous methods have been developed to induce direct degradation of a POI by harnessing the endogenous ubiquitin-proteasome system of a cell to circumvent the previously mentioned problems. However, these technologies are still limited in mouse models. Recently, a number of groups have reported employing inducible systems such as dTAG and AID for acutely degrading proteins in mice. Nonetheless, these approaches did not provide tissue specificity since the degron tool was expressed in the whole system, and the drug that controls degron expression is administered systemically. For the first time, this study demonstrates inducible tissue-specific protein degradation in mice.

4.2.1 Key Features and Advantages of mAdPROM

I showed that mAdPROM is a valuable tool for rapidly targeting GFP-tagged proteins in as little as 6 hours. To test the kinetics of this tool, I used the cortically located protein ZO1-GFP. However, the degradation dynamics of different proteins may vary depending on the POI's cellular location. Even though mAdPROM recognizes its target using a nanobody—one variable domain of a heavy-chain antibody—this small component adds about 15 kDa to the degron (Bever et al., 2016), potentially affecting degron accessibility to a cell compartment. For example, proteins located inside other organelles, like the nucleus, may take different time to be degraded. Therefore, it would be necessary to empirically test the minimum degradation time of a POI if this factor significantly influences the study at hand.

Another advantage of using tools that degrade proteins is the reversibility of the targeted protein. After stopping degron induction, I tested the time it would take for GFP to come back. I

observed degron expression in the epidermis for up to 8 days after dox administration was stopped in the epidermis of neonate mice. This might be due to the long half-life of degron itself and the time it takes to be naturally degraded. However, degron stability may vary depending on the tissue in which it is expressed. Experiments to characterize degron kinetics, including the time required for POI-GFP degradation and GFP recovery, are needed for each POI.

4.2.2 Applications and Implications of mAdPROM

Lastly, mAdPROM was able to deplete GR-GFP in either the basal layer or the suprabasal cells, which recapitulated different phenotypes observed in epidermal GR knockout mice previously studied. This indicates that GR serves distinct functions based on the cellular compartment of the epidermis in which it is expressed. This opens the possibility that the same may occur in different compartments within other tissues, especially for transcription factors with a wide range of downstream effects. Our results emphasize the importance of analyzing a protein's role in each distinct cell type, for which mAdPROM could serve as a useful resource.

4.2.3 Concluding remarks and future directions

In the second part of my dissertation, I developed a tool for rapid conditional protein degradation, enabling tissue-specificity in mice for the first time. This tool works to degrade GFP-tagged proteins in different cell compartments and cell populations. Future directions for this project involve exploring the utility of mAdPROM in different tissues beyond epithelia, potentially making it a widely valuable resource for rapidly knocking down intracellular proteins, including in brain studies. Moreover, exploring ways to increase the instability of the degron, ensuring it is expressed solely during doxycycline exposure, represents a crucial avenue for future research. Rapid POI degradation and swift endogenous protein recovery may enhance mAdPROM’s application in research where quick reversibility is crucial. In this way, mAdPROM could be a useful tool for more tunable regulation of protein function.

Also, a powerful utility for this tool is to differentiate the role of a protein in different cell populations of a tissue. Here, I demonstrated that a protein expressed throughout the epidermis, GR, seems to have different roles in stem cells and differentiated cells. An exciting future direction for the use of this tool is to clarify which cellular compartment in the epidermis drives the inflammatory responses observed in GR^{eKO} mice. Determining whether these immune responses arise from defects in epidermal differentiation that compromise the epidermal barrier, from progenitor cells initiating downstream immune signaling, or from a combination of both could deepen our understanding of glucocorticoids' anti-inflammatory mechanisms. This insight could lead to more effective and targeted treatments for patients undergoing glucocorticoid therapy, potentially minimizing side effects and improving therapeutic outcomes. The only way to gain these insights is by directly degrading the protein of interest, as our system does.

In conclusion, mAdPROM is a powerful tool that enables a deeper investigation into the precise mechanisms of a protein's action. It allows us to address questions that were previously beyond reach using traditional loss-of-function approaches.

4.3 Author contributions

I (Alexandra Prado Mantilla) am the sole author of this chapter.

References

Abuhashem, A., Lee, A. S., Joyner, A. L., & Hadjantonakis, A.-K. (2022). Rapid and efficient degradation of endogenous proteins in vivo identifies stage-specific roles of RNA Pol II pausing in mammalian development. *Developmental Cell*, *57*(8). https://doi.org/10.1016/j.devcel.2022.03.013

Akiyama, M. (2010). ABCA12 mutations and autosomal recessive congenital ichthyosis: a review of genotype/phenotype correlations and of pathogenetic concepts. *Hum Mutat*, *31*(10), 1090-1096. https://doi.org/10.1002/humu.21326

Angulo-Urarte, A., van der Wal, T., & Huveneers, S. (2020). Cell-cell junctions as sensors and transducers of mechanical forces. *Biochim Biophys Acta Biomembr*, *1862*(9), 183316. https://doi.org/10.1016/j.bbamem.2020.183316

Aragona, M., Dekoninck, S., Rulands, S., Lenglez, S., Mascre, G., Simons, B. D., & Blanpain, C. (2017). Defining stem cell dynamics and migration during wound healing in mouse skin epidermis. *Nat Commun*, *8*, 14684. https://doi.org/10.1038/ncomms14684

Aragona, M., Sifrim, A., Malfait, M., Song, Y., Van Herck, J., Dekoninck, S., Gargouri, S., Lapouge, G., Swedlund, B., Dubois, C., Baatsen, P., Vints, K., Han, S., Tissir, F., Voet, T., Simons, B. D., & Blanpain, C. (2020). Mechanisms of stretch-mediated skin expansion at single-cell resolution. *Nature*, *584*(7820), 268-273. https://doi.org/10.1038/s41586-020-2555-7

Ashburner, M., Ball, C. A., Blake, J. A., Botstein, D., Butler, H., Cherry, J. M., Davis, A. P., Dolinski, K., Dwight, S. S., Eppig, J. T., Harris, M. A., Hill, D. P., Issel-Tarver, L., Kasarskis, A., Lewis, S., Matese, J. C., Richardson, J. E., Ringwald, M., Rubin, G. M., & Sherlock, G. (2000). Gene ontology: tool for the unification of biology. The Gene Ontology Consortium. *Nat Genet*, *25*(1), 25-29. https://doi.org/10.1038/75556

Aw, W. Y., Heck, B. W., Joyce, B., & Devenport, D. (2016). Transient Tissue-Scale Deformation Coordinates Alignment of Planar Cell Polarity Junctions in the Mammalian Skin. *Curr Biol*, *26*(16), 2090-2100. https://doi.org/10.1016/j.cub.2016.06.030

Babicki, S., Arndt, D., Marcu, A., Liang, Y., Grant, J. R., Maciejewski, A., & Wishart, D. S. (2016). Heatmapper: web-enabled heat mapping for all. *Nucleic Acids Res*, *44*(W1), W147-153. https://doi.org/10.1093/nar/gkw419

Baroni, A., Buommino, E., De Gregorio, V., Ruocco, E., Ruocco, V., & Wolf, R. (2012). Structure and function of the epidermis related to barrier properties. *Clin Dermatol*, *30*(3), 257-262. https://doi.org/10.1016/j.clindermatol.2011.08.007

Bayo, P., Sanchis, A., Bravo, A., Cascallana, J. L., Buder, K., Tuckermann, J., Schutz, G., & Perez, P. (2008). Glucocorticoid receptor is required for skin barrier competence. *Endocrinology*, *149*(3), 1377-1388. https://doi.org/10.1210/en.2007-0814

Bever, C. S., Dong, J.-X., Vasylieva, N., Barnych, B., Cui, Y., Xu, Z.-L., Hammock, B. D., & Gee, S. J. (2016). VHH antibodies: emerging reagents for the analysis of environmental

chemicals. *Analytical and Bioanalytical Chemistry*, *408*(22), 5985-6002. https://doi.org/10.1007/s00216-016-9585-x

Bikle, D. D., Ratnam, A., Mauro, T., Harris, J., & Pillai, S. (1996). Changes in calcium responsiveness and handling during keratinocyte differentiation. Potential role of the calcium receptor. *J Clin Invest*, *97*(4), 1085-1093. https://doi.org/10.1172/JCI118501

Bisia, A. M., Costello, I., Xypolita, M. E., Harland, L. T. G., Kurbel, P. J., Bikoff, E. K., & Robertson, E. J. (2023). A degron-based approach to manipulate Eomes functions in the context of the developing mouse embryo. *Proc Natl Acad Sci U S A*, *120*(44), e2311946120. https://doi.org/10.1073/pnas.2311946120

Blank, I. H. (1953). Further observations on factors which influence the water content of the stratum corneum. *J Invest Dermatol*, *21*(4), 259-271. https://doi.org/10.1038/jid.1953.100

Blanpain, C., Lowry, W. E., Pasolli, H. A., & Fuchs, E. (2006). Canonical notch signaling functions as a commitment switch in the epidermal lineage. *Genes Dev*, *20*(21), 3022-3035. https://doi.org/10.1101/gad.1477606

Bondeson, D. P., Mullin-Bernstein, Z., Oliver, S., Skipper, T. A., Atack, T. C., Bick, N., Ching, M., Guirguis, A. A., Kwon, J., Langan, C., Millson, D., Paolella, B. R., Tran, K., Wie, S. J., Vazquez, F., Tothova, Z., Golub, T. R., Sellers, W. R., & Ianari, A. (2022). Systematic profiling of conditional degron tag technologies for target validation studies. *Nat Commun*, *13*(1), 5495. https://doi.org/10.1038/s41467-022-33246-4

Bouwstra, J. A., & Ponec, M. (2006). The skin barrier in healthy and diseased state. *Biochim Biophys Acta*, *1758*(12), 2080-2095. https://doi.org/10.1016/j.bbamem.2006.06.021

Box, K., Joyce, B. W., & Devenport, D. (2019). Epithelial geometry regulates spindle orientation and progenitor fate during formation of the mammalian epidermis. *Elife*, *8*. https://doi.org/10.7554/eLife.47102

Brabec, R. K., Peters, B. P., Bernstein, I. A., Gray, R. H., & Goldstein, I. J. (1980). Differential lectin binding to cellular membranes in the epidermis of the newborn rat. *Proc Natl Acad Sci U S A*, *77*(1), 477-479. https://www.ncbi.nlm.nih.gov/pubmed/6928640

Branda, C. S., & Dymecki, S. M. (2004). Talking about a revolution: The impact of site-specific recombinases on genetic analyses in mice. *Dev Cell*, *6*(1), 7-28. https://doi.org/10.1016/s1534-5807(03)00399-x

Brandner, J. M., Zorn-Kruppa, M., Yoshida, T., Moll, I., Beck, L. A., & De Benedetto, A. (2015). Epidermal tight junctions in health and disease. *Tissue Barriers*, *3*(1-2), e974451. https://doi.org/10.4161/21688370.2014.974451

Brennan, D., Hu, Y., Joubeh, S., Choi, Y. W., Whitaker-Menezes, D., O'Brien, T., Uitto, J., Rodeck, U., & Mahoney, M. G. (2007). Suprabasal Dsg2 expression in transgenic mouse skin confers a hyperproliferative and apoptosis-resistant phenotype to keratinocytes. *J Cell Sci*, *120*(Pt 5), 758-771. https://doi.org/10.1242/jcs.03392

Brewer, J. A., Sleckman, B. P., Swat, W., & Muglia, L. J. (2002). Green fluorescent protein-glucocorticoid receptor knockin mice reveal dynamic receptor modulation during

thymocyte development. *J Immunol*, *169*(3), 1309-1318. https://doi.org/10.4049/jimmunol.169.3.1309

Byrd, K. M., Lough, K. J., Patel, J. H., Descovich, C. P., Curtis, T. A., & Williams, S. E. (2016). LGN plays distinct roles in oral epithelial stratification, filiform papilla morphogenesis and hair follicle development. *Development*, *143*(15), 2803-2817. https://doi.org/10.1242/dev.136010

Byrne, C., Tainsky, M., & Fuchs, E. (1994). Programming gene expression in developing epidermis. *Development*, *120*(9), 2369-2383. https://doi.org/10.1242/dev.120.9.2369

Cai, W., & Yang, H. (2016). The structure and regulation of Cullin 2 based E3 ubiquitin ligases and their biological functions. *Cell Div*, *11*, 7. https://doi.org/10.1186/s13008-016-0020-7

Candi, E., Rufini, A., Terrinoni, A., Dinsdale, D., Ranalli, M., Paradisi, A., De Laurenzi, V., Spagnoli, L. G., Catani, M. V., Ramadan, S., Knight, R. A., & Melino, G. (2006). Differential roles of p63 isoforms in epidermal development: selective genetic complementation in p63 null mice. *Cell Death Differ*, *13*(6), 1037-1047. https://doi.org/10.1038/sj.cdd.4401926

Carley, E., Stewart, R. M., Zieman, A., Jalilian, I., King, D. E., Zubek, A., Lin, S., Horsley, V., & King, M. C. (2021). The LINC complex transmits integrin-dependent tension to the nuclear lamina and represses epidermal differentiation. *Elife*, *10*. https://doi.org/10.7554/eLife.58541

Chalmers, A. D., Lachani, K., Shin, Y., Sherwood, V., Cho, K. W., & Papalopulu, N. (2006). Grainyhead-like 3, a transcription factor identified in a microarray screen, promotes the specification of the superficial layer of the embryonic epidermis. *Mech Dev*, *123*(9), 702-718. https://doi.org/10.1016/j.mod.2006.04.006

Chen, S. Y., Ishii, M. A., Cheng, B., Otten, A. B. C., & Sun, B. K. (2019). HOPX Is a ZNF750 Target that Promotes Late Epidermal Differentiation. *J Invest Dermatol*, *139*(9), 2039-2042 e2032. https://doi.org/10.1016/j.jid.2019.03.1141

Ciechanover, A., Elias, S., Heller, H., Ferber, S., & Hershko, A. (1980). Characterization of the heat-stable polypeptide of the ATP-dependent proteolytic system from reticulocytes. *J Biol Chem*, *255*(16), 7525-7528. https://www.ncbi.nlm.nih.gov/pubmed/6249802

Clackson, T., Yang, W., Rozamus, L. W., Hatada, M., Amara, J. F., Rollins, C. T., Stevenson, L. F., Magari, S. R., Wood, S. A., Courage, N. L., Lu, X., Cerasoli, F., Jr., Gilman, M., & Holt, D. A. (1998). Redesigning an FKBP-ligand interface to generate chemical dimerizers with novel specificity. *Proc Natl Acad Sci U S A*, *95*(18), 10437-10442. https://doi.org/10.1073/pnas.95.18.10437

Cockburn, K., Annusver, K., Gonzalez, D. G., Ganesan, S., May, D. P., Mesa, K. R., Kawaguchi, K., Kasper, M., & Greco, V. (2022). Gradual differentiation uncoupled from cell cycle exit generates heterogeneity in the epidermal stem cell layer. *Nat Cell Biol*, *24*(12), 1692-1700. https://doi.org/10.1038/s41556-022-01021-8

Cong, L., Ran, F. A., Cox, D., Lin, S., Barretto, R., Habib, N., Hsu, P. D., Wu, X., Jiang, W., Marraffini, L. A., & Zhang, F. (2013). Multiplex genome engineering using CRISPR/Cas systems. *Science*, *339*(6121), 819-823. https://doi.org/10.1126/science.1231143

D'Angelo, M. A., Raices, M., Panowski, S. H., & Hetzer, M. W. (2009). Age-dependent deterioration of nuclear pore complexes causes a loss of nuclear integrity in postmitotic cells. *Cell*, *136*(2), 284-295. https://doi.org/10.1016/j.cell.2008.11.037

Dai, X., Schonbaum, C., Degenstein, L., Bai, W., Mahowald, A., & Fuchs, E. (1998). The ovo gene required for cuticle formation and oogenesis in flies is involved in hair formation and spermatogenesis in mice. *Genes & Development*, *12*(21), 3452-3463. https://doi.org/10.1101/gad.12.21.3452

Damen, M., Wirtz, L., Soroka, E., Khatif, H., Kukat, C., Simons, B. D., & Bazzi, H. (2021). High proliferation and delamination during skin epidermal stratification. *Nat Commun*, *12*(1), 3227. https://doi.org/10.1038/s41467-021-23386-4

De Groote, P., Tran, H. T., Fransen, M., Tanghe, G., Urwyler, C., De Craene, B., Leurs, K., Gilbert, B., Van Imschoot, G., De Rycke, R., Guérin, C. J., Holland, P., Berx, G., Vandenabeele, P., Lippens, S., Vleminckx, K., & Declercq, W. (2015). A novel RIPK4–IRF6 connection is required to prevent epithelial fusions characteristic for popliteal pterygium syndromes. *Cell Death & Differentiation*, *22*(6), 1012-1024. https://doi.org/10.1038/cdd.2014.191

de Guzman Strong, C., Wertz, P. W., Wang, C., Yang, F., Meltzer, P. S., Andl, T., Millar, S. E., Ho, I. C., Pai, S. Y., & Segre, J. A. (2006). Lipid defect underlies selective skin barrier impairment of an epidermal-specific deletion of Gata-3. *J Cell Biol*, *175*(4), 661-670. https://doi.org/10.1083/jcb.200605057

den Hollander, L., Han, H., de Winter, M., Svensson, L., Masich, S., Daneholt, B., & Norlen, L. (2016). Skin Lamellar Bodies are not Discrete Vesicles but Part of a Tubuloreticular Network. *Acta Derm Venereol*, *96*(3), 303-308. https://doi.org/10.2340/00015555-2249

DuBrul, E. F. (1972). Fine structure of epidermal differentiation in the mouse. *J Exp Zool*, *181*(2), 145-158. https://doi.org/10.1002/jez.1401810202

Eckhart, L., Lippens, S., Tschachler, E., & Declercq, W. (2013). Cell death by cornification. *Biochim Biophys Acta*, *1833*(12), 3471-3480. https://doi.org/10.1016/j.bbamcr.2013.06.010

Elbashir, S. M., Harborth, J., Lendeckel, W., Yalcin, A., Weber, K., & Tuschl, T. (2001). Duplexes of 21-nucleotide RNAs mediate RNA interference in cultured mammalian cells. *Nature*, *411*(6836), 494-498. https://doi.org/10.1038/35078107

Elias, P. M., Cullander, C., Mauro, T., Rassner, U., Komuves, L., Brown, B. E., & Menon, G. K. (1998). The secretory granular cell: the outermost granular cell as a specialized secretory cell. *J Investig Dermatol Symp Proc*, *3*(2), 87-100. https://doi.org/10.1038/jidsymp.1998.20

Elias, P. M., & Wakefield, J. S. (2014). Mechanisms of abnormal lamellar body secretion and the dysfunctional skin barrier in patients with atopic dermatitis. *J Allergy Clin Immunol*, *134*(4), 781-791 e781. https://doi.org/10.1016/j.jaci.2014.05.048

Engler, A. J., Sen, S., Sweeney, H. L., & Discher, D. E. (2006). Matrix elasticity directs stem cell lineage specification. *Cell*, *126*(4), 677-689. https://doi.org/10.1016/j.cell.2006.06.044

Feingold, K. R. (2012). Lamellar bodies: the key to cutaneous barrier function. *J Invest Dermatol*, *132*(8), 1951-1953. https://doi.org/10.1038/jid.2012.177

Feng, X., Li, G. Y., Ramier, A., Eltony, A. M., & Yun, S. H. (2022). In vivo stiffness measurement of epidermis, dermis, and hypodermis using broadband Rayleigh-wave optical coherence elastography. *Acta Biomater*. https://doi.org/10.1016/j.actbio.2022.04.030

Festa, E., Fretz, J., Berry, R., Schmidt, B., Rodeheffer, M., Horowitz, M., & Horsley, V. (2011). Adipocyte lineage cells contribute to the skin stem cell niche to drive hair cycling. *Cell*, *146*(5), 761-771. https://doi.org/10.1016/j.cell.2011.07.019

Fiore, V. F., Krajnc, M., Quiroz, F. G., Levorse, J., Pasolli, H. A., Shvartsman, S. Y., & Fuchs, E. (2020). Mechanics of a multilayer epithelium instruct tumour architecture and function. *Nature*, *585*(7825), 433-439. https://doi.org/10.1038/s41586-020-2695-9

Flora, P., & Ezhkova, E. (2020). Regulatory mechanisms governing epidermal stem cell function during development and homeostasis. *Development*, *147*(22), dev194100. https://doi.org/10.1242/dev.194100

Foote, H. P., Sumigray, K. D., & Lechler, T. (2013). FRAP Analysis Reveals Stabilization of Adhesion Structures in the Epidermis Compared to Cultured Keratinocytes. *PLoS ONE*, *8*(8), e71491. https://doi.org/10.1371/journal.pone.0071491

Fornasiero, E. F., & Savas, J. N. (2023). Determining and interpreting protein lifetimes in mammalian tissues. *Trends Biochem Sci*, *48*(2), 106-118. https://doi.org/10.1016/j.tibs.2022.08.011

Freeman, S. C., & Sonthalia, S. (2024). Histology, Keratohyalin Granules. In *StatPearls*. https://www.ncbi.nlm.nih.gov/pubmed/30725734

Fuchs, E. (2007). Scratching the surface of skin development. *Nature*, *445*(7130), 834-842. https://doi.org/10.1038/nature05659

Fulcher, L. J., Macartney, T., Bozatzi, P., Hornberger, A., Rojas-Fernandez, A., & Sapkota, G. P. (2016). An affinity-directed protein missile system for targeted proteolysis. *Open Biol*, *6*(10). https://doi.org/10.1098/rsob.160255

Furue, M. (2020). Regulation of Filaggrin, Loricrin, and Involucrin by IL-4, IL-13, IL-17A, IL-22, AHR, and NRF2: Pathogenic Implications in Atopic Dermatitis. *International Journal of Molecular Sciences*, *21*(15), 5382. https://doi.org/10.3390/ijms21155382

Furuse, M., Hata, M., Furuse, K., Yoshida, Y., Haratake, A., Sugitani, Y., Noda, T., Kubo, A., & Tsukita, S. (2002). Claudin-based tight junctions are crucial for the mammalian

epidermal barrier: a lesson from claudin-1-deficient mice. *J Cell Biol*, *156*(6), 1099-1111. https://doi.org/10.1083/jcb.200110122

Gaj, T., Sirk, S. J., Shui, S. L., & Liu, J. (2016). Genome-Editing Technologies: Principles and Applications. *Cold Spring Harb Perspect Biol*, *8*(12). https://doi.org/10.1101/cshperspect.a023754

Gao, T., Zhou, D., Yang, C., Singh, T., Penzo-Mendez, A., Maddipati, R., Tzatsos, A., Bardeesy, N., Avruch, J., & Stanger, B. Z. (2013). Hippo signaling regulates differentiation and maintenance in the exocrine pancreas. *Gastroenterology*, *144*(7), 1543-1553, 1553 e1541. https://doi.org/10.1053/j.gastro.2013.02.037

Gdula, M. R., Poterlowicz, K., Mardaryev, A. N., Sharov, A. A., Peng, Y., Fessing, M. Y., & Botchkarev, V. A. (2013). Remodeling of three-dimensional organization of the nucleus during terminal keratinocyte differentiation in the epidermis. *J Invest Dermatol*, *133*(9), 2191-2201. https://doi.org/10.1038/jid.2013.66

Gene Ontology, C., Aleksander, S. A., Balhoff, J., Carbon, S., Cherry, J. M., Drabkin, H. J., Ebert, D., Feuermann, M., Gaudet, P., Harris, N. L., Hill, D. P., Lee, R., Mi, H., Moxon, S., Mungall, C. J., Muruganugan, A., Mushayahama, T., Sternberg, P. W., Thomas, P. D.,…Westerfield, M. (2023). The Gene Ontology knowledgebase in 2023. *Genetics*, *224*(1). https://doi.org/10.1093/genetics/iyad031

Getsios, S., Simpson, C. L., Kojima, S.-I., Harmon, R., Sheu, L. J., Dusek, R. L., Cornwell, M., & Green, K. J. (2009). Desmoglein 1–dependent suppression of EGFR signaling promotes epidermal differentiation and morphogenesis. *Journal of Cell Biology*, *185*(7), 1243-1258. https://doi.org/10.1083/jcb.200809044

Gilbert, L. A., Larson, M. H., Morsut, L., Liu, Z., Brar, G. A., Torres, S. E., Stern-Ginossar, N., Brandman, O., Whitehead, E. H., Doudna, J. A., Lim, W. A., Weissman, J. S., & Qi, L. S. (2013). CRISPR-mediated modular RNA-guided regulation of transcription in eukaryotes. *Cell*, *154*(2), 442-451. https://doi.org/10.1016/j.cell.2013.06.044

Goldie, S. J., Cottle, D. L., Tan, F. H., Roslan, S., Srivastava, S., Brady, R., Partridge, D. D., Auden, A., Smyth, I. M., Jane, S. M., Dworkin, S., & Darido, C. (2018). Loss of GRHL3 leads to TARC/CCL17-mediated keratinocyte proliferation in the epidermis. *Cell Death Dis*, *9*(11), 1072. https://doi.org/10.1038/s41419-018-0901-6

Gordon, W. M., Zeller, M. D., Klein, R. H., Swindell, W. R., Ho, H., Espetia, F., Gudjonsson, J. E., Baldi, P. F., & Andersen, B. (2014). A GRHL3-regulated repair pathway suppresses immune-mediated epidermal hyperplasia. *J Clin Invest*, *124*(12), 5205-5218. https://doi.org/10.1172/JCI77138

Gossen, M., & Bujard, H. (1992). Tight control of gene expression in mammalian cells by tetracycline-responsive promoters. *Proc Natl Acad Sci U S A*, *89*(12), 5547-5551. https://doi.org/10.1073/pnas.89.12.5547

Gronostajski, R. M., & Sadowski, P. D. (1985). The FLP recombinase of the Saccharomyces cerevisiae 2 microns plasmid attaches covalently to DNA via a phosphotyrosyl linkage. *Mol Cell Biol*, *5*(11), 3274-3279. https://doi.org/10.1128/mcb.5.11.3274-3279.1985

Haensel, D., Jin, S., Sun, P., Cinco, R., Dragan, M., Nguyen, Q., Cang, Z., Gong, Y., Vu, R., Maclean, A. L., Kessenbrock, K., Gratton, E., Nie, Q., & Dai, X. (2020). Defining Epidermal Basal Cell States during Skin Homeostasis and Wound Healing Using Single-Cell Transcriptomics. *Cell Reports*, *30*(11), 3932-3947.e3936. https://doi.org/10.1016/j.celrep.2020.02.091

Haftek, M. (2014). 'Memory' of the stratum corneum: exploration of the epidermis' past. *Br J Dermatol*, *171 Suppl 3*, 6-9. https://doi.org/10.1111/bjd.13243

Hatzfeld, M., Keil, R., & Magin, T. M. (2017). Desmosomes and Intermediate Filaments: Their Consequences for Tissue Mechanics. *Cold Spring Harbor Perspectives in Biology*, *9*(6), a029157. https://doi.org/10.1101/cshperspect.a029157

Heo, S., Diering, G. H., Na, C. H., Nirujogi, R. S., Bachman, J. L., Pandey, A., & Huganir, R. L. (2018). Identification of long-lived synaptic proteins by proteomic analysis of synaptosome protein turnover. *Proc Natl Acad Sci U S A*, *115*(16), E3827-E3836. https://doi.org/10.1073/pnas.1720956115

Hershko, A., Eytan, E., Ciechanover, A., & Haas, A. L. (1982). Immunochemical analysis of the turnover of ubiquitin-protein conjugates in intact cells. Relationship to the breakdown of abnormal proteins. *J Biol Chem*, *257*(23), 13964-13970. https://www.ncbi.nlm.nih.gov/pubmed/6292216

Hershko, A., Heller, H., Elias, S., & Ciechanover, A. (1983). Components of ubiquitin-protein ligase system. Resolution, affinity purification, and role in protein breakdown. *J Biol Chem*, *258*(13), 8206-8214. https://www.ncbi.nlm.nih.gov/pubmed/6305978

Hinnant, T., Ning, W., & Lechler, T. (2024). Compartment specific responses to contractility in the small intestinal epithelium. *PLoS Genet*, *20*(3), e1010899. https://doi.org/10.1371/journal.pgen.1010899

Hochedlinger, K., Yamada, Y., Beard, C., & Jaenisch, R. (2005). Ectopic expression of Oct-4 blocks progenitor-cell differentiation and causes dysplasia in epithelial tissues. *Cell*, *121*(3), 465-477. https://doi.org/10.1016/j.cell.2005.02.018

Hochstrasser, M. (1995). Ubiquitin, proteasomes, and the regulation of intracellular protein degradation. *Curr Opin Cell Biol*, *7*(2), 215-223. https://doi.org/10.1016/0955-0674(95)80031-x

Holland, P., Willis, C., Kanaly, S., Glaccum, M., Warren, A., Charrier, K., Murison, J., Derry, J., Virca, G., Bird, T., & Peschon, J. (2002). RIP4 is an ankyrin repeat-containing kinase essential for keratinocyte differentiation. *Curr Biol*, *12*(16), 1424-1428. https://doi.org/10.1016/s0960-9822(02)01075-8

Housden, B. E., Muhar, M., Gemberling, M., Gersbach, C. A., Stainier, D. Y., Seydoux, G., Mohr, S. E., Zuber, J., & Perrimon, N. (2017). Loss-of-function genetic tools for animal models: cross-species and cross-platform differences. *Nat Rev Genet*, *18*(1), 24-40. https://doi.org/10.1038/nrg.2016.118

Hu, Y., Baud, V., Delhase, M., Zhang, P., Deerinck, T., Ellisman, M., Johnson, R., & Karin, M. (1999). Abnormal morphogenesis but intact IKK activation in mice lacking the IKKalpha

subunit of IkappaB kinase. *Science*, *284*(5412), 316-320. https://doi.org/10.1126/science.284.5412.316

Huebner, A. J., Dai, D., Morasso, M., Schmidt, E. E., Schafer, M., Werner, S., & Roop, D. R. (2012). Amniotic fluid activates the nrf2/keap1 pathway to repair an epidermal barrier defect in utero [Research Support, N.I.H., Extramural
Research Support, Non-U.S. Gov't]. *Dev Cell*, *23*(6), 1238-1246. https://doi.org/10.1016/j.devcel.2012.11.002

Ihrie, R. A., Marques, M. R., Nguyen, B. T., Horner, J. S., Papazoglu, C., Bronson, R. T., Mills, A. A., & Attardi, L. D. (2005). Perp is a p63-regulated gene essential for epithelial integrity. *Cell*, *120*(6), 843-856. https://doi.org/10.1016/j.cell.2005.01.008

Ingraham, C. R., Kinoshita, A., Kondo, S., Yang, B., Sajan, S., Trout, K. J., Malik, M. I., Dunnwald, M., Goudy, S. L., Lovett, M., Murray, J. C., & Schutte, B. C. (2006). Abnormal skin, limb and craniofacial morphogenesis in mice deficient for interferon regulatory factor 6 (Irf6). *Nature Genetics*, *38*(11), 1335-1340. https://doi.org/10.1038/ng1903

Ishida-Yamamoto, A., Deraison, C., Bonnart, C., Bitoun, E., Robinson, R., O'Brien, T. J., Wakamatsu, K., Ohtsubo, S., Takahashi, H., Hashimoto, Y., Dopping-Hepenstal, P. J., McGrath, J. A., Iizuka, H., Richard, G., & Hovnanian, A. (2005). LEKTI is localized in lamellar granules, separated from KLK5 and KLK7, and is secreted in the extracellular spaces of the superficial stratum granulosum. *J Invest Dermatol*, *124*(2), 360-366. https://doi.org/10.1111/j.0022-202X.2004.23583.x

Ishida-Yamamoto, A., & Igawa, S. (2015). The biology and regulation of corneodesmosomes. *Cell Tissue Res*, *360*(3), 477-482. https://doi.org/10.1007/s00441-014-2037-z

Ishida-Yamamoto, A., Igawa, S., & Kishibe, M. (2018). Molecular basis of the skin barrier structures revealed by electron microscopy. *Exp Dermatol*, *27*(8), 841-846. https://doi.org/10.1111/exd.13674

Ishida-Yamamoto, A., Simon, M., Kishibe, M., Miyauchi, Y., Takahashi, H., Yoshida, S., O'Brien, T. J., Serre, G., & Iizuka, H. (2004). Epidermal lamellar granules transport different cargoes as distinct aggregates. *J Invest Dermatol*, *122*(5), 1137-1144. https://doi.org/10.1111/j.0022-202X.2004.22515.x

Itoh, M., Tsukita, S., Yamazaki, Y., & Sugimoto, H. (2012). Rho GTP exchange factor ARHGEF11 regulates the integrity of epithelial junctions by connecting ZO-1 and RhoA-myosin II signaling. *Proc Natl Acad Sci U S A*, *109*(25), 9905-9910. https://doi.org/10.1073/pnas.1115063109

Jackson, B. W., Grund, C., Winter, S., Franke, W. W., & Illmensee, K. (1981). Formation of cytoskeletal elements during mouse embryogenesis. II. Epithelial differentiation and intermediate-sized filaments in early postimplantation embryos. *Differentiation*, *20*(3), 203-216. https://doi.org/10.1111/j.1432-0436.1981.tb01177.x

Jacob, T., Annusver, K., Czarnewski, P., Dalessandri, T., Kalk, C., Levra Levron, C., Campama Sanz, N., Kastriti, M. E., Mikkola, M. L., Rendl, M., Lichtenberger, B. M., Donati, G., Bjorklund, A. K., & Kasper, M. (2023). Molecular and spatial landmarks of early mouse

skin development. *Dev Cell*, *58*(20), 2140-2162 e2145. https://doi.org/10.1016/j.devcel.2023.07.015

Johnson, J. L., Najor, N. A., & Green, K. J. (2014). Desmosomes: Regulators of Cellular Signaling and Adhesion in Epidermal Health and Disease. *Cold Spring Harbor Perspectives in Medicine*, *4*(11), a015297-a015297. https://doi.org/10.1101/cshperspect.a015297

Jonca, N., Guerrin, M., Hadjiolova, K., Caubet, C., Gallinaro, H., Simon, M., & Serre, G. (2002). Corneodesmosin, a component of epidermal corneocyte desmosomes, displays homophilic adhesive properties. *J Biol Chem*, *277*(7), 5024-5029. https://doi.org/10.1074/jbc.M108438200

Jonca, N., Leclerc, E. A., Caubet, C., Simon, M., Guerrin, M., & Serre, G. (2011). Corneodesmosomes and corneodesmosin: from the stratum corneum cohesion to the pathophysiology of genodermatoses. *Eur J Dermatol*, *21 Suppl 2*, 35-42. https://doi.org/10.1684/ejd.2011.1264

Joodaki, H., & Panzer, M. B. (2018). Skin mechanical properties and modeling: A review. *Proc Inst Mech Eng H*, *232*(4), 323-343. https://doi.org/10.1177/0954411918759801

Kamura, T., Maenaka, K., Kotoshiba, S., Matsumoto, M., Kohda, D., Conaway, R. C., Conaway, J. W., & Nakayama, K. I. (2004). VHL-box and SOCS-box domains determine binding specificity for Cul2-Rbx1 and Cul5-Rbx2 modules of ubiquitin ligases. *Genes & Development*, *18*(24), 3055-3065. https://doi.org/10.1101/gad.1252404

Kashgari, G., Venkatesh, S., Refuerzo, S., Pham, B., Bayat, A., Klein, R. H., Ramos, R., Ta, A. P., Plikus, M. V., Wang, P. H., & Andersen, B. (2021). GRHL3 activates FSCN1 to relax cell-cell adhesions between migrating keratinocytes during wound reepithelialization. *JCI Insight*, *6*(17). https://doi.org/10.1172/jci.insight.142577

Kimura-Yoshida, C., Mochida, K., Nakaya, M.-A., Mizutani, T., & Matsuo, I. (2018). Cytoplasmic localization of GRHL3 upon epidermal differentiation triggers cell shape change for epithelial morphogenesis. *Nature Communications*, *9*(1). https://doi.org/10.1038/s41467-018-06171-8

Knight, A. S., Schutte, B. C., Jiang, R., & Dixon, M. J. (2006). Developmental expression analysis of the mouse and chick orthologues of IRF6: the gene mutated in Van der Woude syndrome. *Dev Dyn*, *235*(5), 1441-1447. https://doi.org/10.1002/dvdy.20598

Kos, C. H. (2004). Cre/loxP system for generating tissue-specific knockout mouse models. *Nutr Rev*, *62*(6 Pt 1), 243-246. https://doi.org/10.1301/nr2004.jun243-246

Koster, M. I., Dai, D., Marinari, B., Sano, Y., Costanzo, A., Karin, M., & Roop, D. R. (2007). p63 induces key target genes required for epidermal morphogenesis. *Proceedings of the National Academy of Sciences*, *104*(9), 3255-3260. https://doi.org/10.1073/pnas.0611376104

Koster, M. I., Kim, S., Huang, J., Williams, T., & Roop, D. R. (2006). TAp63alpha induces AP-2gamma as an early event in epidermal morphogenesis. *Dev Biol*, *289*(1), 253-261. https://doi.org/10.1016/j.ydbio.2005.10.041

Koster, M. I., Kim, S., Mills, A. A., Demayo, F. J., & Roop, D. R. (2004). p63 is the molecular switch for initiation of an epithelial stratification program. *Genes & Development*, *18*(2), 126-131. https://doi.org/10.1101/gad.1165104

Koster, M. I., & Roop, D. R. (2005). Asymmetric cell division in skin development: a new look at an old observation. *Dev Cell*, *9*(4), 444-446. https://doi.org/10.1016/j.devcel.2005.09.009

Kubo, A., Nagao, K., Yokouchi, M., Sasaki, H., & Amagai, M. (2009). External antigen uptake by Langerhans cells with reorganization of epidermal tight junction barriers. *J Exp Med*, *206*(13), 2937-2946. https://doi.org/10.1084/jem.20091527

Kwa, M. Q., Huynh, J., Aw, J., Zhang, L., Nguyen, T., Reynolds, E. C., Sweet, M. J., Hamilton, J. A., & Scholz, G. M. (2014). Receptor-interacting Protein Kinase 4 and Interferon Regulatory Factor 6 Function as a Signaling Axis to Regulate Keratinocyte Differentiation. *Journal of Biological Chemistry*, *289*(45), 31077-31087. https://doi.org/10.1074/jbc.m114.589382

Lai, E. C. (2004). Notch signaling: control of cell communication and cell fate. *Development*, *131*(5), 965-973. https://doi.org/10.1242/dev.01074

Lambeth, T. R., Riggs, D. L., Talbert, L. E., Tang, J., Coburn, E., Kang, A. S., Noll, J., Augello, C., Ford, B. D., & Julian, R. R. (2019). Spontaneous Isomerization of Long-Lived Proteins Provides a Molecular Mechanism for the Lysosomal Failure Observed in Alzheimer's Disease. *ACS Cent Sci*, *5*(8), 1387-1395. https://doi.org/10.1021/acscentsci.9b00369

Landmann, L. (1986). Epidermal permeability barrier: transformation of lamellar granule-disks into intercellular sheets by a membrane-fusion process, a freeze-fracture study. *J Invest Dermatol*, *87*(2), 202-209. https://doi.org/10.1111/1523-1747.ep12695343

Latorre, V., Sevilla, L. M., Sanchis, A., & Perez, P. (2013). Selective ablation of glucocorticoid receptor in mouse keratinocytes increases susceptibility to skin tumorigenesis. *J Invest Dermatol*, *133*(12), 2771-2779. https://doi.org/10.1038/jid.2013.255

Laurikkala, J., Mikkola, M. L., James, M., Tummers, M., Mills, A. A., & Thesleff, I. (2006). p63 regulates multiple signalling pathways required for ectodermal organogenesis and differentiation. *Development*, *133*(8), 1553-1563. https://doi.org/10.1242/dev.02325

le Duc, Q., Shi, Q., Blonk, I., Sonnenberg, A., Wang, N., Leckband, D., & de Rooij, J. (2010). Vinculin potentiates E-cadherin mechanosensing and is recruited to actin-anchored sites within adherens junctions in a myosin II-dependent manner. *J Cell Biol*, *189*(7), 1107-1115. https://doi.org/10.1083/jcb.201001149

Le, H. Q., Ghatak, S., Yeung, C. Y., Tellkamp, F., Gunschmann, C., Dieterich, C., Yeroslaviz, A., Habermann, B., Pombo, A., Niessen, C. M., & Wickstrom, S. A. (2016). Mechanical regulation of transcription controls Polycomb-mediated gene silencing during lineage commitment. *Nat Cell Biol*, *18*(8), 864-875. https://doi.org/10.1038/ncb3387

Le, Y., & Sauer, B. (2000). Conditional Gene Knockout Using Cre Recombinase. https://doi.org/10.1385/1-59259-065-9:477

Lechler, T., & Fuchs, E. (2005). Asymmetric cell divisions promote stratification and differentiation of mammalian skin. *Nature*, *437*(7056), 275-280. https://doi.org/10.1038/nature03922

Lechler, T., & Fuchs, E. (2005). Asymmetric cell divisions promote stratification and differentiation of mammalian skin. *Nature*, *437*(7056), 275-280. https://doi.org/10.1038/nature03922

Lechler, T., & Fuchs, E. (2007). Desmoplakin: an unexpected regulator of microtubule organization in the epidermis. *J Cell Biol*, *176*(2), 147-154. https://doi.org/10.1083/jcb.200609109

Li, S., Teegarden, A., Bauer, E. M., Choi, J., Messaddeq, N., Hendrix, D. A., Ganguli-Indra, G., Leid, M., & Indra, A. K. (2017). Transcription Factor CTIP1/ BCL11A Regulates Epidermal Differentiation and Lipid Metabolism During Skin Development. *Sci Rep*, *7*(1), 13427. https://doi.org/10.1038/s41598-017-13347-7

Li, Y., Giovannini, S., Wang, T., Fang, J., Li, P., Shao, C., Wang, Y., Agostini, M., Bove, P., Mauriello, A., Novelli, G., Piacentini, M., Rovella, V., Scimeca, M., Sica, G., Sun, Q., Tisone, G., Shi, Y., Candi, E.,…Bernassola, F. (2023). p63: a crucial player in epithelial stemness regulation. *Oncogene*, *42*(46), 3371-3384. https://doi.org/10.1038/s41388-023-02859-4

Lin, Z., Jin, S., Chen, J., Li, Z., Lin, Z., Tang, L., Nie, Q., & Andersen, B. (2020). Murine interfollicular epidermal differentiation is gradualistic with GRHL3 controlling progression from stem to transition cell states. *Nat Commun*, *11*(1), 5434. https://doi.org/10.1038/s41467-020-19234-6

Lombardi, M. L., & Lammerding, J. (2011). Keeping the LINC: the importance of nucleocytoskeletal coupling in intracellular force transmission and cellular function. *Biochem Soc Trans*, *39*(6), 1729-1734. https://doi.org/10.1042/BST20110686

Lopez-Pajares, V., Qu, K., Zhang, J., Webster, D. E., Barajas, B. C., Siprashvili, Z., Zarnegar, B. J., Boxer, L. D., Rios, E. J., Tao, S., Kretz, M., & Khavari, P. A. (2015). A LncRNA-MAF:MAFB transcription factor network regulates epidermal differentiation. *Dev Cell*, *32*(6), 693-706. https://doi.org/10.1016/j.devcel.2015.01.028

Macdonald, L., Taylor, G. C., Brisbane, J. M., Christodoulou, E., Scott, L., Kriegsheim, A. v., Rossant, J., Gu, B., & Wood, A. J. (2022). Rapid and specific degradation of endogenous proteins in mouse models using auxin-inducible degrons. *eLife*, *11*. https://doi.org/10.7554/eLife.77987

Macdonald, L., Taylor, G. C., Brisbane, J. M., Christodoulou, E., Scott, L., von Kriegsheim, A., Rossant, J., Gu, B., & Wood, A. J. (2022). Rapid and specific degradation of endogenous proteins in mouse models using auxin-inducible degrons. *Elife*, *11*. https://doi.org/10.7554/eLife.77987

Mahanty, S., & Setty, S. R. G. (2021). Epidermal Lamellar Body Biogenesis: Insight Into the Roles of Golgi and Lysosomes. *Front Cell Dev Biol*, *9*, 701950. https://doi.org/10.3389/fcell.2021.701950

Mali, P., Yang, L., Esvelt, K. M., Aach, J., Guell, M., DiCarlo, J. E., Norville, J. E., & Church, G. M. (2013). RNA-guided human genome engineering via Cas9. *Science*, *339*(6121), 823-826. https://doi.org/10.1126/science.1232033

Mardaryev, A. N., Gdula, M. R., Yarker, J. L., Emelianov, V. U., Poterlowicz, K., Sharov, A. A., Sharova, T. Y., Scarpa, J. A., Joffe, B., Solovei, I., Chambon, P., Botchkarev, V. A., & Fessing, M. Y. (2014). p63 and Brg1 control developmentally regulated higher-order chromatin remodelling at the epidermal differentiation complex locus in epidermal progenitor cells. *Development*, *141*(1), 101-111. https://doi.org/10.1242/dev.103200

Matsui, T. (2023). Epidermal Barrier Development via Corneoptosis: A Unique Form of Cell Death in Stratum Granulosum Cells. *J Dev Biol*, *11*(4). https://doi.org/10.3390/jdb11040043

Matsui, T., Kadono-Maekubo, N., Suzuki, Y., Furuichi, Y., Shiraga, K., Sasaki, H., Ishida, A., Takahashi, S., Okada, T., Toyooka, K., Sharif, J., Abe, T., Kiyonari, H., Tominaga, M., Miyawaki, A., & Amagai, M. (2021). A unique mode of keratinocyte death requires intracellular acidification. *Proc Natl Acad Sci U S A*, *118*(17). https://doi.org/10.1073/pnas.2020722118

Menon, G. K., Grayson, S., & Elias, P. M. (1985). Ionic calcium reservoirs in mammalian epidermis: ultrastructural localization by ion-capture cytochemistry. *J Invest Dermatol*, *84*(6), 508-512. https://doi.org/10.1111/1523-1747.ep12273485

Metsalu, T., & Vilo, J. (2015). ClustVis: a web tool for visualizing clustering of multivariate data using Principal Component Analysis and heatmap. *Nucleic Acids Res*, *43*(W1), W566-570. https://doi.org/10.1093/nar/gkv468

Meyer-ter-Vehn, T., Sieprath, S., Katzenberger, B., Gebhardt, S., Grehn, F., & Schlunck, G. (2006). Contractility as a prerequisite for TGF-beta-induced myofibroblast transdifferentiation in human tenon fibroblasts. *Invest Ophthalmol Vis Sci*, *47*(11), 4895-4904. https://doi.org/10.1167/iovs.06-0118

Miller, J. C., Tan, S., Qiao, G., Barlow, K. A., Wang, J., Xia, D. F., Meng, X., Paschon, D. E., Leung, E., Hinkley, S. J., Dulay, G. P., Hua, K. L., Ankoudinova, I., Cost, G. J., Urnov, F. D., Zhang, H. S., Holmes, M. C., Zhang, L., Gregory, P. D., & Rebar, E. J. (2011). A TALE nuclease architecture for efficient genome editing. *Nat Biotechnol*, *29*(2), 143-148. https://doi.org/10.1038/nbt.1755

Mills, A. A., Zheng, B., Wang, X.-J., Vogel, H., Roop, D. R., & Bradley, A. (1999). p63 is a p53 homologue required for limb and epidermal morphogenesis. *Nature*, *398*(6729), 708-713. https://doi.org/10.1038/19531

Miroshnikova, Y. A., Le, H. Q., Schneider, D., Thalheim, T., Rubsam, M., Bremicker, N., Polleux, J., Kamprad, N., Tarantola, M., Wang, I., Balland, M., Niessen, C. M., Galle, J., & Wickstrom, S. A. (2018). Adhesion forces and cortical tension couple cell proliferation and differentiation to drive epidermal stratification. *Nat Cell Biol*, *20*(1), 69-80. https://doi.org/10.1038/s41556-017-0005-z

Mischke, D., Korge, B. P., Marenholz, I., Volz, A., & Ziegler, A. (1996). Genes encoding structural proteins of epidermal cornification and S100 calcium-binding proteins form a

gene complex ("epidermal differentiation complex") on human chromosome 1q21. *J Invest Dermatol, 106*(5), 989-992. https://doi.org/10.1111/1523-1747.ep12338501

Miyai, M., Hamada, M., Moriguchi, T., Hiruma, J., Kamitani-Kawamoto, A., Watanabe, H., Hara-Chikuma, M., Takahashi, K., Takahashi, S., & Kataoka, K. (2016a). Transcription Factor MafB Coordinates Epidermal Keratinocyte Differentiation. *J Invest Dermatol, 136*(9), 1848-1857. https://doi.org/10.1016/j.jid.2016.05.088

Miyai, M., Hamada, M., Moriguchi, T., Hiruma, J., Kamitani-Kawamoto, A., Watanabe, H., Hara-Chikuma, M., Takahashi, K., Takahashi, S., & Kataoka, K. (2016b). Transcription Factor MafB Coordinates Epidermal Keratinocyte Differentiation. *J Invest Dermatol, 136*(9), 1848-1857. https://doi.org/10.1016/j.jid.2016.05.088

Montpetit, A., Cote, S., Brustein, E., Drouin, C. A., Lapointe, L., Boudreau, M., Meloche, C., Drouin, R., Hudson, T. J., Drapeau, P., & Cossette, P. (2008). Disruption of AP1S1, causing a novel neurocutaneous syndrome, perturbs development of the skin and spinal cord. *PLoS Genet, 4*(12), e1000296. https://doi.org/10.1371/journal.pgen.1000296

Moreci, R. S., & Lechler, T. (2020). Epidermal structure and differentiation. *Curr Biol, 30*(4), R144-R149. https://doi.org/10.1016/j.cub.2020.01.004

Moreci, R. S., & Lechler, T. (2021). KIF18B is a cell type-specific regulator of spindle orientation in the epidermis. *Mol Biol Cell, 32*(21), ar29. https://doi.org/10.1091/mbc.E21-06-0291

Moriyama, M., Durham, A.-D., Moriyama, H., Hasegawa, K., Nishikawa, S.-I., Radtke, F., & Osawa, M. (2008). Multiple Roles of Notch Signaling in the Regulation of Epidermal Development. *Developmental Cell, 14*(4), 594-604. https://doi.org/10.1016/j.devcel.2008.01.017

Muroyama, A., & Lechler, T. (2017). A transgenic toolkit for visualizing and perturbing microtubules reveals unexpected functions in the epidermis. *Elife, 6*. https://doi.org/10.7554/eLife.29834

Muroyama, A., Terwilliger, M., Dong, B., Suh, H., & Lechler, T. (2018). Genetically induced microtubule disruption in the mouse intestine impairs intracellular organization and transport. *Mol Biol Cell, 29*(13), 1533-1541. https://doi.org/10.1091/mbc.E18-01-0057

Nabet, B., Ferguson, F. M., Seong, B. K. A., Kuljanin, M., Leggett, A. L., Mohardt, M. L., Robichaud, A., Conway, A. S., Buckley, D. L., Mancias, J. D., Bradner, J. E., Stegmaier, K., & Gray, N. S. (2020). Rapid and direct control of target protein levels with VHL-recruiting dTAG molecules. *Nat Commun, 11*(1), 4687. https://doi.org/10.1038/s41467-020-18377-w

Nabet, B., Roberts, J. M., Buckley, D. L., Paulk, J., Dastjerdi, S., Yang, A., Leggett, A. L., Erb, M. A., Lawlor, M. A., Souza, A., Scott, T. G., Vittori, S., Perry, J. A., Qi, J., Winter, G. E., Wong, K. K., Gray, N. S., & Bradner, J. E. (2018). The dTAG system for immediate and target-specific protein degradation. *Nat Chem Biol, 14*(5), 431-441. https://doi.org/10.1038/s41589-018-0021-8

Nair, M., Teng, A., Bilanchone, V., Agrawal, A., Li, B., & Dai, X. (2006). Ovol1 regulates the growth arrest of embryonic epidermal progenitor cells and represses c-myc transcription. *J Cell Biol*, *173*(2), 253-264. https://doi.org/10.1083/jcb.200508196

Narangifard, A., den Hollander, L., Wennberg, C. L., Lundborg, M., Lindahl, E., Iwai, I., Han, H., Masich, S., Daneholt, B., & Norlen, L. (2018). Human skin barrier formation takes place via a cubic to lamellar lipid phase transition as analyzed by cryo-electron microscopy and EM-simulation. *Exp Cell Res*, *366*(2), 139-151. https://doi.org/10.1016/j.yexcr.2018.03.010

Narangifard, A., Wennberg, C. L., den Hollander, L., Iwai, I., Han, H., Lundborg, M., Masich, S., Lindahl, E., Daneholt, B., & Norlen, L. (2021). Molecular Reorganization during the Formation of the Human Skin Barrier Studied In Situ. *J Invest Dermatol*, *141*(5), 1243-1253 e1246. https://doi.org/10.1016/j.jid.2020.07.040

Natsume, T., Kiyomitsu, T., Saga, Y., & Kanemaki, M. T. (2016). Rapid Protein Depletion in Human Cells by Auxin-Inducible Degron Tagging with Short Homology Donors. *Cell Rep*, *15*(1), 210-218. https://doi.org/10.1016/j.celrep.2016.03.001

Navon, A., & Ciechanover, A. (2009). The 26 S proteasome: from basic mechanisms to drug targeting. *J Biol Chem*, *284*(49), 33713-33718. https://doi.org/10.1074/jbc.R109.018481

Nguyen, B.-C., Lefort, K., Mandinova, A., Antonini, D., Devgan, V., Della Gatta, G., Koster, M. I., Zhang, Z., Wang, J., Di Vignano, A. T., Kitajewski, J., Chiorino, G., Roop, D. R., Missero, C., & Dotto, G. P. (2006). Cross-regulation between Notch and p63 in keratinocyte commitment to differentiation. *Genes & Development*, *20*(8), 1028-1042. https://doi.org/10.1101/gad.1406006

Niehues, H., Rikken, G., Van Vlijmen-Willems, I. M. J. J., Rodijk-Olthuis, D., Van Erp, P. E. J., Zeeuwen, P. L. J. M., Schalkwijk, J., & Van Den Bogaard, E. H. (2022). Identification of Keratinocyte Mitogens: Implications for Hyperproliferation in Psoriasis and Atopic Dermatitis. *JID Innovations*, *2*(1), 100066. https://doi.org/10.1016/j.xjidi.2021.100066

Niessen, C. M., van der Raaij-Helmer, M. H., Hulsman, E. H., van der Neut, R., Jonkman, M. F., & Sonnenberg, A. (1996). Deficiency of the integrin beta 4 subunit in junctional epidermolysis bullosa with pyloric atresia: consequences for hemidesmosome formation and adhesion properties. *J Cell Sci*, *109 (Pt 7)*, 1695-1706. https://doi.org/10.1242/jcs.109.7.1695

Ning, W., Muroyama, A., Li, H., & Lechler, T. (2021). Differentiated Daughter Cells Regulate Stem Cell Proliferation and Fate through Intra-tissue Tension. *Cell Stem Cell*, *28*(3), 436-452 e435. https://doi.org/10.1016/j.stem.2020.11.002

Nishimura, K., Fukagawa, T., Takisawa, H., Kakimoto, T., & Kanemaki, M. (2009). An auxin-based degron system for the rapid depletion of proteins in nonplant cells. *Nat Methods*, *6*(12), 917-922. https://doi.org/10.1038/nmeth.1401

Norlen, L. (2001). Skin barrier formation: the membrane folding model. *J Invest Dermatol*, *117*(4), 823-829. https://doi.org/10.1046/j.0022-202x.2001.01445.x

Norlen, L., Al-Amoudi, A., & Dubochet, J. (2003). A cryotransmission electron microscopy study of skin barrier formation. *J Invest Dermatol*, *120*(4), 555-560. https://doi.org/10.1046/j.1523-1747.2003.12102.x

Norlen, L., Lundborg, M., Wennberg, C., Narangifard, A., & Daneholt, B. (2022). The Skin's Barrier: A Cryo-EM Based Overview of its Architecture and Stepwise Formation. *J Invest Dermatol*, *142*(2), 285-292. https://doi.org/10.1016/j.jid.2021.06.037

Obarzanek-Fojt, M., Favre, B., Kypriotou, M., Ryser, S., Huber, M., & Hohl, D. (2011). Homeodomain-only protein HOP is a novel modulator of late differentiation in keratinocytes. *Eur J Cell Biol*, *90*(4), 279-290. https://doi.org/10.1016/j.ejcb.2010.11.001

Oberbeck, N., Pham, V. C., Webster, J. D., Reja, R., Huang, C. S., Zhang, Y., Roose-Girma, M., Warming, S., Li, Q., Birnberg, A., Wong, W., Sandoval, W., Komuves, L. G., Yu, K., Dugger, D. L., Maltzman, A., Newton, K., & Dixit, V. M. (2019). The RIPK4-IRF6 signalling axis safeguards epidermal differentiation and barrier function. *Nature*, *574*(7777), 249-253. https://doi.org/10.1038/s41586-019-1615-3

Oberbeck, N., Pham, V. C., Webster, J. D., Reja, R., Huang, C. S., Zhang, Y., Roose-Girma, M., Warming, S., Li, Q., Birnberg, A., Wong, W., Sandoval, W., Kőműves, L. G., Yu, K., Dugger, D. L., Maltzman, A., Newton, K., & Dixit, V. M. (2019). The RIPK4–IRF6 signalling axis safeguards epidermal differentiation and barrier function. *Nature*, *574*(7777), 249-253. https://doi.org/10.1038/s41586-019-1615-3

Olsen, S. N., Godfrey, L., Healy, J. P., Choi, Y. A., Kai, Y., Hatton, C., Perner, F., Haarer, E. L., Nabet, B., Yuan, G. C., & Armstrong, S. A. (2022). MLL::AF9 degradation induces rapid changes in transcriptional elongation and subsequent loss of an active chromatin landscape. *Mol Cell*, *82*(6), 1140-1155 e1111. https://doi.org/10.1016/j.molcel.2022.02.013

Ouspenskaia, T., Matos, I., Mertz, A. F., Fiore, V. F., & Fuchs, E. (2016). WNT-SHH Antagonism Specifies and Expands Stem Cells prior to Niche Formation. *Cell*, *164*(1-2), 156-169. https://doi.org/10.1016/j.cell.2015.11.058

Pajcini, K. V., Xu, L., Shao, L., Petrovic, J., Palasiewicz, K., Ohtani, Y., Bailis, W., Lee, C., Wertheim, G. B., Mani, R., Muthusamy, N., Li, Y., Meijerink, J. P. P., Blacklow, S. C., Faryabi, R. B., Cherry, S., & Pear, W. S. (2017). MAFB enhances oncogenic Notch signaling in T cell acute lymphoblastic leukemia. *Sci Signal*, *10*(505). https://doi.org/10.1126/scisignal.aam6846

Park, S. (2022). Building vs. Rebuilding Epidermis: Comparison Embryonic Development and Adult Wound Repair. *Frontiers in Cell and Developmental Biology*, *9*. https://doi.org/10.3389/fcell.2021.796080

Perez, P. (2011). Glucocorticoid receptors, epidermal homeostasis and hair follicle differentiation. *Dermatoendocrinol*, *3*(3), 166-174. https://doi.org/10.4161/derm.3.3.15332

Phanindhar, K., & Mishra, R. K. (2023). Auxin-inducible degron system: an efficient protein degradation tool to study protein function. *Biotechniques*, *74*(4), 186-198. https://doi.org/10.2144/btn-2022-0108

Pickar-Oliver, A., & Gersbach, C. A. (2019). The next generation of CRISPR-Cas technologies and applications. *Nat Rev Mol Cell Biol*, *20*(8), 490-507. https://doi.org/10.1038/s41580-019-0131-5

Pontiggia, L., Ahuja, A. K., Yosef, H. K., Rütsche, D., Reichmann, E., Moehrlen, U., & Biedermann, T. (2022). Human Basal and Suprabasal Keratinocytes Are Both Able to Generate and Maintain Dermo–Epidermal Skin Substitutes in Long-Term In Vivo Experiments. *Cells*, *11*(14), 2156. https://doi.org/10.3390/cells11142156

Porteus, M. (2008). Design and Testing of Zinc Finger Nucleases for Use in Mammalian Cells. *Chromosomal Mutagenesis*. https://doi.org/10.1007/978-1-59745-232-8_4

Poulson, N. D., & Lechler, T. (2010). Robust control of mitotic spindle orientation in the developing epidermis. *J Cell Biol*, *191*(5), 915-922. https://doi.org/10.1083/jcb.201008001

Powell, B. C., Passmore, E. A., Nesci, A., & Dunn, S. M. (1998). The Notch signalling pathway in hair growth. *Mech Dev*, *78*(1-2), 189-192. https://doi.org/10.1016/s0925-4773(98)00177-4

Prado-Mantilla, A., & Lechler, T. (2023a). Polarity in skin development and cancer. *Curr Top Dev Biol*, *154*, 317-336. https://doi.org/10.1016/bs.ctdb.2023.02.003

Prado-Mantilla, A., & Lechler, T. (2023b). Polarity in Skin Development and Cancer. *Current topics in developmental biology*, *154*. https://doi.org/10.1016/bs.ctdb.2023.02.003

Prado-Mantilla, A., Ning, W., & Lechler, T. (2024). Molecular and Mechanical Signatures Contributing to Epidermal Differentiation and Barrier Formation. In: eLife Sciences Publications, Ltd.

Rangarajan, A. (2001). Notch signaling is a direct determinant of keratinocyte growth arrest and entry into differentiation. *The EMBO Journal*, *20*(13), 3427-3436. https://doi.org/10.1093/emboj/20.13.3427

Raymond, A. A., Gonzalez de Peredo, A., Stella, A., Ishida-Yamamoto, A., Bouyssie, D., Serre, G., Monsarrat, B., & Simon, M. (2008). Lamellar bodies of human epidermis: proteomics characterization by high throughput mass spectrometry and possible involvement of CLIP-170 in their trafficking/secretion. *Mol Cell Proteomics*, *7*(11), 2151-2175. https://doi.org/10.1074/mcp.M700334-MCP200

Richardson, R. J., Dixon, J., Malhotra, S., Hardman, M. J., Knowles, L., Boot-Handford, R. P., Shore, P., Whitmarsh, A., & Dixon, M. J. (2006). Irf6 is a key determinant of the keratinocyte proliferation-differentiation switch. *Nature Genetics*, *38*(11), 1329-1334. https://doi.org/10.1038/ng1894

Richardson, R. J., Hammond, N. L., Coulombe, P. A., Saloranta, C., Nousiainen, H. O., Salonen, R., Berry, A., Hanley, N., Headon, D., Karikoski, R., & Dixon, M. J. (2014). Periderm prevents pathological epithelial adhesions during embryogenesis. *J Clin Invest*, *124*(9), 3891-3900. https://doi.org/10.1172/JCI71946

Rolfs, Z., Frey, B. L., Shi, X., Kawai, Y., Smith, L. M., & Welham, N. V. (2021). An atlas of protein turnover rates in mouse tissues. *Nat Commun*, *12*(1), 6778. https://doi.org/10.1038/s41467-021-26842-3

Romano, R. A., Birkaya, B., & Sinha, S. (2007). A functional enhancer of keratin14 is a direct transcriptional target of deltaNp63. *J Invest Dermatol*, *127*(5), 1175-1186. https://doi.org/10.1038/sj.jid.5700652

Rompolas, P., Mesa, K. R., Kawaguchi, K., Park, S., Gonzalez, D., Brown, S., Boucher, J., Klein, A. M., & Greco, V. (2016). Spatiotemporal coordination of stem cell commitment during epidermal homeostasis. *Science*, *352*(6292), 1471-1474. https://doi.org/10.1126/science.aaf7012

Rousselle, P., Laigle, C., & Rousselet, G. (2022). The basement membrane in epidermal polarity, stemness, and regeneration. *American Journal of Physiology-Cell Physiology*, *323*(6), C1807-C1822. https://doi.org/10.1152/ajpcell.00069.2022

Rubsam, M., Mertz, A. F., Kubo, A., Marg, S., Jungst, C., Goranci-Buzhala, G., Schauss, A. C., Horsley, V., Dufresne, E. R., Moser, M., Ziegler, W., Amagai, M., Wickstrom, S. A., & Niessen, C. M. (2017). E-cadherin integrates mechanotransduction and EGFR signaling to control junctional tissue polarization and tight junction positioning. *Nat Commun*, *8*(1), 1250. https://doi.org/10.1038/s41467-017-01170-7

Ruzzi, L., Gagnoux-Palacios, L., Pinola, M., Belli, S., Meneguzzi, G., D'Alessio, M., & Zambruno, G. (1997). A homozygous mutation in the integrin alpha6 gene in junctional epidermolysis bullosa with pyloric atresia. *J Clin Invest*, *99*(12), 2826-2831. https://doi.org/10.1172/JCI119474

Sakai, K., Akiyama, M., Sugiyama-Nakagiri, Y., McMillan, J. R., Sawamura, D., & Shimizu, H. (2007). Localization of ABCA12 from Golgi apparatus to lamellar granules in human upper epidermal keratinocytes. *Exp Dermatol*, *16*(11), 920-926. https://doi.org/10.1111/j.1600-0625.2007.00614.x

Sauer, B., & Henderson, N. (1988). Site-specific DNA recombination in mammalian cells by the Cre recombinase of bacteriophage P1. *Proc Natl Acad Sci U S A*, *85*(14), 5166-5170. https://doi.org/10.1073/pnas.85.14.5166

Savas, J. N., Toyama, B. H., Xu, T., Yates, J. R., 3rd, & Hetzer, M. W. (2012). Extremely long-lived nuclear pore proteins in the rat brain. *Science*, *335*(6071), 942. https://doi.org/10.1126/science.1217421

Schlegelmilch, K., Mohseni, M., Kirak, O., Pruszak, J., Rodriguez, J. R., Zhou, D., Kreger, B. T., Vasioukhin, V., Avruch, J., Brummelkamp, T. R., & Camargo, F. D. (2011). Yap1 acts downstream of alpha-catenin to control epidermal proliferation. *Cell*, *144*(5), 782-795. https://doi.org/10.1016/j.cell.2011.02.031

Schwanhäusser, B., Busse, D., Li, N., Dittmar, G., Schuchhardt, J., Wolf, J., Chen, W., & Selbach, M. (2011). Global quantification of mammalian gene expression control. *Nature*, *473*(7347), 337-342. https://doi.org/10.1038/nature10098

Segre, J. A., Bauer, C., & Fuchs, E. (1999). Klf4 is a transcription factor required for establishing the barrier function of the skin. *Nat Genet*, *22*(4), 356-360. https://doi.org/10.1038/11926

Seldin, L., Muroyama, A., & Lechler, T. (2016). NuMA-microtubule interactions are critical for spindle orientation and the morphogenesis of diverse epidermal structures. *Elife*, *5*. https://doi.org/10.7554/eLife.12504

Senoo, M., Pinto, F., Crum, C. P., & Mckeon, F. (2007). p63 Is Essential for the Proliferative Potential of Stem Cells in Stratified Epithelia. *Cell*, *129*(3), 523-536. https://doi.org/10.1016/j.cell.2007.02.045

Sevilla, L. M., Bayo, P., Latorre, V., Sanchis, A., & Perez, P. (2010). Glucocorticoid receptor regulates overlapping and differential gene subsets in developing and adult skin. *Mol Endocrinol*, *24*(11), 2166-2178. https://doi.org/10.1210/me.2010-0183

Sevilla, L. M., Latorre, V., Sanchis, A., & Perez, P. (2013). Epidermal inactivation of the glucocorticoid receptor triggers skin barrier defects and cutaneous inflammation. *J Invest Dermatol*, *133*(2), 361-370. https://doi.org/10.1038/jid.2012.281

Shalom-Feuerstein, R., Lena, A. M., Zhou, H., De La Forest Divonne, S., Van Bokhoven, H., Candi, E., Melino, G., & Aberdam, D. (2011). DeltaNp63 is an ectodermal gatekeeper of epidermal morphogenesis. *Cell Death Differ*, *18*(5), 887-896. https://doi.org/10.1038/cdd.2010.159

Sharpe, G. R., Gillespie, J. I., & Greenwell, J. R. (1989). An increase in intracellular free calcium is an early event during differentiation of cultured human keratinocytes. *FEBS Lett*, *254*(1-2), 25-28. https://doi.org/10.1016/0014-5793(89)81002-6

Simpson, C. L., Patel, D. M., & Green, K. J. (2011). Deconstructing the skin: cytoarchitectural determinants of epidermal morphogenesis. *Nature Reviews Molecular Cell Biology*, *12*(9), 565-580. https://doi.org/10.1038/nrm3175

Singh, A., & Tiwari, V. K. (2023). Transcriptional networks of transient cell states during human prefrontal cortex development. *Front Mol Neurosci*, *16*, 1126438. https://doi.org/10.3389/fnmol.2023.1126438

Smart, I. H. (1970). Variation in the plane of cell cleavage during the process of stratification in the mouse epidermis. *Br J Dermatol*, *82*(3), 276-282. https://doi.org/10.1111/j.1365-2133.1970.tb12437.x

Sumigray, K., Zhou, K., & Lechler, T. (2014). Cell-cell adhesions and cell contractility are upregulated upon desmosome disruption. *PLoS One*, *9*(7), e101824. https://doi.org/10.1371/journal.pone.0101824

Sumigray, K. D., Chen, H., & Lechler, T. (2011). Lis1 is essential for cortical microtubule organization and desmosome stability in the epidermis. *J Cell Biol*, *194*(4), 631-642. https://doi.org/10.1083/jcb.201104009

Sumigray, K. D., Foote, H. P., & Lechler, T. (2012a). Non-centrosomal microtubules and type II myosins potentiate epidermal cell adhesion and barrier formation. *J Cell Biol*, *199*(3).

Sumigray, K. D., Foote, H. P., & Lechler, T. (2012b). Noncentrosomal microtubules and type II myosins potentiate epidermal cell adhesion and barrier formation. *J Cell Biol*, *199*(3), 513-525. https://doi.org/10.1083/jcb.201206143

Sumigray, K. D., & Lechler, T. (2015). Cell adhesion in epidermal development and barrier formation. *Curr Top Dev Biol*, *112*, 383-414. https://doi.org/10.1016/bs.ctdb.2014.11.027

Suski, J. M., Ratnayeke, N., Braun, M., Zhang, T., Strmiska, V., Michowski, W., Can, G., Simoneau, A., Snioch, K., Cup, M., Sullivan, C. M., Wu, X., Nowacka, J., Branigan, T. B., Pack, L. R., DeCaprio, J. A., Geng, Y., Zou, L., Gygi, S. P.,…Sicinski, P. (2022). CDC7-independent G1/S transition revealed by targeted protein degradation. *Nature*, *605*(7909), 357-365. https://doi.org/10.1038/s41586-022-04698-x

Tajik, A., Zhang, Y., Wei, F., Sun, J., Jia, Q., Zhou, W., Singh, R., Khanna, N., Belmont, A. S., & Wang, N. (2016). Transcription upregulation via force-induced direct stretching of chromatin. *Nat Mater*, *15*(12), 1287-1296. https://doi.org/10.1038/nmat4729

Tan, X., Calderon-Villalobos, L. I., Sharon, M., Zheng, C., Robinson, C. V., Estelle, M., & Zheng, N. (2007). Mechanism of auxin perception by the TIR1 ubiquitin ligase. *Nature*, *446*(7136), 640-645. https://doi.org/10.1038/nature05731

Tellkamp, F., Vorhagen, S., & Niessen, C. M. (2014). Epidermal polarity genes in health and disease. *Cold Spring Harb Perspect Med*, *4*(12), a015255. https://doi.org/10.1101/cshperspect.a015255

Thomas, A. C., Cullup, T., Norgett, E. E., Hill, T., Barton, S., Dale, B. A., Sprecher, E., Sheridan, E., Taylor, A. E., Wilroy, R. S., DeLozier, C., Burrows, N., Goodyear, H., Fleckman, P., Stephens, K. G., Mehta, L., Watson, R. M., Graham, R., Wolf, R.,…Kelsell, D. P. (2006). ABCA12 is the major harlequin ichthyosis gene. *J Invest Dermatol*, *126*(11), 2408-2413. https://doi.org/10.1038/sj.jid.5700455

Thomas, P. D., Ebert, D., Muruganujan, A., Mushayahama, T., Albou, L. P., & Mi, H. (2022). PANTHER: Making genome-scale phylogenetics accessible to all. *Protein Sci*, *31*(1), 8-22. https://doi.org/10.1002/pro.4218

Ting, S. B., Caddy, J., Hislop, N., Wilanowski, T., Auden, A., Zhao, L. L., Ellis, S., Kaur, P., Uchida, Y., Holleran, W. M., Elias, P. M., Cunningham, J. M., & Jane, S. M. (2005). A homolog of Drosophila grainy head is essential for epidermal integrity in mice. *Science*, *308*(5720), 411-413. https://doi.org/10.1126/science.1107511

Ting, S. B., Caddy, J., Wilanowski, T., Auden, A., Cunningham, J. M., Elias, P. M., Holleran, W. M., & Jane, S. M. (2005). The epidermis of grhl3-null mice displays altered lipid processing and cellular hyperproliferation. *Organogenesis*, *2*(2), 33-35. https://doi.org/10.4161/org.2.2.2167

Toyama, B. H., Savas, J. N., Park, S. K., Harris, M. S., Ingolia, N. T., Yates, J. R., 3rd, & Hetzer, M. W. (2013). Identification of long-lived proteins reveals exceptional stability of essential cellular structures. *Cell*, *154*(5), 971-982. https://doi.org/10.1016/j.cell.2013.07.037

Tu, C. L., Chang, W., & Bikle, D. D. (2011). The calcium-sensing receptor-dependent regulation of cell-cell adhesion and keratinocyte differentiation requires Rho and filamin A. *J Invest Dermatol*, *131*(5), 1119-1128. https://doi.org/10.1038/jid.2010.414

Tu, C. L., Crumrine, D. A., Man, M. Q., Chang, W., Elalieh, H., You, M., Elias, P. M., & Bikle, D. D. (2012). Ablation of the calcium-sensing receptor in keratinocytes impairs epidermal differentiation and barrier function. *J Invest Dermatol*, *132*(10), 2350-2359. https://doi.org/10.1038/jid.2012.159

Tu, C. L., & You, M. (2014). Obligatory roles of filamin A in E-cadherin-mediated cell-cell adhesion in epidermal keratinocytes. *J Dermatol Sci*, *73*(2), 142-151. https://doi.org/10.1016/j.jdermsci.2013.09.007

Tumbar, T., Guasch, G., Greco, V., Blanpain, C., Lowry, W. E., Rendl, M., & Fuchs, E. (2004). Defining the epithelial stem cell niche in skin. *Science*, *303*(5656), 359-363. https://doi.org/10.1126/science.1092436

Tunggal, J. A., Helfrich, I., Schmitz, A., Schwarz, H., Gunzel, D., Fromm, M., Kemler, R., Krieg, T., & Niessen, C. M. (2005). E-cadherin is essential for in vivo epidermal barrier function by regulating tight junctions. *EMBO J*, *24*(6), 1146-1156. https://doi.org/10.1038/sj.emboj.7600605

Urlinger, S., Baron, U., Thellmann, M., Hasan, M. T., Bujard, H., & Hillen, W. (2000). Exploring the sequence space for tetracycline-dependent transcriptional activators: novel mutations yield expanded range and sensitivity. *Proc Natl Acad Sci U S A*, *97*(14), 7963-7968. https://doi.org/10.1073/pnas.130192197

Urwyler-Rösselet, C., Tanghe, G., Leurs, K., Gilbert, B., De Rycke, R., De Bruyne, M., Lippens, S., Bartunkova, S., De Groote, P., Niessen, C., Haftek, M., Vandenabeele, P., & Declercq, W. (2018). Keratinocyte-Specific Ablation of RIPK4 Allows Epidermal Cornification but Impairs Skin Barrier Formation. *Journal of Investigative Dermatology*, *138*(6), 1268-1278. https://doi.org/10.1016/j.jid.2017.12.031

Uyttendaele, H., Panteleyev, A. A., de Berker, D., Tobin, D. T., & Christiano, A. M. (2004). Activation of Notch1 in the hair follicle leads to cell-fate switch and Mohawk alopecia. *Differentiation*, *72*(8), 396-409. https://doi.org/10.1111/j.1432-0436.2004.07208006.x

van der Neut, R., Krimpenfort, P., Calafat, J., Niessen, C. M., & Sonnenberg, A. (1996). Epithelial detachment due to absence of hemidesmosomes in integrin beta 4 null mice. *Nat Genet*, *13*(3), 366-369. https://doi.org/10.1038/ng0796-366

Varshavsky, A. (1991). Naming a targeting signal. *Cell*, *64*(1), 13-15. https://doi.org/10.1016/0092-8674(91)90202-a

Varshavsky, A. (2006). The early history of the ubiquitin field. *Protein Sci*, *15*(3), 647-654. https://doi.org/10.1110/ps.052012306

Verma, R., Mohl, D., & Deshaies, R. J. (2020). Harnessing the Power of Proteolysis for Targeted Protein Inactivation. *Mol Cell*, *77*(3), 446-460. https://doi.org/10.1016/j.molcel.2020.01.010

Vietri Rudan, M., & Watt, F. M. (2021). Mammalian Epidermis: A Compendium of Lipid Functionality. *Front Physiol, 12*, 804824. https://doi.org/10.3389/fphys.2021.804824

Vining, K. H., & Mooney, D. J. (2017). Mechanical forces direct stem cell behaviour in development and regeneration. *Nat Rev Mol Cell Biol*, *18*(12), 728-742. https://doi.org/10.1038/nrm.2017.108

Wang, S., Drummond, M. L., Guerrero-Juarez, C. F., Tarapore, E., Maclean, A. L., Stabell, A. R., Wu, S. C., Gutierrez, G., That, B. T., Benavente, C. A., Nie, Q., & Atwood, S. X. (2020). Single cell transcriptomics of human epidermis identifies basal stem cell transition states. *Nature Communications*, *11*(1). https://doi.org/10.1038/s41467-020-18075-7

Wang, X., Agrawal, V., Dunton, C. L., Liu, Y., Virk, R. K. A., Patel, P. A., Carter, L., Pujadas, E. M., Li, Y., Jain, S., Wang, H., Ni, N., Tsai, H. M., Rivera-Bolanos, N., Frederick, J., Roth, E., Bleher, R., Duan, C., Ntziachristos, P.,…Ameer, G. A. (2023). Chromatin reprogramming and bone regeneration in vitro and in vivo via the microtopography-induced constriction of cell nuclei. *Nat Biomed Eng*, *7*(11), 1514-1529. https://doi.org/10.1038/s41551-023-01053-x

Wang, Z., Sun, Y., Lou, F., Bai, J., Zhou, H., Cai, X., Sun, L., Yin, Q., Tang, S., Wu, Y., Fan, L., Xu, Z., Wang, H., Hu, X., & Wang, H. (2022). Targeting the transcription factor HES1 by L-menthol restores protein phosphatase 6 in keratinocytes in models of psoriasis. *Nat Commun*, *13*(1), 7815. https://doi.org/10.1038/s41467-022-35565-y

Weiss, L. W., & Zelickson, A. S. (1975). Embryology of the epidermis: ultrastructural aspects. II. Period of differentiation in the mouse with mammalian comparisons. *Acta Derm Venereol*, *55*(5), 321-329. http://www.ncbi.nlm.nih.gov/pubmed/52965

Williams, R. R., Broad, S., Sheer, D., & Ragoussis, J. (2002). Subchromosomal positioning of the epidermal differentiation complex (EDC) in keratinocyte and lymphoblast interphase nuclei. *Exp Cell Res*, *272*(2), 163-175. https://doi.org/10.1006/excr.2001.5400

Williams, S. E., Beronja, S., Pasolli, H. A., & Fuchs, E. (2011). Asymmetric cell divisions promote Notch-dependent epidermal differentiation. *Nature*, *470*(7334), 353-358. https://doi.org/10.1038/nature09793

Williams, S. E., Ratliff, L. A., Postiglione, M. P., Knoblich, J. A., & Fuchs, E. (2014). Par3-mInsc and Galphai3 cooperate to promote oriented epidermal cell divisions through LGN. *Nat Cell Biol*, *16*(8), 758-769. https://doi.org/10.1038/ncb3001

Wurm, S., Zhang, J., Guinea-Viniegra, J., Garcia, F., Munoz, J., Bakiri, L., Ezhkova, E., & Wagner, E. F. (2015). Terminal epidermal differentiation is regulated by the interaction of Fra-2/AP-1 with Ezh2 and ERK1/2. *Genes Dev*, *29*(2), 144-156. https://doi.org/10.1101/gad.249748.114

Yamanishi, H., Soma, T., Kishimoto, J., Hibino, T., & Ishida-Yamamoto, A. (2019). Marked Changes in Lamellar Granule and Trans-Golgi Network Structure Occur during Epidermal Keratinocyte Differentiation. *J Invest Dermatol*, *139*(2), 352-359. https://doi.org/10.1016/j.jid.2018.07.043

Yang, A., Kaghad, M., Wang, Y., Gillett, E., Fleming, M. D., Dötsch, V., Andrews, N. C., Caput, D., & Mckeon, F. (1998). p63, a p53 Homolog at 3q27–29, Encodes Multiple Products with Transactivating, Death-Inducing, and Dominant-Negative Activities. *Molecular Cell*, *2*(3), 305-316. https://doi.org/10.1016/s1097-2765(00)80275-0

Yang, A., Schweitzer, R., Sun, D., Kaghad, M., Walker, N., Bronson, R. T., Tabin, C., Sharpe, A., Caput, D., Crum, C., & Mckeon, F. (1999). p63 is essential for regenerative proliferation in limb, craniofacial and epithelial development. *Nature*, *398*(6729), 714-718. https://doi.org/10.1038/19539

Yesbolatova, A., Saito, Y., Kitamoto, N., Makino-Itou, H., Ajima, R., Nakano, R., Nakaoka, H., Fukui, K., Gamo, K., Tominari, Y., Takeuchi, H., Saga, Y., Hayashi, K. I., & Kanemaki, M. T. (2020). The auxin-inducible degron 2 technology provides sharp degradation control in yeast, mammalian cells, and mice. *Nat Commun*, *11*(1), 5701. https://doi.org/10.1038/s41467-020-19532-z

Yonemura, S., Wada, Y., Watanabe, T., Nagafuchi, A., & Shibata, M. (2010). alpha-Catenin as a tension transducer that induces adherens junction development. *Nat Cell Biol*, *12*(6), 533-542. https://doi.org/10.1038/ncb2055

Yoshida, K., Yokouchi, M., Nagao, K., Ishii, K., Amagai, M., & Kubo, A. (2013). Functional tight junction barrier localizes in the second layer of the stratum granulosum of human epidermis. *J Dermatol Sci*, *71*(2), 89-99. https://doi.org/10.1016/j.jdermsci.2013.04.021

Yu, F., White, S. B., Zhao, Q., & Lee, F. S. (2001). HIF-1α binding to VHL is regulated by stimulus-sensitive proline hydroxylation. *Proceedings of the National Academy of Sciences*, *98*(17), 9630-9635. https://doi.org/10.1073/pnas.181341498

Yu, Z., Gong, Y., Cui, L., Hu, Y., Zhou, Q., Chen, Z., Yu, Y., Chen, Y., Xu, P., Zhang, X., Guo, C., & Shi, Y. (2020). High-throughput transcriptome and pathogenesis analysis of clinical psoriasis. *J Dermatol Sci*, *98*(2), 109-118. https://doi.org/10.1016/j.jdermsci.2020.03.006

Yu, Z., Lin, K. K., Bhandari, A., Spencer, J. A., Xu, X., Wang, N., Lu, Z., Gill, G. N., Roop, D. R., Wertz, P., & Andersen, B. (2006). The Grainyhead-like epithelial transactivator Get-1/Grhl3 regulates epidermal terminal differentiation and interacts functionally with LMO4. *Dev Biol*, *299*(1), 122-136. https://doi.org/10.1016/j.ydbio.2006.07.015

Zaidel-Bar, R., Zhenhuan, G., & Luxenburg, C. (2015). The contractome--a systems view of actomyosin contractility in non-muscle cells. *J Cell Sci*, *128*(12), 2209-2217. https://doi.org/10.1242/jcs.170068

Zhang, C., Merana, G. R., Harris-Tryon, T., & Scharschmidt, T. C. (2022). Skin immunity: dissecting the complex biology of our body's outer barrier. *Mucosal Immunol*, *15*(4), 551-561. https://doi.org/10.1038/s41385-022-00505-y

Zhang, H., Pasolli, H. A., & Fuchs, E. (2011). Yes-associated protein (YAP) transcriptional coactivator functions in balancing growth and differentiation in skin [Research Support, N.I.H., Extramural
Research Support, Non-U.S. Gov't]. *Proc Natl Acad Sci U S A*, *108*(6), 2270-2275. https://doi.org/10.1073/pnas.1019603108

Zhang, L., Stokes, N., Polak, L., & Fuchs, E. (2011). Specific microRNAs are preferentially expressed by skin stem cells to balance self-renewal and early lineage commitment. *Cell Stem Cell*, *8*(3), 294-308. https://doi.org/10.1016/j.stem.2011.01.014

Zhong, T., Wu, X., Xie, W., Luo, X., Song, T., Sun, S., Luo, Y., Li, D., Liu, M., Xie, S., & Zhou, J. (2022). ENKD1 promotes epidermal stratification by regulating spindle orientation in basal keratinocytes. *Cell Death Differ*. https://doi.org/10.1038/s41418-022-00958-5

Zhou, X., Chen, Y., Cui, L., Shi, Y., & Guo, C. (2022). Advances in the pathogenesis of psoriasis: from keratinocyte perspective. *Cell Death Dis*, *13*(1), 81. https://doi.org/10.1038/s41419-022-04523-3

Zhu, X. D., & Sadowski, P. D. (1995). Cleavage-dependent ligation by the FLP recombinase. Characterization of a mutant FLP protein with an alteration in a catalytic amino acid. *J Biol Chem*, *270*(39), 23044-23054. https://doi.org/10.1074/jbc.270.39.23044

Biography

Alexandra Prado Mantilla received her B.S. in Biology from Universidad Peruana Cayetano Heredia in Lima in 2016. In August 2018, she began her Ph.D. studies at Duke University in the Developmental and Stem Cell Biology program, joining the Lechler lab and affiliating with the Cell Biology Department.

Her research includes authoring the paper, “Molecular and Mechanical Signatures Contributing to Epidermal Differentiation and Barrier Formation,” which forms Chapter 2 of her dissertation. She is also preparing another first-author manuscript based on Chapter 3 of this work. During graduate school, Alexandra was awarded the ASCB International Federation of Cell Biology Scholarship, enabling her to attend the Neurobiology course at The Marine Biological Laboratory in Woods Hole.

Beyond her scientific pursuits, Alexandra discovered a passion for painting in her third year of graduate studies. She showcased her artwork in the 2024 DUU VisArts Student Art Gallery at Duke University and in the Our House Exhibition at the Durham Arts Council.